

# **A First Introduction to Discrete Exterior Calculus**

## **Masterarbeit**

der Philosophisch-naturwissenschaftlichen Fakultät  
der Universität Bern

vorgelegt von

Peter Bertholet

2012

Leiter der Arbeit:  
Claude Knaus  
Prof. Dr. Matthias Zwicker  
Institut für Informatik und angewandte Mathematik



## Abstract

Discrete exterior calculus (DEC) provides tools to discretize partial differential equations (PDEs) defined on manifolds. The discretized PDE's can be described using global sparse linear equations defined on discrete manifolds. DEC has successfully been used in various computer graphics applications. Nevertheless, DEC is not directly accessible to many graduate students in computer sciences, as they can have varying mathematical backgrounds, from basic to very advanced. DEC is directly related to exterior calculus (EC) and EC is often not covered in the math covered standard computer science course.

This textbook aims to render DEC easily accessible to a broader public, by giving an introduction to DEC alongside of EC. Only a basic knowledge of calculus and linear algebra is assumed, covering even basic notions like manifolds. The geometric aspects of both DEC and EC are emphasized in order to put across the insights behind the DEC and EC formalisms. More advanced DEC and EC results are given in the context of applications, where their relevance is demonstrated at once. The use of DEC is demonstrated in the context of surface parametrization, vector field design, and fluid simulations.

This text provides a working knowledge of both exterior calculus and discrete exterior calculus, enabling the reader to apply and adapt DEC to new problems and to follow reasonings made using EC.



## **Acknowledgements**

I would like to thank Claude Knaus for the long discussions, the good suggestions and the competent supervision of this thesis. I also greatly thank Professor Matthias Zwicker for giving me the opportunity to get acquainted with discrete differential forms, and for his valuable feedback. Also I wish to thank Gian Calgeer, Marco Manzi and Patrik Rauber for telling me on a regular basis not to get lost in details, and for making the time I worked on this thesis much more fun. Finally, I owe many thanks to my parents for their unwavering support and for giving me the possibility to take this masters course.



# Contents

<b>1. Introduction</b>	<b>3</b>
1.1. Goal of this Thesis . . . . .	3
1.2. Why Use DEC? . . . . .	3
1.3. A Glimpse of DEC . . . . .	4
1.4. Structure of this Thesis . . . . .	6
1.5. Disclaimer . . . . .	7
<b>2. Manifolds and Meshes</b>	<b>9</b>
2.1. Manifolds . . . . .	10
2.1.1. Describing Manifolds . . . . .	10
2.1.2. Tangential Spaces . . . . .	12
2.1.3. Orientations . . . . .	13
2.1.4. The Border Operator . . . . .	14
2.1.5. Differential Calculus on Manifolds . . . . .	16
2.1.6. Summary . . . . .	18
2.2. Discrete Manifolds . . . . .	19
2.2.1. Simplices and Simplicial Complexes . . . . .	19
2.2.2. Orientations . . . . .	20
2.2.3. Formal Sums, k-Chains and Vectors . . . . .	22
2.2.4. The Border Operator . . . . .	24
2.2.5. Oriented Discrete Manifold . . . . .	26
2.2.6. Summary . . . . .	26
2.3. Implementation Notes . . . . .	28
2.3.1. A Word on Sparse Matrices . . . . .	28
2.3.2. Implementing Simplicial 2-Complexes . . . . .	28
2.3.3. Implementing Simplicial k-Complexes . . . . .	29
2.3.4. Simple Example Applications . . . . .	31
<b>3. Differential Forms</b>	<b>33</b>
3.1. Smooth Differential Forms . . . . .	33
3.1.1. The Perfect Thing to Integrate . . . . .	34
3.1.2. Forms . . . . .	36
3.1.3. The Wedge Product . . . . .	39
3.1.4. Differential Forms . . . . .	41
3.1.5. Interpretation of Differential Forms in $\mathbb{R}^3$ . . . . .	41
3.1.6. Integration of Forms . . . . .	44

---

3.1.7. Pull-Backs . . . . .	47
3.2. Discrete Differential Forms . . . . .	47
3.2.1. Sampling Forms . . . . .	48
3.2.2. Integration of Discrete Forms . . . . .	50
<b>4. Exterior Calculus &amp; Discrete Exterior Calculus</b>	<b>53</b>
4.1. The Exterior Derivative $d$ . . . . .	54
4.1.1. Definition . . . . .	54
4.1.2. Properties . . . . .	55
4.1.3. The Exterior Derivative in Euclidean Coordinates . . . . .	55
4.2. Stokes' Theorem . . . . .	57
4.2.1. Proof Sketch . . . . .	57
4.2.2. The Geometry of $d$ . . . . .	61
4.2.3. The Geometry of Classical Differential Operators . . . . .	61
4.3. The Hodge Star . . . . .	63
4.3.1. Intuition . . . . .	63
4.3.2. Dual Forms . . . . .	64
4.3.3. Realization of $\star$ in Standard Calculus . . . . .	67
4.4. Exterior Calculus . . . . .	68
4.4.1. The Coderivative . . . . .	69
4.5. Discrete Exterior Calculus . . . . .	71
4.5.1. The Discrete Exterior Derivative . . . . .	71
4.5.2. The Dual Mesh . . . . .	73
4.5.3. Discrete Dual Forms . . . . .	76
4.5.4. The Discrete Hodge Star . . . . .	77
4.5.5. A Fully Formulated Example . . . . .	78
4.5.6. The Discrete Coderivative . . . . .	81
4.5.7. This is Discrete Exterior Calculus . . . . .	83
<b>5. Conformal Mesh Parametrization</b>	<b>85</b>
5.1. Problem Statement . . . . .	85
5.2. Conformal Embeddings with DEC . . . . .	88
5.2.1. Graph Theory . . . . .	89
5.2.2. Fixed Border Constraints . . . . .	92
5.2.3. Multiple Borders . . . . .	93
5.2.4. Results . . . . .	95
<b>6. Vector Field Design and the General Laplacian</b>	<b>99</b>
6.1. Problem Statement . . . . .	100
6.2. The Hopf Index Theorem . . . . .	101
6.3. Harmonic, Closed and Coclosed Forms . . . . .	102
6.3.1. General Laplacian . . . . .	103
6.3.2. Curl- and Divergence-Freeness . . . . .	103
6.3.3. Poincaré-Lemma . . . . .	104

6.3.4. Hodge Decomposition . . . . .	104
6.3.5. Discrete Hodge Decomposition . . . . .	106
6.3.6. Dimension of Harmonic Spaces . . . . .	107
6.4. Application: Vector Field Design . . . . .	108
6.4.1. 1-Form to Vector Field . . . . .	109
6.4.2. Directional Constraints . . . . .	110
6.4.3. Results . . . . .	111
6.4.4. Border Constraints . . . . .	111
<b>7. A Fluid Simulation with DEC</b>	<b>117</b>
7.1. Problem Statement . . . . .	117
7.1.1. Navier Stokes . . . . .	118
7.1.2. A Numerical Integration Scheme . . . . .	120
7.1.3. From Vorticities to Velocities . . . . .	121
7.2. Implementation . . . . .	123
7.2.1. Sampling Scheme . . . . .	124
7.2.2. Algorithm Overview . . . . .	124
7.2.3. Interpolation and Pathtracing . . . . .	125
7.2.4. Diffusion and Additional Forces . . . . .	129
7.2.5. The Harmonic Component . . . . .	130
7.2.6. Recovering $d\mathbf{a}$ . . . . .	133
7.3. Results . . . . .	135
<b>8. Discussion and Further Literature</b>	<b>139</b>
<b>A. Further Details</b>	<b>141</b>
A.1. The Well-Definedness of the Integral for Differential Forms . . . . .	141
A.2. The Dual Discrete Border Operator . . . . .	142
<b>. Bibliography</b>	<b>143</b>



# 1. Introduction

## 1.1. Goal of this Thesis

This thesis introduces the reader to exterior calculus (EC) and discrete exterior calculus (DEC). Exterior calculus provides a very elegant way to formulate important operators and relations from standard calculus and leads to deeper insights about various differential operators. Discrete exterior calculus mirrors exterior calculus, but is defined directly on triangle meshes and simplicial complexes. It allows to reformulate and approximate equations from exterior calculus with matrices, such that the equations can be solved computationally directly on the meshes.

After reading this thesis a reader should have a working knowledge of both exterior calculus and discrete exterior calculus, such that you can apply discrete exterior calculus to problems and reason (or at least follow reasonings) using exterior calculus.

Both EC and DEC are, under a layer of abstraction, of a very geometric nature. This thesis also attempts to help a reader see the simplicity and beauty of the underlying relations used by and described by EC and DEC.

## 1.2. Why Use DEC?

DEC provides one way to discretize partial differential equations, and naturally allows the treatment of differential equations on curved discrete surfaces or spaces, described by triangle meshes or more general simplicial complexes. The major DEC features are:

- DEC is designed to preserve the geometry behind differential equations. The preservation of visually striking geometric features is important for computer graphic applications.
- DEC provides a set of coherently discretized differential operators like the gradient, the curl or the divergence. The relationship between these differential operators is preserved to a large extent by their DEC discretizations. For example Stokes' theorem and the Hodge decomposition theorem are preserved by DEC.
- For DEC there is no need to introduce local coordinates on meshes. The DEC operators are coordinate free.
- DEC is designed to be used on triangle mesh surfaces, tetrahedral meshes or more general simplicial complexes representing curved spaces. This is appealing for computer graphic applications, as triangle meshes and tetrahedral meshes are widely used.

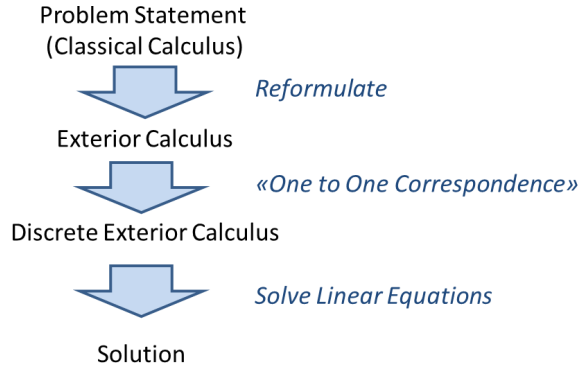


Figure 1.1.: Ideal solution process using DEC.

- DEC discretizations naturally lead to sparse linear systems that can be solved efficiently by standard solvers.

### 1.3. A Glimpse of DEC

Broadly speaking, DEC provides a set of matrices that correspond to EC operators. EC operators on the other hand generalize standard calculus operators, like the divergence or gradient operator. The application of DEC to a problem usually follows the general pattern, sketched in Figure 1.1. At the beginning stands a problem statement or solution process expressed in standard calculus terms. In a first step the standard calculus equations are reformulated using exterior calculus operators. This is done in order to use the correspondence between EC operators and DEC matrices: in the exterior calculus formulation, the exterior calculus operators can be substituted directly by the corresponding discrete exterior calculus matrices. This produces linear equations that finally can be solved computationally, using standard sparse linear solvers.

We illustrate this pattern with an application from Desbrun et al. [DMSB99], [MDSB02]: the smoothing of two-dimensional meshes. This application can be based on the theory of minimal surfaces. In the setting of minimal surfaces a so called area minimizing flow, or mean curvature flow arises, see e.g. [Car92] or [CM11]. For a curved surface, this flow is described by a set of vectors orthogonal to the surface. Then, if the whole surface is slightly moved in these directions, it is guaranteed that the area of the surface is decreased everywhere. Say  $M$  is our surface and  $V$  is the set of directions describing the mean curvature flow, then in a sloppy notation

$$\frac{\partial}{\partial t} \text{area}(M + t \cdot V) \Big|_{t=0} \leq 0.$$

Now it turns out that the mean curvature flow can be described by applying the Laplace

operator  $\Delta_M$  defined on the surface  $M$ , to the coordinates of the surface  $M$ ,

$$V = \begin{pmatrix} \Delta_M M.x \\ \Delta_M M.y \\ \Delta_M M.z \end{pmatrix}.$$

For the moment it is not important how a Laplacian is defined *on* a surface, this will be described in Chapter 4. Important is only, that  $\Delta$  is a standard calculus differential operator that can be expressed using exterior calculus operators, namely  $d$  and  $\partial$ :

$$\Delta = \partial d.$$

This gives us a description of the area minimizing process in exterior calculus terms; if the surface positions are changed over time according to the following equation, its area gets minimized:

$$\frac{\partial}{\partial t} \begin{pmatrix} M_t.x \\ M_t.y \\ M_t.z \end{pmatrix} = \begin{pmatrix} \partial d M_t.x \\ \partial d M_t.y \\ \partial d M_t.z \end{pmatrix}.$$

Now suppose we have a triangle mesh and we want to minimize its surface. Wanting to minimize the surface of a mesh is not an exotic idea. In this example the surface minimization is used to smooth a surface. If a surface is bumpy, minimizing the surface locally will flatten the bumps. DEC now provides the possibility to directly use the description of the area minimizing flow on the triangle mesh. The area minimizing process is described in exterior calculus terms. Discrete exterior calculus mirrors exterior calculus: it provides two matrices  $\partial^{\text{discrete}}$  and  $d^{\text{discrete}}$  that correspond to the EC operators  $\partial$  and  $d$ . Then we simply replace the exterior calculus operator  $\Delta = \partial d$  with the discrete exterior calculus matrix  $\Delta^{\text{discrete}} = \partial^{\text{discrete}} \cdot d^{\text{discrete}}$  and the surface coordinates of  $M$  by the coordinates of the mesh vertices  $v$  and we get

$$\frac{\partial}{\partial t} \begin{pmatrix} v_t.x \\ v_t.y \\ v_t.z \end{pmatrix} = \begin{pmatrix} \Delta^{\text{discrete}} v_t.x \\ \Delta^{\text{discrete}} v_t.y \\ \Delta^{\text{discrete}} v_t.z \end{pmatrix}.$$

This describes three equations, one for each coordinate, that need to be integrated. These equations can be integrated computationally, either using explicit integration,

$$v_{t_{n+1}}.x = v_{t_n}.x + (t_{n+1} - t_n) \Delta^{\text{discrete}} v_{t_n}.x,$$

or using implicit Euler integration,

$$v_{t_{n+1}}.x = v_{t_n}.x + (t_{n+1} - t_n) \Delta^{\text{discrete}} v_{t_{n+1}}.x,$$

which means solving the following sparse linear equation for  $v_{t_{n+1}}.x$  in every time step, solving for the  $x$ -coordinates of all vertices at once

$$\underbrace{(Id - (t_{n+1} - t_n) \Delta^{\text{discrete}})}_{\text{square matrix of dim } \# \text{vertices}} v_{t_{n+1}}.x = v_{t_n}.x .$$



Figure 1.2.: Smoothing a dragon mesh, using the implicit integration scheme.

Implicit integration is much more stable than explicit integration and is the option that should be chosen. Lastly the mesh needs to be rescaled after every step, because it shrinks. For example it could be rescaled such that its volume stays constant. And then... this is it! This is all it takes to smooth surfaces as in Figure 1.2. For implementation details see [DMSB99] and [MDSB02]; note that there the application is derived without the use of DEC.

This is an ideal use-case of DEC and nothing is ever as simple as motivational examples make believe. The formulation with EC must be chosen carefully such that the translation to DEC works. In order to choose a good EC formulation a good knowledge of EC and its relation to DEC is vital. Often the DEC matrices need to be adapted before they can be used.

## 1.4. Structure of this Thesis

The thesis has three pillars: smooth theory, discrete theory and applications/ implementations of example problems. As far as it is possible, the smooth theory is introduced alongside the corresponding discrete theory, such that the reasons and assumptions behind the discretizations become clear. The emphasis is to convey an intuitive understanding of the smooth theory rather than giving a rigorous mathematical introduction.

Chapter 2 introduces manifolds and discrete manifolds, or more generally simplicial complexes. We cover orientations and border operators and sketch how manifolds allow calculus *on* them. We also give some suggestions on how to implement discrete manifolds in a DEC setting.

In Chapter 3 we explain differential forms and discrete differential forms. We introduce the  $\wedge$  and  $\sharp$  operators and tie differential forms to standard calculus objects. We also consider integrals of differential forms and how discrete differential forms can be interpreted as sampled differential forms.

Chapter 4 introduces the remaining exterior calculus operators, the exterior derivative  $d$ , the coderivative  $\partial$  and the Hodge star  $\star$ . We look at Stokes' theorem, which explains

the geometry of the exterior derivative and the standard calculus operators *curl* and *div* and focus on understanding the geometry of the Hodge star. These insights then are used for the definition of the DEC operators.

The Chapters 5, 6 and 7 then use EC and DEC for different computer graphics applications. We broaden the understanding of EC and DEC by explaining application dependent results and also shortly introduce application dependent theory.

In Chapter 5 we consider conformal parameterizations of mesh patches with DEC. We mention Gortler’s extension of Tutte’s theorem and give simple boundary constraints to compute parametrizations. The computation of mesh parametrizations is for example useful to generate texture maps.

In chapter 6 we use DEC for vector field design. Being able to design vector fields can be a useful element for various applications, for example texture generation, as it is used in the original paper [FSDH07] or guided surface crack generation, as in [Rau12]. In this context we present the Hodge decomposition and its discrete variant, results about harmonic forms and look at the Poincaré Hopf index theorem to highlight the influence of surface topology on solution spaces of problem statements.

Chapter 7 describes a fluid simulation with DEC. Here DEC is used in a more complex setting; this application highlights best how problem statements need to be carefully reformulated for DEC to be applicable. We consider harmonic forms once more, and look at a result from de Rham which describes the degrees of freedom of harmonicity depending on the topology of the manifold, and how the degrees of freedom can be controlled on closed manifolds.

## 1.5. Disclaimer

This thesis focuses on introducing readers without any prior experience with DEC and only a basic knowledge of calculus to DEC. But we omit many important subjects in this introduction to EC and DEC. We do not consider any error analysis or compare DEC to finite element methods or any other alternatives. Furthermore, EC is not introduced rigorously, many technical details are omitted or only sketched. We refer to standard works for details, see also the discussion in Chapter 8.



## 2. Manifolds and Meshes

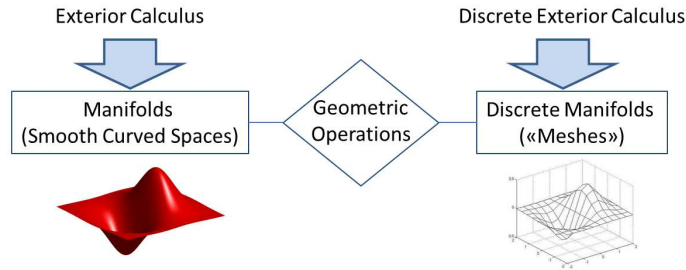


Figure 2.1.: Exterior calculus is defined on manifolds, discrete exterior calculus on discrete manifolds. The continuous and the discrete theory are related via the geometric operations that manifolds and discrete manifolds have in common. This chapter covers manifolds, discrete manifolds and geometric operations.

This chapter introduces the geometric objects exterior calculus (EC) and discrete exterior calculus (DEC) deal with. Everything treated in this thesis is inherently geometric, and geometric relations of objects lie at the heart of exterior calculus and discrete exterior calculus, as depicted in Figure 2.1. Geometric relations are meant in their broadest sense. How is an object oriented relatively to another? What is the geometric boundary of an object? How is a boundary oriented relatively to the interior of the object? The core realization in Chapter 4 is that the most important differential operators are in some sense nothing else than boundary operators.

This chapter covers the description of manifolds and some of their geometric features. Local coordinates, tangential spaces, orientations and the border operator are introduced. We also treat how directional derivatives can be computed *on* manifolds, which allows differential calculus on manifolds. These topics form the Section 2.1 of this chapter.

Section 2.2 treats the discretization of manifolds: simplicial complexes. These allow the definition of orientations and border operators, thereby discretizing the geometric operations introduced on manifolds.

The last section of this chapter is of a more practical nature. It can be used as a guideline when implementing discrete manifolds for DEC. As application some geometric operations on meshes and discrete manifolds are described.

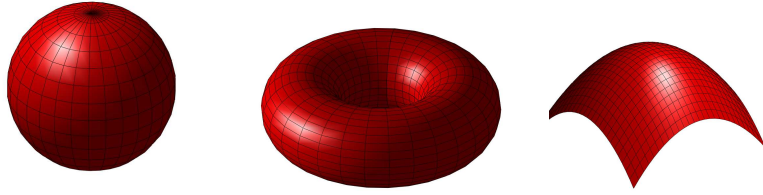


Figure 2.2.: Three simple 2-manifolds; the surfaces of the sphere and the torus do not have any borders, the third surface has. The volume contained by the sphere and the torus are 3-manifolds with border, their borders being the surfaces.

## 2.1. Manifolds

We introduce manifolds as smooth curved  $k$ -dimensional subsets of  $\mathbb{R}^n$ . In this section we cover the following topics on manifolds:

1. The description of manifolds using local maps
2. Tangential spaces
3. The orientation of manifolds
4. The border operator and the orientation of borders
5. Differential calculus on manifolds (derivatives of functions on manifolds)

### 2.1.1. Describing Manifolds

A  $k$ -dimensional manifold, or short  $k$ -manifold, is an object that locally looks like  $\mathbb{R}^k$  and possibly has one or multiple  $k - 1$  dimensional boundaries. Some examples are given in Figure 2.2.

Manifolds are described using local maps. Local maps describe small portions of manifolds. There are two types of maps: maps that describe manifolds around inner points and maps that describe manifolds around border points, as depicted in Figure 2.3. Generally, a  $k$ -dimensional manifold  $M$  lying in  $\mathbb{R}^n$  is a geometric object that locally looks like  $\mathbb{R}^k$  or, at its boundaries, like the halfspace  $\mathbb{H}^k = \{x = (x_1, \dots, x_k) \in \mathbb{R}^k : x_k \geq 0\}$ . Formally this is guaranteed by requiring that for every point on the manifold there is a map linking some neighborhood of the point to  $\mathbb{R}^k$  or  $\mathbb{H}^k$ .

For simplicity we assume henceforth that all functions and mappings are infinitely differentiable.

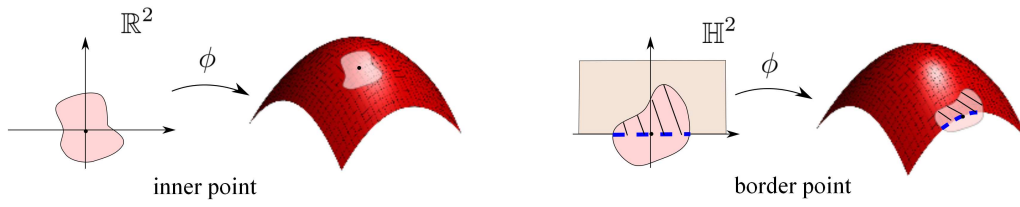


Figure 2.3.: An example of a bordered 2-manifold. Left: a local map  $\phi$  at some inner point. Right: a local map at a border point. The map at the border has the additional restriction that the border of the halfspace  $\mathbb{H}^2$  is mapped to the border of the manifold.

**Definition (Map)** *A  $k$ -dimensional map or parametrization is a differentiable mapping*

$$\phi : U \rightarrow \phi(U) \subset \mathbb{R}^n,$$

$$\begin{pmatrix} u_1 \\ \vdots \\ u_k \end{pmatrix} \rightarrow \begin{pmatrix} x_1(u_1, \dots, u_k) \\ x_2(u_1, \dots, u_k) \\ \vdots \\ x_n(u_1, \dots, u_k) \end{pmatrix},$$

that is injective and whose Jacobi matrix  $D\phi$ ,

$$D\phi = \begin{pmatrix} \frac{\partial \phi_1}{\partial u_1} & \dots & \frac{\partial \phi_1}{\partial u_k} \\ \vdots & & \vdots \\ \frac{\partial \phi_n}{\partial u_1} & \dots & \frac{\partial \phi_n}{\partial u_k} \end{pmatrix},$$

has rank  $k$  on all  $U$ , where  $U$  is some open subset of  $\mathbb{R}^k$  or  $\mathbb{H}^k$  (Figure 2.3).

There are some important details in the definition of maps. The injectivity of the maps prevents self intersecting manifolds, and the constraint on the rank of the Jacobi matrix makes sure that the image of a map  $\phi$  does not degenerate. For example the image of a two dimensional map should not degenerate to a point or a line. A  $k$ -manifold then is an object where you can find local maps everywhere:

**Definition (Manifold)** *A subset  $S \subset \mathbb{R}^n$  is a  $k$ -manifold, if for each point  $p \in S$  there exist an open set  $V \subset \mathbb{R}^k$  such that there is a bijective map  $\phi : U \rightarrow \phi(U) = V \cap S$ .*

Note that in the condition  $\phi(U) = V \cap S$  the additional constraint that the boundary of  $\mathbb{H}^k$  is mapped to the boundary of  $M$  is hidden. Also, technically, the surface patches in the Figures 2.2 and 2.3 that are sold as 2-manifolds with boundary do not fulfill our definition of a manifold. The problem lies in the sharp corners, the corner points do not allow the definition of a smooth border map. But as rounding up the corners any little bit solves this problem they can still be used for illustration purposes.

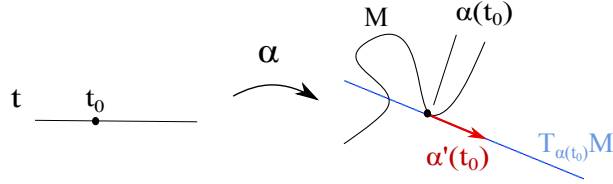


Figure 2.4.: A curve  $M$  parametrized by  $\alpha$ , together with the vector  $\alpha'$  and the tangential space  $T_{\alpha(t_0)}M$  at  $t_0$ .

### Local Coordinates

Any local map  $\phi : U \subset \mathbb{R}^k \rightarrow M$  assigns *local* coordinates to a manifold  $M$ . The values of the tuple  $u = (u_1, \dots, u_k) \in U$  are called the local coordinates of the point  $\phi(u)$ , in the map  $\phi$ . A classic example for local coordinates is to parametrize the sphere by two angles using a map like

$$\phi(a, b) = (\sin(a)\sin(b), \sin(a)\cos(b), \cos(a)).$$

This assigns coordinates  $(a, b)$  to the sphere in the same way as longitude and latitude are used as coordinate for the world.<sup>1</sup>

Functions  $f : M \rightarrow V$  that map the manifold to some arbitrary space  $V$ , can also be expressed in the local coordinates given by a map  $\phi$ . This means that you consider  $f \circ \phi : U \subset \mathbb{R}^k \rightarrow V$  instead of  $f$ , such that you can use the local coordinates  $(u_1, \dots, u_k)$  as parameters of  $f$  instead of the position on the manifold.

#### 2.1.2. Tangential Spaces

Manifolds have tangential spaces. For curves calculating tangents is easy. Given a parametrization  $\alpha(t) : I \subset \mathbb{R} \rightarrow \mathbb{R}^n$  of some curve  $M$ , then

$$\alpha'(t) = (\alpha'_1(t), \alpha'_2(t), \dots, \alpha'_n(t))$$

is a tangential vector of the curve at the position  $\alpha(t)$ . While the length of  $\alpha'(t)$  at the point  $\alpha(t)$  depends on the parametrization  $\alpha$ , the *tangential space*

$$T_{\alpha(t)}M = \text{span}(\alpha'(t)) = \{x \in \mathbb{R}^n : x = c \cdot \alpha'(t), c \in \mathbb{R}\}$$

does only depend on the position  $\alpha(t)$  on the curve, as depicted in Figure 2.4. On a  $k$ -dimensional manifold  $M$ , the tangential space  $T_pM$  at a point  $p$  can be characterized by any of the following ways:

1. The tangential space is the vector space  $T_pM \subset \mathbb{R}^n$  such that the affine linear space  $p + T_pM$  approximates the surface in the best way, locally at  $p$ .

<sup>1</sup>But note that you can not parametrize the whole sphere at once if the source domain of your map is an open set and the map has to be injective.

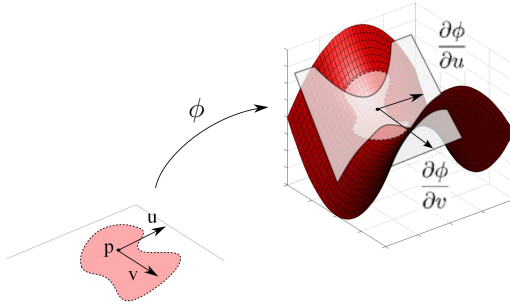


Figure 2.5.: A map  $\phi$  on a 2-manifold  $M$  is used to determine the tangential space  $T_p M$  at some point  $p$ .

2. The tangential space is the vector space  $T_p M \subset \mathbb{R}^n$  made up by the tangents of all curves on the surface that go through  $p$ .
3. For a given parametrization  $\phi : \mathbb{R}^k \rightarrow \mathbb{R}^n$ ,  $\phi(u) = (\phi_1(u), \dots, \phi_n(u))$  the tangential plane  $T_{\phi(u)} M$  is given by

$$\text{span}\left(\frac{\partial \phi}{\partial u_1}, \dots, \frac{\partial \phi}{\partial u_k}\right) = \text{span}\left(\begin{pmatrix} \frac{\partial \phi_1}{\partial u_1} \\ \frac{\partial \phi_2}{\partial u_1} \\ \vdots \\ \frac{\partial \phi_n}{\partial u_1} \end{pmatrix}, \dots, \begin{pmatrix} \frac{\partial \phi_1}{\partial u_k} \\ \frac{\partial \phi_2}{\partial u_k} \\ \vdots \\ \frac{\partial \phi_n}{\partial u_k} \end{pmatrix}\right),$$

as depicted in Figure 2.5 for a 2-manifold. Here the role of the restriction that maps have a Jacobi matrix with full rank is clear, as it means that the partial derivatives are linearly independent.

The tangential space is defined for every point of a manifold. A manifold then is an object with vector spaces glued to all positions. While the tangential spaces  $T_p M$  are well defined, the choice of a basis for  $T_p M$  is open. Maps  $\phi$  induce bases  $\frac{\partial \phi}{\partial u_i}$ , therefore a map can be used not only to parametrize the manifold but also the tangential spaces. But note that, just as it is sketched in Figure 2.5, these vectors are in general not orthogonal or normalized.

### 2.1.3. Orientations

The orientation of volumes and manifolds is, together with the border operator, the geometric property that plays the most important part in EC and DEC. But what is orientation? Orientation is to assign signs to volumes. A volume can be positive or negative. To decide which it is, you need a reference – you can only say how a volume is oriented relative to something.

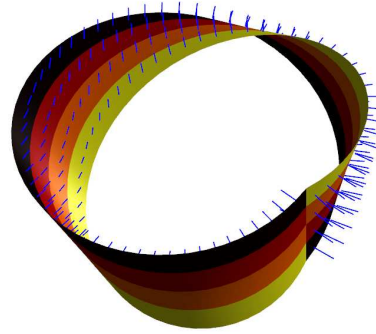


Figure 2.6.: The Moebius strip, the pathological example of a non-orientable manifold.

For a vector space you can encode orientation in the ordering of basis vectors. Two ordered bases  $v_1, \dots, v_k$  and  $w_1, \dots, w_k$  describe the same orientation if the matrix that describes the change of bases has a positive determinant. If a base is chosen, the determinant can also be used to measure the signed volume spanned by a set of vectors.

In the previous section we introduced tangential spaces and emphasized that every point gets its own proper tangential vector space. Tangential spaces of points that are close together are very similar and it makes sense to ask them to have the same orientation. A manifold is oriented by orienting its tangential spaces.

Local maps provide bases for tangential spaces. One single parametrization induces consistent orientations to the tangential spaces of all points it hits. Therefore we say that a manifold is oriented if all tangential spaces are oriented consistently:

**Definition (Oriented Manifold)** *A manifold is orientable if there exists a set of maps  $\mathcal{A} = \{\phi : U_\phi \rightarrow \phi(U_\phi) \subset M\}$  such that the maps describe the whole manifold and any two maps  $\phi, \psi$  which describe a common patch  $\psi(U_\psi) \cap \phi(U_\phi)$  result in the same orientations, i.e., the base change matrix  $C$  from the base formed by the columns of the Jacobian  $D\phi$  to the base formed by the columns of  $D\psi$  has a positive determinant,*

$$\det(C) > 0.$$

*A manifold is oriented if for all tangential spaces a consistent orientation has been chosen.*

For 2-manifolds in  $\mathbb{R}^3$ , orienting a surface is equivalent to consistently choosing a surface normal, as tried in Figure 2.6.

#### 2.1.4. The Border Operator

The border operator describes a special geometric operation for manifolds. We denote the border of a manifold  $M$  by  $\delta M$  and call  $\delta$  the border operator. From the way maps

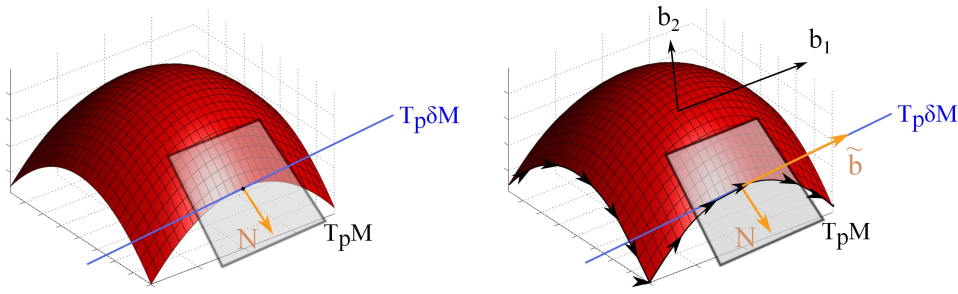


Figure 2.7.: On bordered manifold two tangential spaces  $T_pM$  and  $T_p\delta M$  are present at boundary points.  $N$  is the outward pointing border normal (left image). The base  $(b_1, b_2)$  is oriented according to the manifold. The induced border orientation is given by a vector  $\tilde{b}$  such that  $(N, \tilde{b})$  is oriented like  $b_1, b_2$ .

were defined at border points follows that the border of a manifold is again a manifold, and the dimension is decreased by one. Also, the border of a manifold always is a manifold without border, as can be seen with the interior of spheres or tori (see Figure 2.2). This border of a border of a manifold is empty,

$$\delta\delta M = \emptyset.$$

A central point is that an oriented manifold induces an orientation to its border, as sketched in Figure 2.7. Therefore we can define the border operator  $\delta$  such that it takes an oriented manifold and returns an oriented manifold with an induced orientation. What follows is a short technical description of how the induced orientation on the border is defined formally.

As the orientation of a manifold is defined by the orientation of its tangential spaces we need to take a closer look at the tangential spaces of bordered manifolds. At boundary points two tangential spaces are present. One is the tangential space of the manifold  $T_pM$  and is  $k$ -dimensional, the other one is the  $k - 1$  dimensional tangential space of the border manifold  $T_p\delta M$ , as depicted in Figure 2.7 (left). Inducing an orientation to the border means inducing an orientation to  $T_p\delta M$  using the orientation of  $T_pM$ . This happens by defining normals on the border.

For any border point one can define a border normal  $N$ . The border normal  $N$  is the vector in  $T_pM$  with:

- $N$  is orthogonal to  $T_p\delta M$
- $N$  has length 1
- $N$  points outside

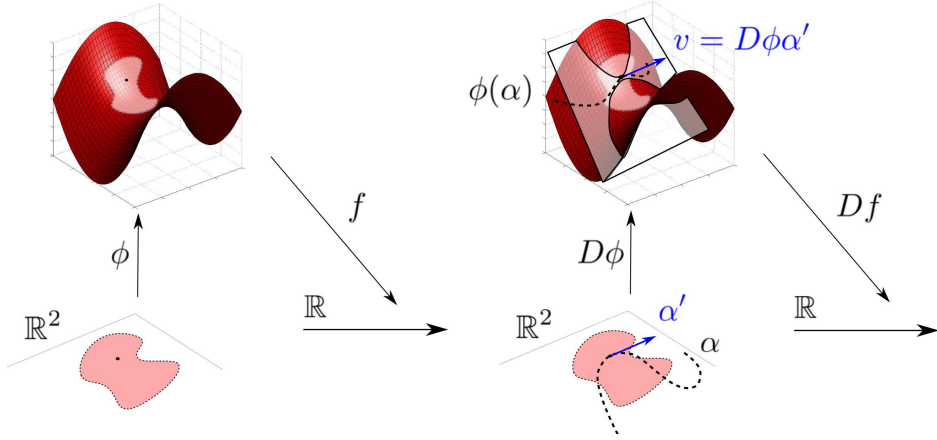


Figure 2.8.: Construction of the total derivative of a real valued function  $f$  defined on a manifold locally parametrized by  $\phi$ .  $Df$  at a point  $p$  is a linear mapping from the tangential space  $T_p M$  to  $\mathbb{R}$ .

Orientation is encoded in the enumeration of basis vectors. If  $b_1, \dots, b_k$  gives the orientation of  $T_p M$ , a basis  $\tilde{b}_1, \dots, \tilde{b}_{k-1}$  of the tangential space of the border  $T_p \delta M$  is oriented according to the manifold, if prepending the normal  $N$  to the basis leads to a basis  $(N, \tilde{b}_1, \dots, \tilde{b}_{k-1})$  that has the same orientation as  $b_1, \dots, b_k$ . This is illustrated in Figure 2.7.

### 2.1.5. Differential Calculus on Manifolds

So far we have seen tangential spaces, orientations and the border operator. The last property of smooth manifolds that needs to be covered is that manifolds allow differentiation to be done *on* them. In this section we explain how mappings  $f : M \rightarrow M'$  between two manifolds  $M$  and  $M'$  are differentiated *on* the manifolds. With this, manifolds become more than geometric objects; they become spaces where differential calculus is possible, just as it is on  $\mathbb{R}^n$ .

#### Total Derivative

Given a manifold  $M$  and a function  $f : M \rightarrow \mathbb{R}^n$ , what is the total derivative of  $f$ ? We want the derivative to be something very similar to the total derivative  $Dh$  of a function  $h : \mathbb{R}^k \rightarrow \mathbb{R}^n$ . In this case  $Dh$  is the linear mapping that locally approximates  $h$  and can be used to give the directional derivative for a direction  $v$ . For a fixed  $p$ , the Jacobian  $Dh(p)$  is a  $n \times k$  matrix; with  $t \in \mathbb{R}$  close to 0 and  $v \in \mathbb{R}^k$  we have

$$h(p + t v) \approx h(p) + Dh(p) \cdot t v.$$

We want the same for functions  $f$  on manifolds:  $Df$  should be a linear mapping that maps a direction to the vector that describes the change of  $f$  when going in that direction.

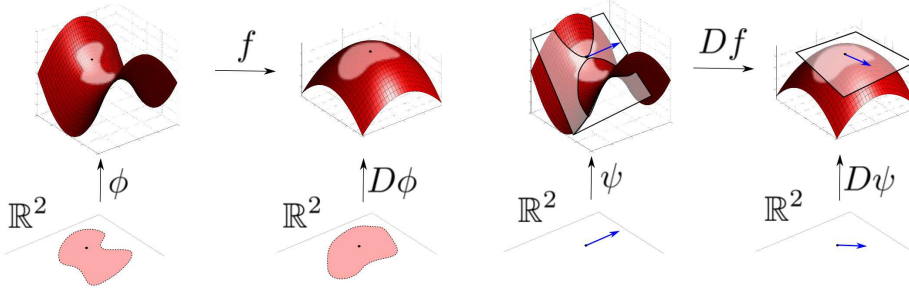


Figure 2.9.: Two 2-manifolds  $M$  and  $M'$  with local parametrizations  $\phi$  and  $\psi$  and a mapping  $f : M \rightarrow M'$ . The total derivative  $Df$  at a point  $p$  is a linear mapping from the tangential space  $T_p M$  to  $T_{f(p)} M'$ .  $D\phi$  and  $D\psi$  parametrize the tangential spaces and  $Df$  can be represented as a  $2 \times 2$  matrix.

But a direction on a manifold at some position is a tangential vector. Therefore, the differential  $Df$  is a mapping from the *tangential spaces* to vectors.

We can express the idea that  $Df \cdot v$  describes the change of  $f$  in the direction  $v$  readily by using a curve  $\alpha(t)$  with a tangent  $\frac{d\alpha(0)}{dt} = v$  in the wished direction  $v$ , as depicted in Figure 2.8 :

$$Df \cdot v := \frac{\partial}{\partial t} f(\alpha(t)) \quad (2.1)$$

As  $f(\alpha(t))$  is simply a function  $\mathbb{R} \rightarrow \mathbb{R}^n$  we know how to calculate the right hand side of Equation 2.1. We can also express the derivative in the local coordinates given by a parametrization  $\phi(u_1, \dots, u_k)$ .

As we have seen, a parametrization provides a base for the tangential space, namely

$$\frac{\partial \phi}{\partial u_1}, \dots, \frac{\partial \phi}{\partial u_k}.$$

We then express  $\alpha$ ,  $f$  and the tangential vector  $\alpha'$  in the map  $\phi$ :

$$\begin{aligned} \alpha(t) &= \phi(u_1(t), \dots, u_k(t)), \\ \alpha'(t) &= \frac{\partial \phi}{\partial u_1} u'_1 + \dots + \frac{\partial \phi}{\partial u_k} u'_k, \\ f(u_1, \dots, u_k) &= f(\phi(u_1, \dots, u_k)) \\ &= f_1(\phi(u_1, \dots, u_k)), \dots, f_n(\phi(u_1, \dots, u_k)). \end{aligned}$$

Then Equation 2.1 becomes

$$Df \cdot \alpha'(t) = \frac{\partial}{\partial t} f(u_1(t), \dots, u_k(t)) = \left( \frac{\partial f}{\partial u_1}, \dots, \frac{\partial f}{\partial u_k} \right) \cdot \begin{pmatrix} u'_1 \\ \vdots \\ u'_k \end{pmatrix}.$$

Therefore,  $Df$  in the local coordinates given by  $\phi$  is given by the  $n \times k$  matrix  $(\frac{\partial f}{\partial u_1}, \dots, \frac{\partial f}{\partial u_k})$  and if some tangential vector  $v$  is described in the same map  $v = v_1 \frac{\partial \phi}{\partial u_1} + \dots + v_k \frac{\partial \phi}{\partial u_k}$ :

$$Df \cdot v = \left( \frac{\partial f}{\partial u_1}, \dots, \frac{\partial f}{\partial u_k} \right) \cdot \begin{pmatrix} v_1 \\ \vdots \\ v_k \end{pmatrix}.$$

### Mappings between Manifolds

We can also consider the total derivative of mappings going from one manifold  $M$  to another manifold  $M'$ ,

$$f : M \rightarrow M',$$

as shown in Figure 2.9. We look again at Equation 2.1:

$$Df \cdot v := \frac{\partial}{\partial t} f(\alpha(t)).$$

Note that  $f(\alpha(t))$  is a curve on  $M'$  and  $\frac{\partial}{\partial t} f(\alpha(t))$  therefore is a tangential vector to this curve and lies in  $T_{f(\alpha(t))} M'$ . Then  $Df \cdot v$  has to be a vector in the tangential space of  $M'$ . This means that the derivative  $D_p f$  at some point  $p$  is a linear mapping from the tangential space  $T_p M$  to the tangential space  $T_{f(p)} M'$ , i.e.,

$$D_p f = T_p M \rightarrow T_{f(p)} M'.$$

If  $M$  is a  $k$ -manifold and  $M'$  a  $l$ -manifold,  $Df$  can be expressed as a  $l \times k$  matrix, described relatively to two sets of local coordinates  $\phi \rightarrow M$  and  $\psi \rightarrow M'$ .

#### 2.1.6. Summary

Manifolds are objects with geometric features, for example the orientation of volume and the definition of a border operator, but they also allow differential calculus on their surfaces. Tangential spaces play a crucial role by allowing local properties to be pointwisely defined on them and differentiation leads to linear mappings between tangential spaces.

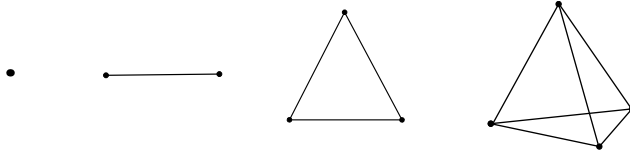


Figure 2.10.: A 0-simplex (point), 1-simplex (line), 2-simplex (triangle), and 3-simplex (tetrahedron).

## 2.2. Discrete Manifolds

In the last sections we had a look at the geometric objects exterior calculus will be defined on, i.e. smooth surfaces and manifolds. The next step is to introduce the discrete analogues we want to do computations with: triangle meshes, or more generally simplices and simplicial complexes. Simplices are for example points (0-dimensional), lines (1-dimensional) triangles (2-dimensional) and tetrahedra (3-dimensional). Simplicial complexes are ‘meshes’ made out of them. The definitions are taken from [DKT08] and [Fra11].

### 2.2.1. Simplices and Simplicial Complexes

A  $k$ -simplex is the most basic geometric object with a  $k$ -dimensional volume: the convex hull of  $k+1$  points, as depicted in Fig. 2.10. No point should lie in the convex hull of the others; else no  $k$ -dimensional volume is spanned and the simplex is called degenerated.

**Definition (Simplex)** *A non degenerated  $k$ -simplex is the convex hull of  $k+1$  points  $p_1, \dots, p_{k+1}$ , where the vectors  $p_2 - p_1, p_3 - p_1, \dots, p_{k+1} - p_1$  are linearly independent. It is represented as a tuple of its corner vertices  $\{p_1, \dots, p_{k+1}\}$ .*

Every simplex has faces of various dimensions: any combination of  $l+1$  of its corner vertices forms an  $l$ -dimensional face. For example a tetrahedron has 4 2-dimensional faces (triangles), 6 1-dimensional faces (edges) and 4 0-dimensional faces (vertices), see Figure 2.10. A 4-simplex would have 5 tetrahedral faces and so on.

Out of simplices one can build simplicial complexes, in the same way as meshes are built out of triangles. The restrictions are the usual: the interior of any two simplices should not overlap, and if the intersection of two simplices is not empty, the intersection has to be a face of both simplices. A simplicial complex then is a list of simplices, following these restrictions.

If a simplicial complex contains a  $k$ -simplex  $\sigma$ , we also demand that all faces of  $\sigma$  are part of the simplicial complex. This is not just a tedious technical detail; we explicitly want to associate different values to all faces of simplices. In a triangle mesh, for example, we will need to keep track not only of triangles and vertices but also of the edges.

**Definition (Simplicial Complex)** *A simplicial complex is a collection  $\kappa$  of simplices, such that if a simplex is contained in  $\kappa$ , all its faces are too. Furthermore the intersection*

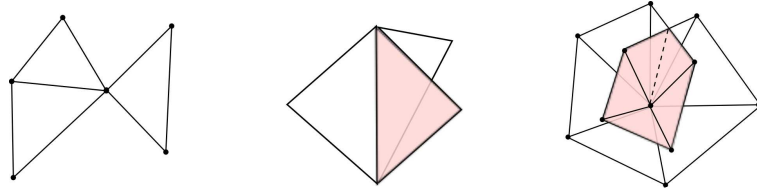


Figure 2.11.: These are not discrete 2-manifolds: the first mesh has a dangling triangle, the second mesh has a ‘wheel’ and is not locally equivalent to a plane, the same holds for the third mesh.

*of any two simplices in  $\kappa$  is either empty or a common face.*

Lastly we do not want our discrete manifolds to have the analogue of dangling triangles (Figures 2.11 and 2.13). To ensure this formally one has to make a restriction that is similar to the definition of manifolds. Just as we ensured that a  $k$ -manifold locally looks like  $\mathbb{R}^k$  or  $\mathbb{H}^k$ , we want to make sure our discrete manifold looks locally like either a  $k$ -dimensional ball or a  $k$ -dimensional half-ball, as depicted in Figure 2.12. This gets rid of dangling things.

**Definition (Discrete Manifold)** *A  $k$ -dimensional discrete Manifold is a simplicial complex where for every vertex in  $\kappa$  the union of all incident simplices is equivalent to a  $k$ -dimensional ball or a  $k$ -dimensional half ball.*

On discrete manifolds we can define orientations and a border operator with the same geometric meaning as on smooth manifolds.

### 2.2.2. Orientations

Orientations can be treated on discrete manifolds similarly as on continuous manifolds. Orientations are quite of practical importance and a notorious source of switched sign errors in the context of discrete exterior calculus.

We can assign one of two orientations to a simplex of any dimension, meaning that the volume represented by the simplex should be considered as positive or negative. While we coded orientation before in the enumeration of basis vectors, we encode the orientation of simplices in the enumeration of their corner vertices. For edges it is the most intuitive what this means: we assign a direction to the edge  $\{p_1, p_2\}$  by saying that the first vertex listed is the start vertex of the edge. Note that for an edge or any geometric object there is not a strict ‘positive’ or a ‘negative’ orientation; we can only say how something is oriented relative to something else. For example the edge  $\{p_1, p_2\}$  is oriented negatively to the edge  $\{p_2, p_1\}$ ; this is noted as

$$-\{p_1, p_2\} = \{p_2, p_1\}.$$

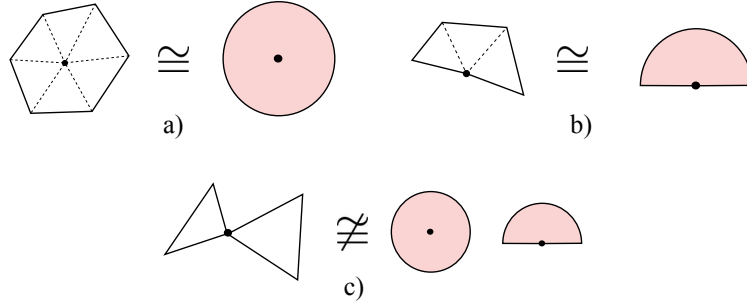


Figure 2.12.: Discrete manifolds are asked to be locally ‘equivalent’ to balls or half-balls.

This is meant in the sense of homeomorphism: there should exist a homeomorphism, a continuous bijective mapping, between 1-neighborhoods and either balls or half-balls. In (a) the 1-neighborhood of the marked vertex is homeomorph to a 2D ball, i.e. a disk, in (b) the 1-neighborhood is homeomorph to a half-ball, and in (c) there exists no homeomorphism to either a half-disk or a disk.

So the orientation of a  $k$ -simplex depends on the way its corner vertices are enumerated. Two enumerations of corner vertices result in the same orientation if they are related by an even permutation. A permutation is called even, if it can be reproduced by switching pairs of vertices an even number of times. E.g.

$$\{a, b, c, d\} = \{c, a, b, d\}$$

$$\{a, b, c, d\} \rightarrow \{c, b, a, d\} \rightarrow \{c, a, b, d\},$$

where we get from the first tuple to the second by swapping  $a$  and  $c$  and then  $a$  and  $b$ , i.e. with two swaps. Alternatively, determinants can be used to determine the sign of a permutation; just calculate the determinant of the permutation matrix

$$\{a, b, c, d\} \rightarrow \{c, a, b, d\},$$

$$\begin{pmatrix} c \\ a \\ b \\ d \end{pmatrix} = \begin{pmatrix} 0 & 0 & 1 & 0 \\ 1 & 0 & 0 & 0 \\ 0 & 1 & 0 & 0 \\ 0 & 0 & 0 & 1 \end{pmatrix} \begin{pmatrix} a \\ b \\ c \\ d \end{pmatrix}.$$

Or again you can use the simplex to induce a base to the affine vector space it is aligned to

$$p_1 - p_2, \dots, p_k - p_{k+1},$$

and two vertex enumerations induce the same orientation if the induced bases have the same orientation. This also shows that defining the orientation of a simplex by looking at the ordering of its corner vertices amounts to the same as orienting volumes by choosing bases.

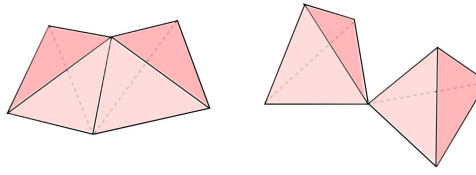


Figure 2.13.: If tetrahedra are not connected by two dimensional faces, they are ‘dangling’.

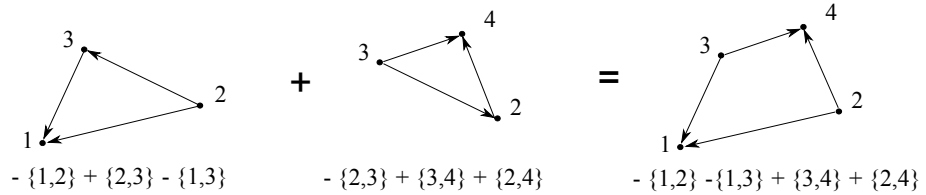


Figure 2.14.: Two sets of edges expressed as formal sums that get summed up.

One exception are vertices or 0-simplices  $\{v_0\}$ , where orientation is not encodable in the enumeration of the vertex. We need to assign orientations to single points too and say that  $-\{v_0\}$  is the negatively oriented version of  $\{v_0\}$ . Orientation is ‘imprinted’ on the point. The best way of thinking of orientation is that orientation adds a sign to volumes. A negatively oriented point is then a point whose 0-dimensional volume is negative. The 0-dimensional volume of any single point is defined to be either 1 or  $-1$  and the 0 dimensional volume of a point set is  $\#positive\ points - \#negative\ points$ .

As long as you stick with calculations in  $\mathbb{R}^3$  it stays pretty simple to determine if two orientations of a simplex are the same, if you stick with triangle meshes it is trivial. Just make sure you always remember to respect orientations. In Section 2.3.2 we will also come back to the question of how to compute relative orientations in practice.

### 2.2.3. Formal Sums, k-Chains and Vectors

Single oriented  $k$ -simplices are represented as ordered tuples of vertices, optionally with a sign to denote switched orientation. A set of  $k$ -simplices can then be described by a *formal sum*, and is also called a *simplicial  $k$ -chain*. For example the set of the three edges  $\{v_0, v_1\}$ ,  $\{v_1, v_2\}$  and  $\{v_2, v_0\}$  written as a formal sum is

$$\{v_0, v_1\} + \{v_1, v_2\} + \{v_2, v_0\}.$$

Additionally, a simplicial  $k$ -chain is allowed to have multiple ‘copies’ or negatively oriented copies of some simplex. This is taken account of by associating integer values from  $\mathbb{Z}$  to the simplices, for example

$$3\{v_0, v_1\} - 2\{v_1, v_2\} + \{v_2, v_0\}$$

Vertices	Edges	Faces
[0] $v_0$	[0] $e_0 = \{v_0, v_2\}$	[0] $f_0 = \{v_0, v_2, v_1\}$
[1] $v_1$	[1] $e_1 = \{v_0, v_1\}$	[1] $f_1 = \{v_2, v_3, v_1\}$
[2] $v_2$	[2] $e_2 = \{v_2, v_1\}$	
[3] $v_3$	[3] $e_3 = \{v_3, v_1\}$	
	[4] $e_4 = \{v_3, v_2\}$	

Figure 2.15.: A simple simplicial complex with a fixed enumeration of the occurring simplices; for each simplex a reference orientation has been chosen.

would have three copies of  $\{v_0, v_1\}$  and so on. The negative integers denote a change of orientation as described in the last section; the formal sum could be rewritten without the use of negative integers as

$$3\{v_0, v_1\} + 2\{v_2, v_1\} + \{v_2, v_0\}.$$

Two  $k$ -Chains can be combined by summing them up,

$$\begin{aligned} c &= \sum_{i=1}^N c_i \sigma_i, & d &= \sum_{i=1}^N d_i \sigma_i, \\ c + d &= \sum_{i=1}^N (c_i + d_i) \sigma_i, \end{aligned}$$

where the  $c_i$  and  $d_i$  are integers from  $\mathbb{Z}$  and the  $\sigma_i$  are  $k$ -simplices. This reflects that if in the set  $c$  there are  $c_i$  copies of  $\sigma_i$  and in  $d$  there are  $d_i$  copies, then in the combined set  $c + d$  there have to be  $c_i + d_i$  copies of  $\sigma_i$ . In particular, oppositely oriented simplices cancel out, see also Figure 2.14.

Formal sums are one way to describe sets of oriented  $k$ -simplices. Equivalently the  $k$ -chains can be written as a vector of integers if a global enumeration of all  $k$ -simplices has been chosen and one reference orientation has been assigned to every simplex. For example consider the enumeration of vertices, edges and faces in Figure 2.15. Note that every kind of simplices is enumerated separately. With this fixed enumeration a set of vertices can be described as vector in  $\mathbb{Z}^4$ , a set of edges as a vector in  $\mathbb{Z}^5$  and a set of faces as a vector in  $\mathbb{Z}^2$ . Generally a set of  $k$ -simplices can then be identified with an integer vector with the dimension of the number of occurring  $k$ -simplices, i.e. a vector from  $\mathbb{Z}^{\#k\text{-simplices}}$ . The  $i$ th value in such a vector then denotes the number of occurrences of the  $i$ th simplex. For example, using the enumeration of Figure 2.15, the formal sum  $e_0 - e_1 + 2e_2$  would be described by the vector  $(1, -1, 2, 0, 0)$ .

For computations the vector notation for  $k$ -chains is the most useful; but in order to use it a global enumeration and fixed reference orientations of the simplices need to be chosen first.

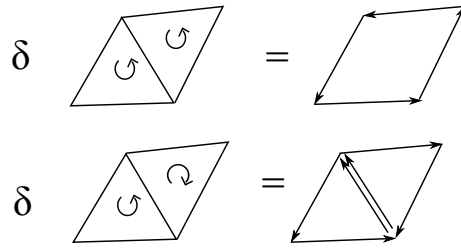


Figure 2.16.: The border operator that respects orientation only makes sense with oriented discrete manifolds. Orientation of faces is depicted by an arrow that says what orientation a simplex induces to its border.

#### 2.2.4. The Border Operator

Discrete manifolds or any set of simplices allow the definition of a border operator similar to the border operator defined on continuous manifolds. And just on continuous manifolds, an oriented discrete manifold induces an orientation to its border.

The border of a single  $k$ -simplex is the following formal sum

$$\delta\{v_0, v_1, \dots, v_k\} = \sum_{j=0}^k (-1)^j \{v_0, \dots, \hat{v_j}, \dots, v_k\},$$

where the  $\hat{v_j}$  means omitting  $v_j$ . This expresses that the border of the simplex is a set of  $k - 1$  simplices. The orientations they get are the ones that the simplex induces. Note that prepending the omitted vertex  $v_j$  to  $(-1)^j \{v_0, \dots, \hat{v_j}, \dots, v_k\}$  leads to a simplex with the orientation of  $\{v_0, v_1, \dots, v_k\}$ . This is consistent with the way we defined that orientation should be induced to borders of smooth manifolds.

For example the border of a triangle  $\{a, b, c\}$  is

$$\{b, c\} - \{a, c\} + \{a, b\} = \{a, b\} + \{b, c\} + \{c, a\},$$

just as it should be.

But if we can take the border of single simplices, we can also take the border of a set of simplices or of discrete manifolds; it is simply the formal sum of the borders of the  $k$ -simplices the discrete  $k$ -manifold is made out of. Formally, the border operator maps simplicial  $k$ -chains to simplicial  $k - 1$ -chains and is a linear mapping; if  $c$  and  $\tilde{c}$  are two  $k$ -chains, the border operator fulfills

$$\delta(c + \tilde{c}) = \delta c + \delta \tilde{c}.$$

Another point is that, as you see in the Figure 2.16, the border operator gives a ‘wrong’ result when a discrete manifold is oriented inconsistently.

### The Border Operator as a Matrix

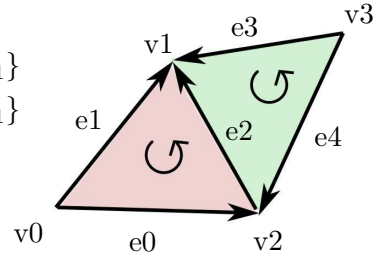
Instead of representing the border operator as a formal sum we can write it as a matrix, provided that an enumeration and reference orientation of the simplices has been chosen. The sets of  $k$ -simplices are described by integer vectors as introduced in Section 2.2.3. The border operator  $\delta_k$  for  $k$ -simplices is a linear mapping from the simplicial  $k$ -chains to the simplicial  $k - 1$ -chains and therefore is a linear mapping

$$\delta_k : \mathbb{Z}^{\#k\text{-simplices}} \rightarrow \mathbb{Z}^{\#k-1\text{-simplices}}.$$

Note that we explicitly make a distinction between the border operators for simplices of different dimensions and annotate the border operators with a subscript  $k$  that describes the dimensionality of the simplices the border operator can be applied to.

These border operator matrices form the backbone of DEC and they will be used excessively throughout this thesis. Also it is very important to understand that they describe a purely geometric operation, namely the operation of going from a  $k$ -dimensional set of simplices to a  $k - 1$ -dimensional set describing the boundary. The border operator matrices are relatively easy to compute and store the relative orientations of  $k$ -simplices and  $k - 1$ -simplices. Consider the following toy-example: we look at the simplicial complex with fixed simplex enumerations and reference orientations from Figure 2.15, which is inlined here once more for convenience.

Vertices	Edges	Faces	
[0] $v_0$	[0] $e_0 = \{v_0, v_2\}$	[0] $f_0 = \{v_0, v_2, v_1\}$	
[1] $v_1$	[1] $e_1 = \{v_0, v_1\}$	[1] $f_1 = \{v_2, v_3, v_1\}$	
[2] $v_2$	[2] $e_2 = \{v_2, v_1\}$		
[3] $v_3$	[3] $e_3 = \{v_3, v_1\}$		
[4] $e_4 = \{v_3, v_2\}$			



Here we have two 2-simplices (triangles), five 1-simplices (edges) and four 0-simplices (vertices). There are two border operator matrices: one to compute boundaries of 2-dimensional sets and one to compute the boundary of 1-dimensional sets. The first one,  $\delta_2$ , maps 2-chains to 1-chains and therefore has to be a linear mapping from  $\mathbb{Z}^2$  to  $\mathbb{Z}^5$ , i.e. a  $5 \times 2$  matrix.

The first row of  $\delta_2$  describes the result of applying the border operator to the first face  $f_0$ , i.e.  $\delta_2 \cdot (1, 0)^T$ . The boundary of the face  $f_0$  is the formal sum  $e_0 + e_2 - e_1$ , which is described by the integer vector  $(1, -1, 1, 0, 0)^T$ . The second row  $\delta_2 \cdot (0, 1)^T$  of  $\delta_2$  describes the boundary of  $f_1$  and is given by the formal sum  $-e_2 - e_4 + e_3$ , i.e.  $(0, 0, -1, 1, -1)^T$ . Therefore the complete matrix is given by

$$\delta_2 = \begin{pmatrix} 1 & -1 & 1 & 0 & 0 \\ 0 & 0 & -1 & 1 & -1 \end{pmatrix}^T.$$

The other border operator matrix,  $\delta_1$ , is a linear mapping from simplicial 1-chains to 0-chains and therefore is a  $4 \times 5$  matrix. Here the  $i$ th matrix row describes the border

of the  $i$ th edge  $e_i$ ; for example the border of the edge  $e_0$  is the formal sum  $v_2 - v_0$  and therefore the first row of  $\delta_1$  has to be  $(-1, 0, 1, 0)^T$ . The complete matrix is given by

$$\delta_1 = \begin{pmatrix} -1 & -1 & 0 & 0 & 0 \\ 0 & 1 & 1 & 1 & 0 \\ 1 & 0 & -1 & 0 & 1 \\ 0 & 0 & 0 & -1 & -1 \end{pmatrix}.$$

Of course, the border matrices can be applied to more complex chains. For example the border of the line segment  $e_0 - e_4 + e_3$  or would be given by

$$\begin{pmatrix} -1 \\ 1 \\ 0 \\ 0 \end{pmatrix} = \delta_1 \begin{pmatrix} 1 \\ 0 \\ 0 \\ 1 \\ -1 \end{pmatrix},$$

which is  $-v_0 + v_1$ , saying that  $v_0$  is the ‘start’ and  $v_1$  the ‘end’ border of the line.

Generally, for a  $k$ -complex there is a total of  $k$  border matrices: the border operator  $\delta_1$  for sets of 1-simplices (edges), the operator  $\delta_2$  for 2-simplices (triangle faces),  $\delta_3$  for 3-simplices and so on. The entry  $(i, j)$  in a border matrix is the relative orientation of the two simplices concerned. In the example above  $\delta_1(0, 1) = -1$  because the vertex  $v_0$  is oriented negatively relative to the edge  $e_1$ , considering the border induced orientation.

### 2.2.5. Oriented Discrete Manifold

Lastly we can not only orient single simplices, but also a whole discrete manifold. This leads to oriented discrete manifolds, which are the discrete analogue to smooth oriented manifolds.

The orientation of a volume is strongly linked to the orientation of borders. For convenience we will define well orientedness of a discrete manifold using the border orientations. Two  $k$ -simplices that share a  $k-1$  dimensional face are oriented consistently exactly if the induced orientation of this face is opposed for both  $k$ -simplices, as depicted in Figure 2.16. A  $k$ -manifold is oriented if all- $k$  simplices are oriented consistently.

### 2.2.6. Summary

Discrete manifolds are geometric objects made out of simplices and allow the definition of orientation and border operators, just like smooth manifolds. Also, applying the discrete border operator twice to an oriented discrete manifold leads to an empty set:

$$\delta_{j-1}\delta_j = 0.$$

This mirrors the property of the smooth border operator. The smooth and the discrete border operator are depicted schematically in Figure 2.17.

Subsets of  $j$ -simplices of a discrete  $k$ -manifold can simply be represented by vectors and the border operators by matrices. Up to now only the geometry of smooth manifolds

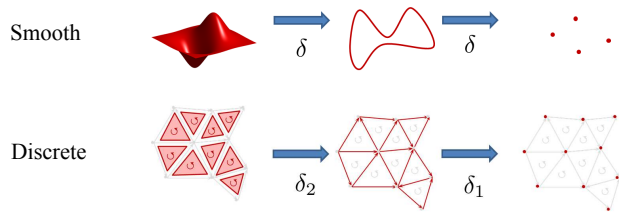


Figure 2.17.: Applying the smooth border operator to a  $k$ -manifold returns a  $k - 1$ -manifold, the same holds in the discrete setting. Also for *oriented* smooth and discrete manifolds  $\delta\delta = 0$  holds.

has been discretized; to develop an analogue to differential calculus on manifolds we will first need to introduce differential forms.

## 2.3. Implementation Notes

This chapter provides a guideline of what needs to be implemented to get DEC and the later applications up and running. The components needed are described and some of the more tricky details are mentioned.

### 2.3.1. A Word on Sparse Matrices

The point of DEC is to reformulate differential equations using sparse matrices. Therefore any implementation of DEC is somewhat centered around sparse matrices.

If you plan to implement your DEC framework you should start by looking for a sparse matrix solver. For all results in this thesis the sparse solver from the Pardiso-Project of the University of Basel has been used as a black box solver [SG04]. Unfortunately it is not freeware but any other sparse solver will do as well.

The Pardiso solver uses the so-called Yale format. The Yale format uses 3 vectors to describe an arbitrary  $n \times m$  matrix  $A$ . The first vector  $a$  stores all non-zero values of  $A$ , enumerated by row. The second vector  $ja$  stores the column indices of the non-zero values, again enumerated by row. The third vector  $ia$  stores for every row the index  $ind$ , such that  $a(ind)$  and  $ja(ind)$  are the value and the column of the first element in the row. Additionally one appends the length of the vector  $a$  to  $ia$ .

For example

$$\begin{pmatrix} 1 & 0 & 0 & 3 \\ 0 & 0 & 0 & 2 \\ 0 & 4 & 2 & 0 \end{pmatrix} \Rightarrow \begin{cases} a = [1, 3, 2, 4, 2] \\ ja = [0, 3, 3, 1, 2] \\ ia = [0, 2, 3, 5] \end{cases}$$

Iterating over the values and indices of the  $k$ th row then amounts to

```
for i = ia(k):ia(k+1) do
    out ← (k, ja(i)) //the index pair
    out ← a(i) //of this value
end for
```

### 2.3.2. Implementing Simplicial 2-Complexes

The applications in this thesis focus on 2-complexes, i.e., classical triangle meshes. You might not need any more general implementation. General  $k$ -complexes are treated separately in the next section.

For DEC we need the complete geometric information of meshes; we have to explicitly keep lists of vertices, edges and faces, the full information about their incidence and border relations, as well as their assigned orientations.

For 2D meshes a winged edge structure is a convenient choice of representation. In a winged edge structure you have the following three objects: vertices, edges and faces, as described in Figure 2.18. Edges are stored once, with an arbitrary chosen orientation. With this information present it is easy to do things like iterating over the incident edges or faces of a vertex or iterate over the edges of a border component following the orientation of the mesh.

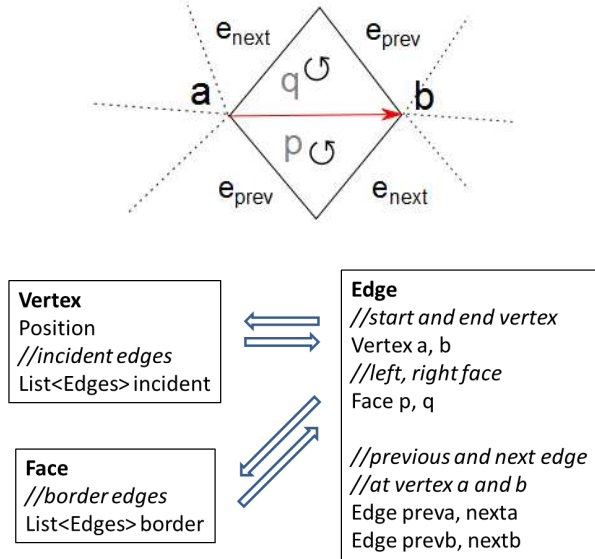


Figure 2.18.: The information stored on a winged edge structure.

Note that, even though the incidence information is stored in a winged mesh structure, for DEC applications the discrete border operator matrices  $\delta_1$  and  $\delta_2$  still need to be computed.

### 2.3.3. Implementing Simplicial k-Complexes

Chances are you do not need simplicial complexes of higher dimensions other than tetrahedral meshes embedded in  $\mathbb{R}^3$ . But one straight forward and for DEC suitable way to implement arbitrary  $k$ -complexes is to store lists of simplices and represent the incidence information explicitly with the sparse border matrices. The border operator matrices play a central role in DEC and need to be set up anyway.

Figure 2.19 depicts a possible implementation of  $k$ -complexes. A  $k$ -complex consists of  $k + 1$  simplex lists and of the border matrices  $\delta_1, \dots, \delta_k$ . The vertices ( $0$ -Simplices) store their positions. A  $j$ -simplex is represented by a  $j$ -tuple of vertex indices, these are the indices of the vertices in the list kept in the  $k$ -complex data structure. The index tuples describing the simplices are sorted, i.e.,

$$(i_1, i_2, \dots, i_j) : i_1 < i_2 < \dots < i_j.$$

Sorted tuples facilitate the computation of the relative orientation of a  $j - 1$  simplex  $(v_0, \dots, \hat{v}_l, \dots, v_j)$  lying on the border of a  $j$  simplex  $(v_0, \dots, \hat{v}_l, \dots, v_j)$ . By the definition of the border operator from Section 2.2.4 their relative orientation simply is:

$$\text{relativeOrientation} = (-1)^l$$

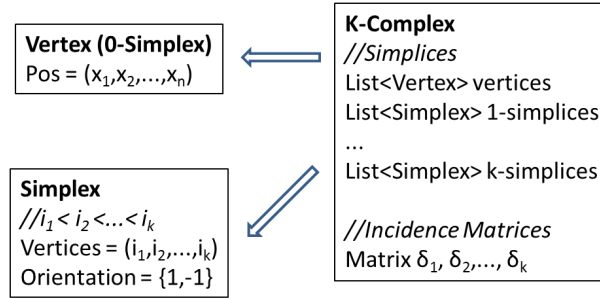


Figure 2.19.: Implementation of a  $k$ -complex that uses tuple of ordered indices to characterize a simplex.

The orientation of most simplices of an oriented simplicial  $k$ -complex can be chosen arbitrarily and we choose the orientation that is defined by the sorted index tuples. Only the  $k$ -simplices of an oriented  $k$ -complex have to be oriented consistently. Therefore, they get an additional ‘orientation’ variable in which is stored if the orientation induced by the ordered tuple is positive or negative relative to the orientation of the  $k$ -complex.

### Setting Up a k-Complex

Setting up the border operator matrices  $\delta_j$  for complexes of arbitrary dimensions can be a fuzz, as you need to excessively compute relative orientations of simplices. Supposing that you have a wireframe model of the  $k$ -complex, i.e., a list of vertex positions and a list of  $k$ -simplices, the full  $k$ -complex with all incidence matrices can be set up in the following way:

1. Reorder the index tuples of the  $k$ -simplices and adapt the orientation accordingly
2. Generate all the  $j$ -simplex lists
3. Set up the matrices  $\delta_j$

#### Reordering tuples:

When reordering the tuples in the first step, you need to keep track of how the orientation changes. This can be done using a so called *inversion table*. Lets say the tuple  $(i_1, \dots, i_n)$  is a permutation of the tuple  $(1, 2, \dots, n)$ . An inversion is an index pair  $(i_l, i_k)$ , where  $l < k$  but  $i_l > i_k$ , i.e., the order of  $i_l, i_k$  is inverted. The relative orientation of the simplex  $\{i_1, \dots, i_n\}$  and the ordered simplex  $\{1, 2, \dots, n\}$  is  $(-1)^{\#inversions}$  where  $\#inversions$  is the total number of inversions.

In the inversion table you count for every index in the tuple the number of elements

```

for ind1 = (0:#j-simplices) do
    //get the ind1th j-simplex:
    {i0, ..., ij}  $\leftarrow$  j-simplex[ind1]
    //Iterate of the bordering j-1 simplices
    for l=(0:j) do
        //Find the index of the lth bordering j-1 simplex
        ind2  $\leftarrow$  index({i0, ..., il, ..., ij})
        //Store the relative orientation of the border simplex
        //and the simplex in  $\delta_j$ 
         $\delta_j$ (ind1,ind2)  $\leftarrow$  (-1)l
    end for
end for

```

Figure 2.20.: An algorithm to set up the border operator matrix  $\delta_j$ .

on its left that are greater. Example:

permuted tuple	3, 2, 5, 4, 1
inversions	0, 1, 0, 1, 4

The first line represents the permuted indices the lower the number of inversions of every index. The total number of inversion is  $1+1+4=6$  and the relative orientation of  $\{3, 2, 5, 4, 1\}$  to  $\{1, 2, 3, 4, 5\}$  is  $(-1)^6 = 1$ .

#### Setting up incidence matrices:

After the steps 1 and 2, all simplices in the simplicial complex have a fixed orientation and a fixed position *ind* in the simplex lists. Setting up the border matrix  $\delta_j$  is then described in the listing in Figure 2.20

#### 2.3.4. Simple Example Applications

Using the border matrices you can easily check if a mesh is well oriented or compute the border components of a mesh.

#### Orientation Test

That a *k*-complex is oriented can be checked by looking at  $\delta_k$ . The condition we gave in Section 2.2.5 for a *k*-complex to be oriented was the following: any  $k - 1$  simplex is either a border simplex, therefore being part of exactly one *k*-simplex, or it is part of two *k*-simplices, having once positive and once negative orientation.

This is exactly the case if any column of  $\delta_k$  has either exactly one entry, which is the case for boundary simplices, or two entries: a one and a minus one.

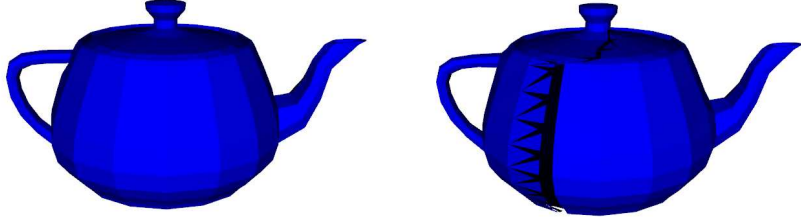


Figure 2.21.: A teapot mesh that on the first look seems to be a discrete borderless 2-manifold but turns out to be a mesh with border and dangling triangles, which makes it a non-manifold mesh and therefore not suited for some DEC applications. The deformed teapot on the right was generated using the area minimizing flow mentioned in the introduction, Section 1.3

### **Check if a 2-Complex is a Discrete Manifold**

DEC applications might fail if a complex is not a discrete manifold. Two dimensional meshes used for displaying purposes are often not discrete manifold. To avoid singular matrices and to eliminate the possibility that bugs occur due to the ill-formedness of a mesh it is good to test a mesh for manifoldness before using it. The mesh in Figure 2.21 is an example of a non-manifold mesh that leads to unexpected results.

In a winged edge mesh, finding dangling faces is fairly simple; at every vertex iterate over all edges and make sure that either exactly 2 or no edges have only one neighbor face.

### **Finding Borders**

Given an oriented discrete  $k$ -manifold we want to find the  $(k - 1)$ -complex that represents its border. This can be easily done by applying the border Operator  $\delta_k$  to the  $(1, 1, 1, 1, 1\dots)$  vector, which represents the whole manifold. The resulting vector then exactly represents the formal sum of  $k - 1$  simplices that describes the border manifold. If multiple borders are present the connected components of this border have to be computed in a separate step.

### 3. Differential Forms

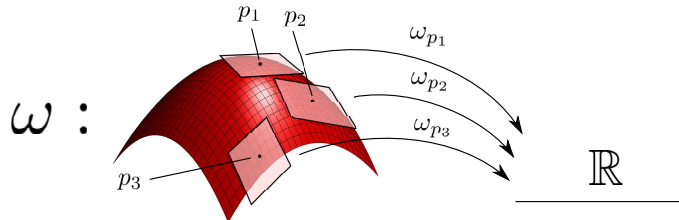


Figure 3.1.: Here a differential form  $\omega$  is represented. A single differential form provides linear mappings  $\omega_p$  at all points  $p$  on a manifold; the mappings  $\omega_p$  map the tangential spaces  $T_p M$  to  $\mathbb{R}$ .

As seen in the last chapter, you can do differential calculus on smooth manifolds. To be able to define discrete calculus on discrete manifolds we first need a geometric understanding of calculus. We get to this understanding by generalizing functions to ‘objects’ that can be integrated over subsets of manifolds. These objects are *differential forms*; one is schematically depicted in Figure 3.1. In a next step we will then define an exterior derivative  $d$  for differential forms, whose geometry is easier to understand and can be used to define a discrete exterior derivative on discrete manifolds. The point why we are interested in differential forms and the exterior derivative  $d$  is that  $d$  unifies many differential operators, like divergence, gradient and curl.

The basic theory for differential forms is split in two chapters. This chapter motivates differential forms, captures them more formally, covers integration of differential forms and relates them to standard calculus objects like real valued functions and vector fields. It ends with the introduction of discrete differential forms.

In the next chapter, Chapter 4, we will then introduce the most important elements of exterior calculus and discrete exterior calculus, like the exterior derivative  $d$ , the operators  $\partial$  and  $\star$  and Stokes theorem, which describes the geometry of the exterior derivative.

#### 3.1. Smooth Differential Forms

We start introducing differential forms by motivating them as objects that fulfill all requirements to be useful under an integral in Section 3.1.1. In Section 3.1.2 we describe the local structure of differential forms. At any point a differential form  $\omega$  provides a *form*

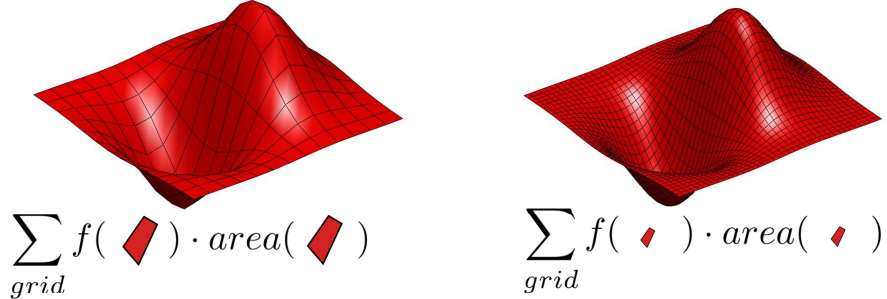


Figure 3.2.: To calculate the Riemann integral over a surface we select a grid and refine it. In the sums  $f$  is evaluated at arbitrary positions in the patches.

$\omega_p$ , a multilinear, antisymmetric mapping. These multilinear mappings form a vector space of a finite dimension. Using the so called wedge product  $\wedge$ , we describe simple bases for them in Section 3.1.3. Having understood the local structure of differential forms we give a clean definition of them in Section 3.1.4 and finally use everything to relate the differential forms to the more intuitive well known objects from standard calculus in Section 3.1.5.

### 3.1.1. The Perfect Thing to Integrate

Differential forms arise very naturally when considering integrals. Suppose that we have a two dimensional surface  $M$  and a function  $f$  defined on the surface. We want to integrate  $f$  over  $M$  i.e. calculate the Riemann integral

$$\int_M f dA.$$

To compute the integral by brute force we can use Riemann sums as depicted in Figure 3.2: we choose a grid, sum up the areas of the parallelograms  $s$  weighted by the function value  $f(s)$ , and take the limit under grid refinement:

$$\lim_{diam(s \in grid) \rightarrow 0} \sum_{s \in grid} f(s) \cdot area(s).$$

We take a step back and consider what is essential for an ‘object’ to be integrated in this way. Basically we can integrate anything that assigns values to areas  $s$ . Say  $\omega_p$  assigns the value  $\omega_p(s)$  to an area  $s$  located at some point  $p$ , then its integral can be computed as:

$$\int_M \omega = \lim_{diam(s \in grid) \rightarrow 0} \sum_{s \in grid} \omega_{p \in s}(s).$$

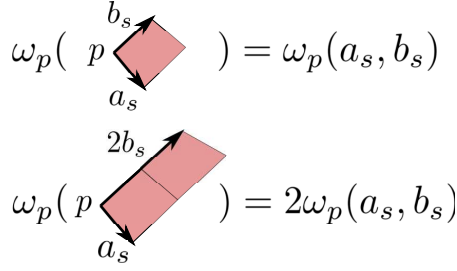


Figure 3.3.: Locally at some point  $p$ , a differential form ‘measures’ volumes and therefore has to be proportional to the volume measured. If the volumes are described by the vectors that span the volume, here  $a_s$  and  $b_s$ , this means that  $\omega$  should be linear in both  $a_s$  and  $b_s$ .

Obviously  $\omega_p$  has to follow some rules to be useful for integration. For one it should scale with the area of  $s$ . Assume a grid segment  $s$  is spanned by two vectors  $a_s, b_s$ , then we can write  $\omega_p(s)$  as  $\omega_p(a_s, b_s)$ , see Figure 3.3. For  $\omega_p$  to be proportional to the area of  $s$  we need it to be linear in both  $a_s$  and  $b_s$ ,

$$\begin{aligned}\omega_p(\lambda a_s, b_s) &= \lambda \omega_p(a_s, b_s), \\ \omega_p(a_s, \lambda b_s) &= \lambda \omega_p(a_s, b_s).\end{aligned}$$

Furthermore,  $\omega$  should behave well when the parameters are swapped, as the vector pairs  $(a_s, b_s)$  and  $(b_s, a_s)$  span the same area, but for orientation. There are two possibilities that make sense: we can choose  $\omega$  to be symmetric or to be antisymmetric:

$$\begin{aligned}\omega(a_s, b_s) &= \omega(b_s, a_s), \\ \omega(a_s, b_s) &= -\omega(b_s, a_s).\end{aligned}$$

Symmetry would mean that  $\omega$  only depends on the absolute area of  $s$ . Antisymmetry means that  $\omega$  respects the orientation of  $s$ . We choose antisymmetry,  $\omega$  then is a *differential form*. The first variant would lead to so called *pseudo forms*.

Lastly we have to clarify what  $a_s$  and  $b_s$  are. The vectors  $a_s$  and  $b_s$  are bound to some position  $p$ . Also, if you look at the grid in Figure 3.2, you see that the grid elements nearly lie in the tangential spaces of the surface  $M$ . At least they do so in the limit. This gets us to the full definition of a differential form on a two dimensional surface: a differential form  $\omega$  provides at any point  $p$  on the surface  $M$  a mapping  $\omega_p$  that takes two vectors from the tangential space  $T_p M$ , is linear in both arguments and antisymmetric. I.e., for all points  $p \in M$  the following holds:

$$\omega_p : T_p M \times T_p M \rightarrow \mathbb{R}$$

$$\begin{aligned}\omega_p(\lambda a, b) &= \lambda \omega_p(a, b) = \omega_p(a, \lambda b) && \text{bilinearity} \\ \omega_p(a, b) &= -\omega_p(b, a) && \text{antisymmetry}\end{aligned}$$

A differential form  $\omega$  should also change smoothly between neighboring  $p$ s.

### 3.1.2. Forms

We motivated that differential forms have a position  $p$  and some number of tangential vectors from  $T_p M$  as input variables. And for a fixed  $p$  the differential form should be multilinear and antisymmetric. Before we give a full definition of differential forms, we have a look at how they behave at single points. A multilinear antisymmetric mapping is called a form (without the word ‘differential’). Forms form a finite dimensional vector space and allow the definition of a wedge product. This is important for us because this will let us describe differential forms with greater ease and let us relate differential forms to standard calculus objects.

#### Defining k-Forms

A  $k$ -form on  $\mathbb{R}^l$  is a multilinear antisymmetric mapping  $\mathbb{R}^l \times \dots \times \mathbb{R}^l \rightarrow \mathbb{R}$  which depends on  $k$  vectors from  $\mathbb{R}^l$ :

**Definition ( $k$ -form)** *A  $k$ -form (not a differential  $k$ -form, mind you) on a  $l$  dimensional space  $\mathbb{R}^l$  is a mapping  $\omega : \mathbb{R}^l \times \mathbb{R}^l \times \dots \times \mathbb{R}^l \rightarrow \mathbb{R}$  with the following properties:*

1.  $\omega(x_1, \dots, x_k)$  is linear in all  $k$  parameters, meaning that

$$\omega(x_1, \dots, \lambda a + b, \dots, x_k) = \lambda \omega(x_1, \dots, a, \dots, x_k) + \omega(x_1, \dots, b, \dots, x_k).$$

2.  $\omega(x_1, \dots, x_k)$  is skew symmetric or antisymmetric, meaning that switching any two variables leads to a change of sign:

$$\omega(x_1, \dots, x_i, \dots, x_j, \dots, x_k) = -\omega(x_1, \dots, x_j, \dots, x_i, \dots, x_k).$$

3. In particular:

$$\omega(x_1, \dots, x_k) = 0 \text{ if } x_1, \dots, x_k \text{ are linearly dependent.}$$

To denote that a form  $\omega$  is a  $k$ -form we will sometimes add a superscript  $k$  and denote the form by  $\omega^k$ .

The first property makes sure that  $\omega$  is proportional to the volume spanned by the input vectors, while the second ensures that  $\omega$  respects the orientation of the input. The third property follows from the first two.<sup>1</sup> The space of all  $k$ -Forms on  $\mathbb{R}^l$  is denoted by  $\Lambda^k(\mathbb{R}^l)$  and is a vector space: if  $\omega$  and  $\nu$  are  $k$  forms so are  $\omega + \nu$  and any multiples  $\lambda\omega$ . A natural question is what dimension  $\Lambda^k(\mathbb{R}^l)$  has and to find a suitable basis of this space.

---

<sup>1</sup>From  $\omega$ 's antisymmetry follows  $\omega(\dots, v, \dots, v, \dots) = -\omega(\dots, v, \dots, v, \dots)$ , i.e.  $\omega(\dots, v, \dots, v, \dots) = 0$ . Then from the linearity directly follows  $\omega(x_1, \dots, x_{k-1}, \sum_{j=1}^{k-1} a_j x_j) = 0$

### Basis and Dimension of $\Lambda^k(\mathbb{R}^l)$

Given a  $k$ -form  $\omega$  on  $\mathbb{R}^l$  and a basis  $e_1, \dots, e_l$  of  $\mathbb{R}^l$ , then  $\omega(a_1, \dots, a_k)$  can be rewritten the following way: we express the parameters  $a_j$  explicitly as a sum of basis vectors,

$$a_j = \sum_{i=1}^l a_j^i e_i,$$

where  $a_j^i \in \mathbb{R}$  denotes the coordinate of  $a_j \in \mathbb{R}^l$  corresponding to the basis vector  $e_i$ . Using the linearity of forms we get

$$\begin{aligned} \omega(a_1, \dots, a_k) &= \omega\left(\sum_{i_1=1}^l a_1^{i_1} e_{i_1}, \dots, \sum_{i_k=1}^l a_k^{i_k} e_{i_k}\right) \\ &= \sum_{i_1, \dots, i_k \in \{1, \dots, l\}} a_1^{i_1} \cdot \dots \cdot a_k^{i_k} \omega(e_{i_1}, \dots, e_{i_k}). \end{aligned}$$

The sum on the second line is equivalent to separately summing up every  $i_j$  from 1 to  $l$ . But written like this we express that this actually is one sum over all possible tuples  $(i_1, \dots, i_k)$  with  $i_1, \dots, i_k$  being integer values between 1 and  $l$ .

We can reorder this sum such that all terms treating the same set of basis vectors are grouped together,

$$\omega(a_1, \dots, a_k) = \sum_{i_1 < \dots < i_k} \left( \sum_{\sigma \in S^k} a_1^{i_{\sigma(1)}} \cdot \dots \cdot a_k^{i_{\sigma(k)}} \omega(e_{i_{\sigma(1)}}, \dots, e_{i_{\sigma(k)}}) \right). \quad (3.1)$$

Here the permutation group  $S^k$  is used to express that the inner sum goes over all orderings of basis vectors. Because of the antisymmetry of forms, reordering  $e_{i_{\sigma(1)}}, \dots, e_{i_{\sigma(k)}}$  to  $e_{i_1}, \dots, e_{i_k}$  such that  $i_1 < \dots < i_k$ , affects only the sign of  $\omega(e_{i_1}, \dots, e_{i_k})$ :

$$\omega(e_{i_1}, \dots, e_{i_k}) = \text{sgn}(\sigma) \omega(e_{i_{\sigma(1)}}, \dots, e_{i_{\sigma(k)}}).$$

Rewriting the sum 3.1 yields

$$\begin{aligned} &\sum_{i_1 < \dots < i_k} \left( \sum_{\sigma \in S^k} \text{sgn}(\sigma) a_1^{i_{\sigma(1)}} \cdot \dots \cdot a_k^{i_{\sigma(k)}} \right) \omega(e_{i_1}, \dots, e_{i_k}) \\ &= \sum_{i_1 < \dots < i_k} \det_{i_1, \dots, i_k}(a_1, \dots, a_k) \omega(e_{i_1}, \dots, e_{i_k}), \end{aligned}$$

where  $\det_{i_1, \dots, i_k}(a_1, \dots, a_k)$  is a sub determinant of the matrix formed by the vectors  $a_1, \dots, a_k$  restricted to the lines  $i_1, \dots, i_k$ :

$$\det_{i_1, \dots, i_k}(a_1, \dots, a_k) = \det \begin{pmatrix} a_1^{i_1} & a_2^{i_1} & \dots & a_k^{i_1} \\ \vdots & & & \vdots \\ a_1^{i_k} & a_2^{i_k} & \dots & a_k^{i_k} \end{pmatrix}.$$

Put on one line we get

$$\omega(a_1, \dots, a_k) = \sum_{i_1 < \dots < i_k} \omega(e_{i_1}, \dots, e_{i_k}) \cdot \det_{i_1, \dots, i_k}(a_{i_1}, \dots, a_{i_k}).$$

We can read a few things out of this. For one, the  $k$ -form  $\omega$  is determined uniquely by the values it assumes on  $k$ -tuples of basis vectors  $e_{i_1}, \dots, e_{i_k}$  with  $i_1 < \dots < i_k$ . And the  $k$ -forms

$$\det_{i_1, \dots, i_k}(a_1, \dots, a_k),$$

which calculate  $k$ -subdeterminants of the input vectors, form a basis of  $\Lambda^k(\mathbb{R}^l)$ . From this follows directly that the dimension of the space of  $k$ -forms on  $\mathbb{R}^l$  equals the number of ordered tuples  $i_1 < \dots < i_k$  of integers  $i_1, \dots, i_k \in \{1, \dots, l\}$ , i.e.,

$$\dim(\Lambda^k(\mathbb{R}^l)) = \binom{l}{k}.$$

In particular, the space of  $k$ -forms on  $\mathbb{R}^l$  with  $k > l$  is 0-dimensional, which means that there are no  $k > l$ -forms.

### Examples

As an example we have a look at 2-forms in  $\mathbb{R}^2$  and  $\mathbb{R}^3$ . A 2-form has to take two input vectors and return a value in  $\mathbb{R}$ . On  $\mathbb{R}^2$  with the standard basis, an example is the determinant:

$$\omega(a, b) = \det \begin{pmatrix} a_1 & b_1 \\ a_2 & b_2 \end{pmatrix} = a_1 b_2 - a_2 b_1.$$

You can easily check that this is a 2-form. We have linearity,  $\omega(\lambda a + b, c) = \lambda\omega(a, c) + \omega(b, c)$ , and antisymmetry,  $\omega(a, b) = -\omega(b, a)$ . But for a multiple this is the only 2-form on  $\mathbb{R}^2$ , every other 2-form  $\tilde{\omega}$  is a multiple of the determinant,

$$\tilde{\omega}(a, b) = \mu \det \begin{pmatrix} a_1 & b_1 \\ a_2 & b_2 \end{pmatrix} = \mu (a_1 b_2 - a_2 b_1),$$

with some weight  $\mu \in \mathbb{R}$ . The dimension of the space of all 2-forms on  $\mathbb{R}^2$  therefore is one,

$$\dim(\Lambda^2(\mathbb{R}^2)) = 1.$$

On  $\mathbb{R}^3$  an example 2-form is

$$\omega(a, b) = \langle a \times b, \hat{w} \rangle, \tag{3.2}$$

where the cross product of the input vectors  $a, b$  is projected on some arbitrary vector  $\hat{w} \in \mathbb{R}^3$ . This obviously is a 2-form, we have linearity in both  $a$  and  $b$  and antisymmetry, as the cross product is antisymmetric:

$$a \times b = -b \times a.$$

Lets consider the basis of the space of 2-forms in  $\mathbb{R}^3$ ,  $\Lambda^2(\mathbb{R}^3)$ , as described in the last section. The basis elements are

$$\det_{2,3}(a, b) = a_2 b_3 - b_2 a_3,$$

$$\det_{3,1}(a, b) = a_3 b_1 - b_3 a_1,$$

$$\det_{1,2}(a, b) = a_1 b_2 - b_1 a_2.$$

Any 2-form in  $\Lambda^2(\mathbb{R}^3)$  is a linear combination, i.e., a weighted sum, of these three basis elements. So any 2-form can be expressed with three weights  $\hat{w}_1, \hat{w}_2, \hat{w}_3 \in \mathbb{R}$  as

$$\hat{w}_1 \cdot (a_2 b_3 - b_2 a_3) + \hat{w}_2 \cdot (a_3 b_1 - b_3 a_1) + \hat{w}_3 \cdot (a_1 b_2 - b_1 a_2).$$

But this is exactly the same as in Equation 3.2, with  $\hat{w} = (\hat{w}_1, \hat{w}_2, \hat{w}_3)$ . So every 2-form in  $\mathbb{R}^3$  can be thought of as a projection of the cross product of the input vectors onto some vector  $\hat{w}$ .

### 3.1.3. The Wedge Product

The wedge product for forms is a way to create higher order forms out of lower order forms, for example out of a  $j$  form  $\omega^j$  and a  $k$  form  $\nu^k$  you can make a  $j+k$  form  $\omega^j \wedge \nu^k$ . The important points to understand in this section are that the wedge product can be used to create higher order forms and to simply describe a base of the space of  $k$ -Forms  $\Lambda^k(\mathbb{R}^l)$ . Furthermore, the wedge product is associative, distributive and has some symmetry.

#### Definition of the Wedge Product

The wedge product is easy to define but not very intuitive. You directly define the wedge product as

$$\omega^j \wedge \nu^k(v_1, \dots, v_{l+k}) = \frac{1}{k!l!} \sum_{\sigma \in S^{k+l}} \operatorname{sgn}(\sigma) \omega^j(v_{\sigma(1)}, \dots, v_{\sigma(j)}) \nu^l(v_{\sigma(k+1)}, \dots, v_{\sigma(k+l)}).$$

The wedge product has the following properties, as is easy to show and is done e.g. in [AF01]. These algebraic rules are handy for calculations.

1. *Linearity in both arguments*, i.e.  $(\lambda \omega_1^k + \omega_2^k) \wedge \nu^l = \lambda (\omega_1^k \wedge \nu^l) + \omega_2^k \wedge \nu^l$  and the same for  $\nu^l$ .
2. *Associativity*, i.e.  $(\omega^j \wedge \nu^k) \wedge \mu^l = \omega^j \wedge (\nu^k \wedge \mu^l)$ .
3. *Symmetry*:  $\omega^k \wedge \nu^l = (-1)^{kl} \nu^l \wedge \omega^k$ .

The wedge product is closely connected to determinants. For two arbitrary 1-forms  $\omega^1, \nu^1$  we get

$$\omega^1 \wedge \nu^1(a, b) = \det \begin{pmatrix} \omega(a) & \omega(b) \\ \nu(a) & \nu(b) \end{pmatrix},$$

and wedging  $k$  one forms  $\omega_1^1, \dots, \omega_k^1$  leads to

$$\omega_1^1 \wedge \omega_2^1 \wedge \dots \wedge \omega_k^1(a_1, \dots, a_k) := \det \begin{pmatrix} \omega_1(a_1) & \dots & \omega_1(a_k) \\ \vdots & & \vdots \\ \omega_k(a_1) & \dots & \omega_k(a_k) \end{pmatrix}.$$

### Describing a Basis using the Wedge Product

The wedge product allows to elegantly describe a basis for the space of  $k$ -forms  $\Lambda^k(\mathbb{R}^l)$  using a basis  $e_1, \dots, e_l$  of  $\mathbb{R}^l$ . The space of 1-forms  $\Lambda^1(\mathbb{R}^l)$  has dimension  $l$  and is spanned by the special set of basis forms

$$de_i(a) := \det_i \begin{pmatrix} a^1 \\ \vdots \\ a^l \end{pmatrix} = a^i,$$

i.e., the forms that project  $a$  to the  $i$ th coordinate  $a^i$  of  $a$  with respect to the chosen base  $e_1, \dots, e_l$ . If multiple indices are present, we denote components by superscripts and elements by subscripts. E.g.  $a_i^j$  is the  $j$ th component of  $a_i$ . If we apply the wedge product to the ‘standard’ basis 1-forms  $de_1, \dots, de_l$ , we get

$$de_{i_1} \wedge de_{i_2} \wedge \dots \wedge de_{i_k}(a_1, \dots, a_k) = \det \begin{pmatrix} de_{i_1}(a_1) & \dots & de_{i_1}(a_k) \\ \vdots & & \vdots \\ de_{i_k}(a_1) & \dots & de_{i_k}(a_k) \end{pmatrix},$$

which is  $\det_{i_1, \dots, i_k}(a_1, \dots, a_k)$  when  $i_1 < \dots < i_k$ . These are exactly the ‘standard’ basis forms for the space of  $k$ -forms from the Section 3.1.2. This means that a basis of  $\mathbb{R}^l$  induces a basis to the space of forms and any  $k$ -form can be written as a linear combination,

$$\omega^k = \sum_{i_1 < \dots < i_k} w_{i_1, \dots, i_k} de_{i_1} \wedge \dots \wedge de_{i_k},$$

where  $w_{i_1, \dots, i_k} \in \mathbb{R}$  is the weight corresponding to the basis element  $de_{i_1} \wedge \dots \wedge de_{i_k}$ . Note that often  $x_1, \dots, x_l$  or  $x, y, z$  or similar is chosen to denote the base of  $\mathbb{R}^l$  and the basis forms consequently are denoted by  $dx_1, \dots, dx_l$  or  $dx, dy, dz, dx \wedge dy$  and so on.

### Examples

We can again look at 2-forms on  $\mathbb{R}^2$  and  $\mathbb{R}^3$ , when both spaces are equipped with the standard basis. A single basis element  $de_i \wedge de_j$  is given by

$$de_i \wedge de_j(a, b) = a^i b^j - a^j b^i.$$

Then, as we have seen in the last section’s example, all 2-forms and 3-forms are all of the form

$$\omega^2 = w_1 de_1 \wedge de_2,$$

$$\omega^3 = w_1 de_2 \wedge de_3 + w_2 de_3 \wedge de_1 + w_3 de_1 \wedge de_2,$$

with weights  $w, w_1, w_2, w_3 \in \mathbb{R}$ .

### 3.1.4. Differential Forms

Now we can correctly define differential forms. They are exactly as motivated in the beginning of this chapter; a differential form assigns to each point  $p$  of a manifold  $M$  a form  $\omega_p$  defined on the tangential space  $T_p M$ . With the wedge product we can now formulate that the differential form should vary smoothly between points. A local map

$$\phi : U \subset \mathbb{R}^l \rightarrow M$$

induces a basis to all tangential spaces of points in  $\phi(U)$ , namely  $\frac{\partial \phi}{\partial u_i}$ . We can directly use this basis to induce a basis to the space of  $k$ -forms, as done in the last section. Henceforth we will use the following notation for the basis forms induced by a map  $\phi$ :

$$du_i := d \frac{\partial \phi}{\partial u_i}.$$

**Definition (Differential Form)** *A differential  $k$ -form  $\omega^k$  is a mapping that assigns a  $k$ -form  $\omega_p \in \Lambda^k(T_p M)$  to every point  $p \in M$ .*

*Given a local map  $\phi : U \rightarrow M$  all  $k$ -forms  $\omega_p$  with  $p \in \phi(M)$  can be expressed in the coordinates induced by  $\phi$ ,*

$$\omega_p = \sum_{i_1 < \dots < i_k} \omega_{i_1, \dots, i_k}(p) \cdot du_{i_1} \wedge \dots \wedge du_{i_k},$$

*with some real-valued functions  $\omega_{i_1, \dots, i_k}(p)$ . We then say that the differential form  $\omega$  is  $k$  times differentiable if expressed in local coordinates, the  $\omega_{i_1, \dots, i_k}(p)$  are  $k$  times differentiable. For simplicity sake we will always assume that  $\omega$  is infinitely often differentiable, i.e. smooth.*

We will see examples and relate differential forms to more common things like vector fields in the next section.

### 3.1.5. Interpretation of Differential Forms in $\mathbb{R}^3$

Differential forms are of high practical relevance because standard calculus objects like vector fields are just realizations of differential forms. Therefore, the theory about differential forms can be applied directly to a wide range of standard problems. In the following we focus on  $\mathbb{R}^3$ , or equivalently, 3-dimensional manifolds, and relate the differential forms to standard calculus objects. The relation is depicted in Figure 3.4.

#### Differential 0-Forms

Differential 0-forms are real valued functions. By definition a differential 0-form assigns a 0-form, i.e. a constant, to every point  $p$  on a manifold. This means a differential 0-form is simply a smooth function  $\omega : M \rightarrow \mathbb{R}$ .

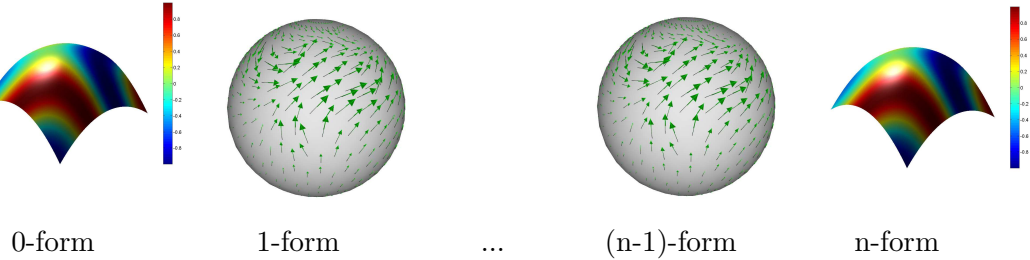


Figure 3.4.: Interpretation of differential forms as standard calculus objects. On a  $n$ -dimensional manifold 0-forms and  $n$ -forms can be identified with real valued functions, 1-forms and  $(n-1)$ -forms as tangential vector fields.

### Differential 1-Forms

Differential 1-forms are equivalent to tangential vector fields. A 1-form is a linear mapping  $\omega : \mathbb{R}^l \rightarrow \mathbb{R}$ . Linear mappings to  $\mathbb{R}$  can be represented as the scalar product of some vector  $\omega^\# \in \mathbb{R}^l$  with the input vector:

$$\omega(v) = \langle \omega^\#, v \rangle.$$

This works just as well on manifolds with tangential spaces; any linear mapping from a tangential space  $T_p M \rightarrow \mathbb{R}$  can be described as the scalar product of the input vector with a fixed vector from  $T_p M$ . Stated differently, any 1-form on  $M$  can be described using a tangential vector field  $\omega^\#$ , i.e., a mapping that provides a vector  $\omega^\# \in T_p M$  for all points  $p \in M$ . The 1-form is then given by

$$\omega(v) = \langle \omega^\#, v \rangle_{T_p M}.$$

Yet, there is an additional difficulty, reflected by the use of the subscript  $T_p M$ : a scalar product needs to be defined on every tangential space. A scalar product that is consistently defined for all tangential spaces is called a *Riemannian metric*. As we look only at manifolds embedded in a higher dimensional space  $M \subset \mathbb{R}^n$ , the natural choice of a scalar product on the tangential spaces is the scalar product induced by the surrounding space.

The operation of going from a 1-form to a vector is denoted by the sharp operator  $\#$ . The reverse operation of making a 1-form out of a vector  $v$  is usually denoted by the ‘flat’ operator  $\flat$ , i.e.  $v^\flat$ .

### Differential n-1-Forms

While general  $k$ -forms on  $n$ -dimensional manifolds are not straight forward to interpret, the interpretation is simple again for  $n - 1$ -forms and  $n$ -forms.

For example, the space of 2-forms on a tangential space of a three-dimensional manifold  $M$ ,  $\Lambda^2(T_p M)$ , has dimension three:

$$\dim \Lambda^2(T_p M) = \binom{3}{2} = 3.$$

Therefore, a differential 2-form can again be represented as a vector field. The components of the vector can be thought of as the weights for the three basis forms given by some parametrization,

$$du_2 \wedge du_3, \ du_3 \wedge du_1, \ du_1 \wedge du_2.$$

In the  $\mathbb{R}^3$  with the standard  $(x, y, z)$  basis and the euclidean scalar product, a basis of  $\Lambda^2(\mathbb{R}^3)$  is given by  $dy \wedge dz, dz \wedge dx, dx \wedge dy$ . If  $\hat{w} = (w_1, w_2, w_3)$  is a vector field, we define the related 2-form as the weighted sum of basis elements,

$$\omega^2 = w_1 dy \wedge dz + w_2 dz \wedge dx + w_3 dx \wedge dy.$$

As the basis forms are given by  $dy \wedge dz(a, b) = a_y b_z - a_z b_y$  and similar, the 2-form  $\omega^2(a, b)$  can be written as:

$$\begin{aligned} \omega^2(a, b) &= (w_1 dy \wedge dz + w_2 dz \wedge dx + w_3 dx \wedge dy)(a, b) \\ &= w_1(a_y b_z - b_y a_z) + w_2(a_z b_x - b_z a_x) + w_3(a_x b_y - a_y b_x) \\ &= \langle \hat{w}, a \times b \rangle. \end{aligned}$$

This means that if we want a vector  $\hat{w} \in \mathbb{R}^3$  to act like a two form on two input vectors  $a, b \in \mathbb{R}^3$ , it amounts to taking the scalar product of  $\hat{w}$  and a vector normal to  $a$  and  $b$ , scaled by the area spanned by  $a, b$ . This can be done for  $(n-1)$ -forms on  $n$ -manifolds in general.

### Volume Forms

Differential 3-forms on  $\mathbb{R}^3$  can again be represented as real valued functions. As can differential  $n$ -forms on  $n$ -dimensional manifolds in general. There is a special differential  $n$ -form on an  $n$  dimensional manifold  $M^n$ : the ‘volume form’. The volume form measures the signed (orientation dependent) volume spanned by the input vectors. In  $\mathbb{R}^n$  with the standard basis  $e_1, \dots, e_n$ , this is exactly the determinant:

$$d\mathbb{R}^n(v_1, \dots, v_n) = \det(v_1, \dots, v_n) = de_1 \wedge \dots \wedge de_n.$$

The volume on some space  $V$  is sometimes denoted as  $dV$  or  $dVol$ . As the dimension of the space of  $n$ -forms on  $T_p M^n$  is

$$\dim(\Lambda^n(\mathbb{R}^n)) = \binom{n}{n} = 1,$$

every  $n$ -form is simply a multiple of the volume form  $dV$ . Therefore any differential  $n$ -form can be represented with a real valued function  $f : M \rightarrow \mathbb{R}$  as

$$\omega^n = f \cdot dVol.$$

### 3.1.6. Integration of Forms

We started this chapter saying that we wanted to design objects that are well suited for integration. We ended up with differential forms that in 3-dimensional spaces turn out to be either vector fields or scalar functions. Let's now look at how differential forms are integrated. We omit various technicalities—for a clean introduction of the integral see e.g. [AF01]; for a very understandable introduction see [Bac06].

A  $k$ -form can be integrated over  $k$ -dimensional regions. In the following,  $\phi : U \subset \mathbb{R}^k \rightarrow M$  is a map,  $M$  a  $k$ -dimensional manifold,  $\omega^k$  a differential  $k$ -form on  $M$ , and  $\Omega = \phi(U)$  a region parametrized by  $\phi$ . The integral of a  $k$ -form looks like the following:

$$\int_{\Omega} \omega^k.$$

Before we go on to the definition of this integral there are a few things to be noted. Note that there are no input parameters for  $\omega^k$  and that the ' $dx_i$ ' usually seen in integrals are absent. This is no accident but an important feature of differential forms. The  $k$  input vectors required by the differential  $k$ -form are provided implicitly by the integral. Intuitively these input parameters are the edges of the cells in the Riemann integral, as motivated in Section 3.1.1. This is the same as in the usual integrals, where parameters are bound by the ' $dx_i$ '. But in contrast to usual integrals, the integral for differential forms is independent of the choice of parametrization. It can be integrated using an arbitrary parametrization and the differential form scales automatically to the grid provided by the parametrization. A  $k$ -form can only be integrated over a  $k$ -dimensional set, as only  $k$ -dimensional 'grid-cells' can be described by exactly  $k$  input vectors, namely the cell's edges.

The integral is defined using a pull-back: using a parametrization  $\phi$  everything is pulled back to  $\mathbb{R}^l$  and integrated there:

$$\int_{\phi(U)} \omega^k = \int_{U \subset \mathbb{R}^k} \omega_{\phi(x_1, \dots, x_k)} \left( \frac{\partial \phi}{\partial x_1}, \dots, \frac{\partial \phi}{\partial x_k} \right) dx_1 \dots dx_k.$$

The integral on the right side integrates a function depending on  $k$  variables over a region  $U$  in  $\mathbb{R}^k$  as usual. Even though the integral for differential forms is defined using a parametrization  $\phi$ , its value is independent of  $\phi$ , and can be computed with any set of coordinates, as is proven in Appendix A.1; as intended  $\omega$  automatically scales according to the volume spanned by the vectors  $\frac{\partial \phi}{\partial x_i}$  for any coordinates  $\phi$ , thereby canceling out the choice of parametrization.

#### Examples

We want to ponder a little bit more on the integration of differential forms and on the independence of the integral to parameterizations.

Lets consider a 1-form  $\omega^1$  on the manifold  $\mathbb{R}^2$ . As  $\mathbb{R}^2$  is a manifold, we can choose an arbitrary parametrization of  $\mathbb{R}^2$ . For now we choose the identity map, which parametrizes  $\mathbb{R}^2$  canonically with  $(x, y)$  coordinates. Every manifold has tangential spaces, and so does

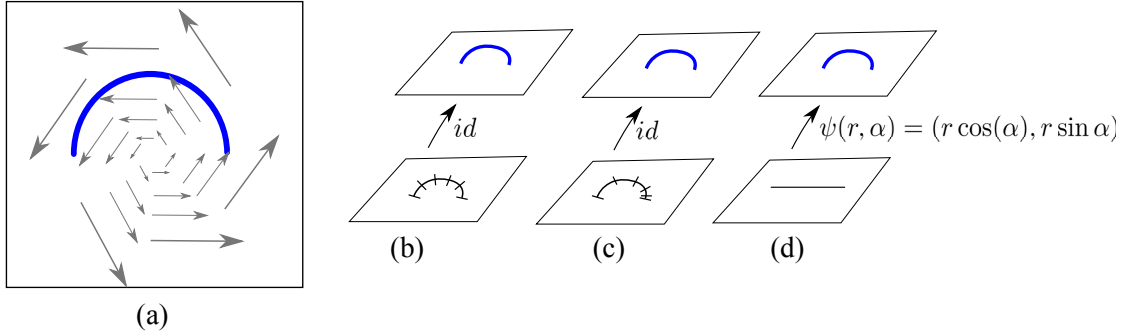


Figure 3.5.: (a) This vector field is integrate along the blue curve. This is done three times, using different parameterizations. In (b) and (c) the manifold  $\mathbb{R}^2$  is parameterized using the identity map, while the curve is parameterized in two different ways. In (d)  $\mathbb{R}^2$  is parameterized using polar coordinates.

$\mathbb{R}^2$ . But its tangential spaces are simply  $\mathbb{R}^2$  again, and every tangential space gets the standard basis induced by the identity map. As an example 1-form we choose the form described by the two dimensional vector field  $\omega_{(x,y)}^\# = (-y, x)$  on  $\mathbb{R}^2$ . Technically the vector field consists of tangential vectors from the tangential spaces. This vector field can be integrated over any curve, and we integrate it over the half circle  $c$  parametrized by  $\phi(t) = (\cos(t), \sin(t))$  with  $t \in [0, \pi]$ . This setting is shown in Figure 3.5 (a) and (b). We compute the integral by pulling everything back using the parameterization of  $c$ . The partial derivative of  $\phi$  is

$$\frac{\partial \phi}{\partial t} = \begin{pmatrix} -\sin(t) \\ \cos(t) \end{pmatrix}.$$

The overall integral is computed as follows, where in the first step we use the definition of the integral and in the second step we express the 1-form using the vector field:

$$\begin{aligned} \int_c \omega^1 &= \int_0^\pi \omega_{\phi(t)}(\frac{\partial \phi}{\partial t}) dt = \int_0^\pi \langle \omega_{(\cos(t), \sin(t))}^\#, \frac{\partial \phi}{\partial t} \rangle dt \\ &= \int_0^\pi \langle \begin{pmatrix} -\sin(t) \\ \cos(t) \end{pmatrix}, \begin{pmatrix} -\sin(t) \\ \cos(t) \end{pmatrix} \rangle dt = \int_0^\pi 1 dt = \pi. \end{aligned}$$

Next we keep the identity as a parametrization for  $\mathbb{R}^2$  but change the parametrization of the curve to

$$\phi(t) = (\cos(t^2), \sin(t^2)),$$

with  $t \in [0, \sqrt{\pi}]$ , this is depicted in Figure 3.5 (c). The result does not change, we get:

$$\begin{aligned} \int_c \omega^1 &= \int_{[0, \sqrt{\pi}]} \omega_{\phi(t)}(\frac{\partial \phi}{\partial t}) dt = \int_{[0, \sqrt{\pi}]} \langle \omega_{(\cos(t^2), \sin(t^2))}^\#, \frac{\partial \phi}{\partial t} \rangle dt \\ &= \int_{[0, \sqrt{\pi}]} \langle \begin{pmatrix} -\sin(t^2) \\ \cos(t^2) \end{pmatrix}, \begin{pmatrix} -2t \sin(t^2) \\ 2t \cos(t^2) \end{pmatrix} \rangle dt = \int_{[0, \sqrt{\pi}]} 2t dt = \pi. \end{aligned}$$

As a last example we change the parametrization of  $\mathbb{R}^2$ , instead of using the identity we use polar coordinates. With polar coordinates we can not parametrize the whole  $\mathbb{R}^2$  with a single map, but if we use the map

$$\psi(r, \alpha) = (r \cos(\alpha), r \sin(\alpha))$$

with  $r > 0$  and  $\alpha \in (-\pi/2, 3\pi/2)$ , the curve lies completely in the region parameterized by this map. As mentioned, the vector field  $\omega^\#$  consists of tangential vectors and the tangential spaces of  $\mathbb{R}^2$  are simply  $\mathbb{R}^2$  again. But if we use  $\psi$  as a parameterization instead of the identity, every tangential space gets a different basis. The tangential space of  $\mathbb{R}^2$  at  $(r \cos(\alpha), r \sin(\alpha))$  has the basis  $\frac{\partial \psi}{\partial x}, \frac{\partial \psi}{\partial y}$ , i.e.,

$$\begin{pmatrix} \cos(\alpha) \\ \sin(\alpha) \end{pmatrix}, \begin{pmatrix} -r \sin(\alpha) \\ r \cos(\alpha) \end{pmatrix}.$$

The vector field under consideration in these coordinates is given by  $\omega_{r,\alpha}^\# = (0, 1)$ . The reason is that at the point  $\psi(r, \alpha) = (r \cos(\alpha), r \sin(\alpha))$ , the vector field should be  $(-r \sin(\alpha), r \cos(\alpha))$ , which exactly is the second basis vector of the tangential space, therefore  $\omega_{r,\alpha}^\# = (0, 1)$ . In these coordinates, the curve  $c$  has the parametrization  $\phi(t) = (1, t)$  with  $t \in [0, \pi]$ , its derivative being  $(0, 1)$ . The scalar product on the tangential space at  $\psi(r, \alpha)$  is given by

$$D\psi^T D\psi = \begin{pmatrix} \cos(\alpha) & \sin(\alpha) \\ -r \sin(\alpha) & r \cos(\alpha) \end{pmatrix} \begin{pmatrix} \cos(\alpha) & -r \sin(\alpha) \\ \sin(\alpha) & r \cos(\alpha) \end{pmatrix} = \begin{pmatrix} 1 & 0 \\ 0 & r^2 \end{pmatrix},$$

$$\langle v, w \rangle_{r,\alpha} = v^T \begin{pmatrix} 1 & 0 \\ 0 & r^2 \end{pmatrix} w.$$

The integral of the vector field in polar coordinates then becomes

$$\begin{aligned} \int_c \omega^1 &= \int_0^\pi \langle \begin{pmatrix} 0 \\ 1 \end{pmatrix}, \begin{pmatrix} 0 \\ 1 \end{pmatrix} \rangle_{(1,t)} dt \\ &= \int_0^\pi (0, 1) \begin{pmatrix} 1 & 0 \\ 0 & 1 \end{pmatrix} \begin{pmatrix} 0 \\ 1 \end{pmatrix} dt = \pi. \end{aligned}$$

This example demonstrates how the integral  $\int_c \omega^1$  is independent of coordinate choices, they all cancel out sooner or later. The integral of a vector field over a curve computes a value that only depends on the geometry of the set up and not on the description of the setting, i.e. the parameterizations. On the other hand, you might be tempted to integrate a vector field over an area too. You might for example suggest to integrate both coordinates independently. But this will *not* be independent of the coordinate choice, as a vector field has only two coordinates with respect to some parametrization.

So  $k$ -forms can only be integrated over smooth  $k$ -dimensional regions. This restriction is softened by the Hodge star operator  $\star$ , introduced in Section 4.3. The  $\star$  will allow to make a  $n - k$ -form out of a  $k$ -form. Like that for example a 0-form can indirectly be integrated over a  $n$ -dimensional set too.

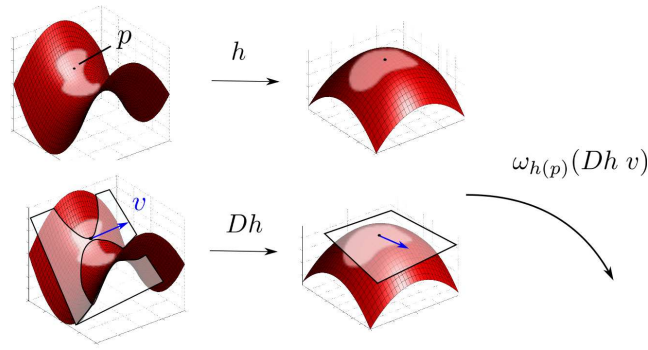


Figure 3.6.: A mapping  $h$  can be used to pull a differential form  $\omega$  back from one manifold to another, as  $h$  provides a mapping between the manifolds and their tangential spaces.

### 3.1.7. Pull-Backs

The ‘pulling back’ used to define an integral can be done more generally. Suppose we have a mapping between two  $n$ -dimensional manifolds  $N$  and  $M$ ,  $h : N \rightarrow M$ , whose total derivative  $Dh$  expressed as a matrix has  $\det(Dh) \neq 0$ . For simplicity we also assume that  $h$  is smooth. As seen in Section 2.1.5,  $Dh$  is a mapping between the tangential spaces of  $N$  and  $M$ . Therefore if we have a differential  $k$ -form  $\omega$  on  $M$  we can ‘pull it back’ to  $N$  via

$$(h^*\omega)_p(v_1, \dots, v_k) := \omega_{h(p)}(Dh v_1, \dots, Dh v_k).$$

The pullback is depicted in Figure 3.6. The action of pulling back  $\omega$  using  $h$  is denoted by  $h^*\omega$ . This mapping preserves the integral (check it by using the definitions!)

$$\int_{h(U) \subset M} \omega = \int_{U \subset N} h^*\omega.$$

This means that we can integrate either  $\omega$  over a subset of  $M$  or the pulled back mapping over a subset of  $N$ . Usually, as in the definition of the integral, you pull back forms to  $\mathbb{R}^k$ , using one of the local maps. The pullback is very powerful as it conserves properties under the integral.

## 3.2. Discrete Differential Forms

Differential forms are defined on Manifolds and, as it is to be expected, discrete forms are defined on discrete manifolds. But there are no tangential spaces on discrete manifolds. While differential forms are spatially varying multilinear mappings, a discrete differential form is something much simpler - it simply is a set of averaged values, as depicted in Figure 3.7.

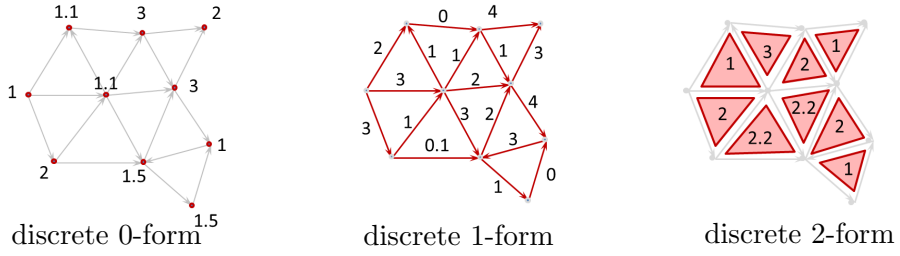


Figure 3.7.: A discrete differential  $k$ -form is a set of values associated to the  $k$ -simplices of a discrete manifold. A value represents the integral of the sampled differential  $k$ -form over the associated simplex.

**Definition (Discrete Form)** *A discrete  $j$ -form on a discrete  $k$ -manifold assigns a real number to every  $j$ -simplex contained in the discrete manifold. This vector of values is also sometimes called a  $j$  co-chain.*

The first question to be answered is how this set of values relates to a non-discrete differential form.

### 3.2.1. Sampling Forms

To relate discrete forms with differential forms, the discrete manifold  $K$  needs to be related somehow to a non-discrete manifold  $M$ . We will just assume that the discrete manifold  $K$  approximates the manifold  $M$  and for any simplex  $\sigma \in K$  there is a continuous analogue  $\sigma \subset M$  on the manifold  $M$ , as in Figure 3.8. We denote both the discrete simplex and the continuous counterpart by the same symbol. Which is meant should be clear from the context.

The relation then is simple: given a differential  $k$ -form  $\omega^k$  on  $M$  the value of the discrete  $k$  form  $\mathbf{w}$  on a  $k$ -simplex  $\sigma$  is value of  $\omega^k$  accumulated over  $\sigma$ ,

$$\mathbf{w}(\sigma) = \int_{\sigma} \omega^k.$$

In the following we look at some examples in  $\mathbb{R}^2$  and  $\mathbb{R}^3$ .

#### Sampling 0-Forms

As seen in Section 3.1.5, 0-forms can simply be represented as functions  $f : M \rightarrow \mathbb{R}$ . A 0-form has to be integrated over 0-dimensional sets, i.e. points. The discrete 0-form is a set of values associated to vertices. The value at a vertex position  $v$  or 0-simplex  $v$  is

$$\mathbf{w}^0(v) = f(v),$$

i.e.  $f$  evaluated at  $v$ .

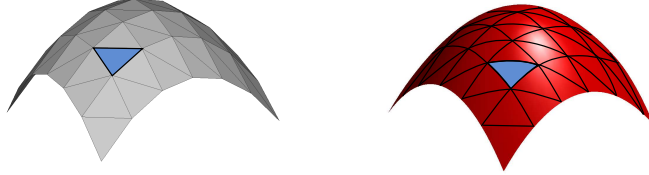


Figure 3.8.: We assume that a simplicial complex samples a manifold, such that every simplex has a related smooth region on the manifold.

### Sampling 1-Forms

A 1-form  $\omega^1$  on a manifold  $M$  can be represented by a tangential vector field  $\nu : M \rightarrow TM$  via

$$\omega_p^1(v) = \langle \nu(p), v \rangle.$$

A 1-form can be integrated over 1-dimensional curves. A discrete 1-form is therefore a set of values associated to the 1-simplices i.e. edges of the discrete manifold. The value on an edge  $e$  is

$$\mathbf{w}^1(e) = \int_e \omega^1 = \int_0^1 \langle \nu(e(t)), \frac{\partial}{\partial t} e(t) \rangle dt,$$

where in the last integral  $e(t)$  is a parametrization of the curve on the manifold  $M$  associated to the edge  $e$ . A discrete 1-form samples a vectorfield by projecting the field on the edge and accumulating these values along the edge. The resulting value can be thought of as measuring how much the vectorfield ‘flows’ along the edge. If the edge  $e$  is a straight line and the vectorfield a constant vector  $\mathbf{w}^1(e)$  is simply the projection of the vector onto the edge,

$$\mathbf{w}^1(e) = \langle \nu, e \rangle.$$

On a 2-manifold there is a second way of how to sample the vectorfield by measuring the flow *through* the edge instead of *along* the edge; we will come back to this in a while when talking about the Hodge star  $\star$  operator in Section 4.3.

$$\mathbf{w}^1(e) = \int_0^1 \langle \nu(e(t)), (\frac{\partial}{\partial t} e(t))^\perp \rangle dt$$

Here  $^\perp$  denotes the vector rotated by  $90^\circ$  according the orientation of the surface. The two sampling schemes are depicted in Figure 3.9.

### Sampling 2-Forms

A 2-form can be integrated over 2D patches and the discrete 2-form associates values to the 2-simplices i.e. the triangles of the discrete manifold.

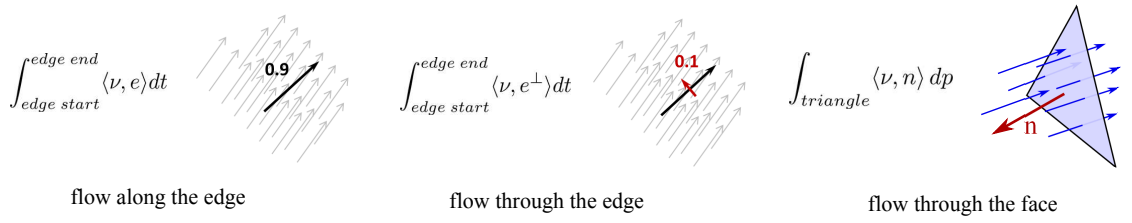


Figure 3.9.: Possibilities to sample 1-forms on 2-manifolds: you can either measure the flow through or along the edge. A 2-form on a 3-manifolds is sampled by measuring the flow through a face.

On a 2-manifold a differential 2-form  $\omega^2$  is represented by a function  $f$ . The value  $w^2(t)$  on a triangle  $t$  is the integral of  $f$  over  $t$ :

$$\mathbf{w}^2(t) = \int_t f \, dVol.$$

On a 3-manifold a differential 2-form  $\omega^2$  is represented by a vectorfield  $\nu : M \rightarrow TM$ , but evaluating it on two vectors amounts to

$$\omega_p(a, b) = \langle \nu(p), a \times b \rangle,$$

such that the value of the discrete 2-form associated to a triangle  $t$  is

$$\mathbf{w}^2(t) = \int_t \langle \nu(p), n(p) \rangle \, dp,$$

where  $n(p)$  denotes the normal on the surface  $t$  at the point  $p$ . This measures the flow of the vectorfield *through* the surface  $t$ , see Figure 3.9.

### 3.2.2. Integration of Discrete Forms

A discrete form can very easily be integrated over a set of simplices. Integrating a discrete  $k$ -Form  $\mathbf{w}^k$  over a set of  $k$ -simplices  $\{\sigma_1, \dots, \sigma_l\}$  can be done simply by summing up the values on those simplices. If  $\mathbf{w}^k$  is the sampled version of  $\omega^k$  this sum is exactly the integral of  $\omega^k$  over the  $k$  dimensional set  $\{\sigma_1, \dots, \sigma_l\}$ :

$$\int_{\{\sigma_1, \dots, \sigma_l\}} \omega^k = \sum_{i=1}^l \mathbf{w}^k(\sigma_i),$$

as

$$\mathbf{w}^k(\sigma_i) = \int_{\sigma_i} \omega^k.$$

As we have seen in Section 2.2.3, we can describe a set of simplices in a discrete manifold as a vector  $\sigma$  of dimension  $\#k$ -simplices consisting of plus ones, minus ones, and zeros.

These vector entries describe if a simplex with a fixed reference orientation occurs within the set with a positive orientation, with a negative orientation, or not at all.

The discrete form  $\mathbf{w}^k$  is a vector of the same dimension, and the discrete integral over  $\sigma$  is simply the scalar product of those two vectors,

$$\langle \sigma, \mathbf{w}^k \rangle.$$

The discrete analogon of the integral is in our setting the scalar product between the simplex vector, i.e. the region, and the discrete form!



## 4. Exterior Calculus & Discrete Exterior Calculus

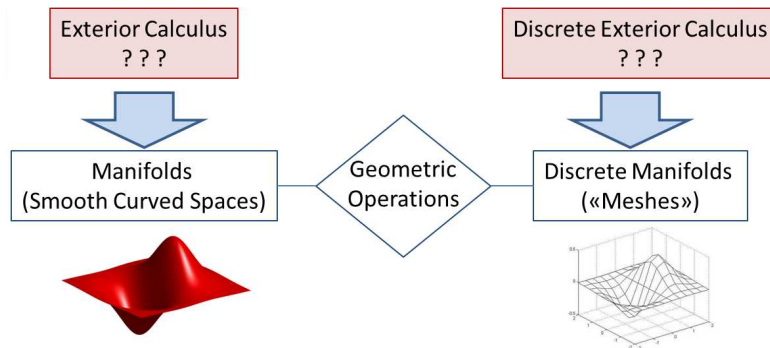


Figure 4.1.: Manifolds, discrete manifolds and differential forms have been covered in the Chapters 2 and 3. The missing elements are exterior calculus (EC) and discrete exterior calculus (DEC). EC and DEC provide operators to manipulate the differential forms on manifolds.

In this chapter we introduce exterior calculus and discrete exterior calculus. Exterior calculus is calculus for differential forms on manifolds. The three operations we introduce for differential forms are the exterior derivative  $d$ , the Hodge star  $\star$  and the coderivative  $\partial$ , which is a concatenation of the  $\star$  and  $d$  operator. Discrete exterior calculus will consist of the same operators, but defined for discrete differential forms.

This chapter is structured as follows: in the Sections 4.1 to 4.4 we introduce exterior calculus, with an emphasis on the geometric structure of the operators and in Section 4.5 we use the geometry of the operators to define the corresponding discrete operators. In more details: Section 4.1 treats the exterior derivative  $d$  and relates it to the standard calculus operators *div*, *curl* and *grad*. In Section 4.2 we consider the geometry of the exterior derivative and its related standard calculus operators. Their geometry is captured by Stokes' theorem. In Section 4.3 the Hodge star operator is introduced, which allows the formulation of higher order derivatives and the coderivative. In Section 4.4 the exterior calculus operators are summarized in the de Rham complex.

In the Section 4.5 finally everything comes together and we use the geometry of the exterior calculus operators to discretize them and build DEC. Discretizing the differential operators  $d$  and  $\star$  is interesting, because they can be used to formulate various operators like the divergence and curl or the Laplacian. By discretizing them we directly get discrete versions of all these operators.

## 4.1. The Exterior Derivative $d$

The exterior derivative  $d$  is a generalization of the usual derivative. But it is better to look at  $d$  as something completely new and unknown, because thinking of it as the ‘derivative for differential forms’ can lead to wrong associations and expectations. For example applying the differential operator multiple times to get an  $n$ th derivative does not make sense. But the exterior derivative generalizes the usual derivative in the sense that the exterior derivative is the counterpart to the integral, by Stokes’ theorem.

The exterior derivative allows a rich theory and is of great practical relevance because many differential operators from classical calculus can be expressed using it. We give examples in Section 4.1.3 and also coordinate free examples in Section 4.2.3.

Note that henceforth we will primarily talk about differential ( $k$ -) forms and often drop the ‘differential’, and refer to them just as ( $k$ -) forms.

### 4.1.1. Definition

The differential operator  $d$  is easy to define on  $\mathbb{R}^n$ , its relevance is not obvious on first sight, but is explained in the following sections.

**Definition (Exterior Derivative on  $\mathbb{R}^n$ )** *The exterior derivative  $d$  maps differential  $k$ -forms to differential  $k + 1$ -forms. If  $\omega^k$  is given in standard coordinates  $x_1, \dots, x_n$  as*

$$\omega_p^k = \sum_{i_1 < \dots < i_k} \omega_{i_1, \dots, i_k}(x) dx_{i_1} \wedge \dots \wedge dx_{i_k},$$

*the exterior derivative is given by*

$$d\omega^k = \sum_{i_1 < \dots < i_k} \sum_{\alpha=1}^n \frac{\partial \omega_{i_1, \dots, i_k}(x)}{\partial x_\alpha} dx_\alpha \wedge dx_{i_1} \wedge \dots \wedge dx_{i_k}.$$

*Note that the term  $dx_\alpha \wedge dx_{i_1} \wedge \dots \wedge dx_{i_k}$  is zero if  $\alpha$  equals some  $i_j$ ,  $\alpha = i_j$ , because the wedge product of linear dependent basis forms is zero. To emphasize that we are talking about the exterior derivative acting on  $k$ -forms for a fixed  $k$ , we sometimes add a subscript to  $d$ ,  $d_k$ .*

To define  $d$  on manifolds in general we use pullbacks, as introduced in Section 3.1.7, namely: if  $M$  is a manifold,  $h$  a local map and  $\omega^k$  a  $k$ -form, then

$$d\omega^k := (h^*)^{-1} d(h^* \omega^k).$$

The first pullback  $h^*$  transforms  $\omega^k$  to a  $k$ -form on  $\mathbb{R}^n$ . On  $\mathbb{R}^n$  the exterior derivative is already defined and can be used. Then the result is pulled back to the manifold.<sup>1</sup>

---

<sup>1</sup>There are some technicalities about  $(h^*)^{-1}$  that are omitted, see e.g. [AF01]. Also note that this definition does not depend on the map  $h$ .

### 4.1.2. Properties

The exterior derivative has the following properties that are more or less straight forward to check by plugging in the definitions; you can find details e.g. in [AF01].

1.  $d(\omega^k + \psi^k) = d\omega^k + d\psi^k$
2.  $d(\omega^k \wedge \psi^l) = (d\omega^k) \wedge \psi^l + (-1)^k \omega^k \wedge (d\psi^l)$
3.  $d(d\omega^k) = 0$
4.  $f^*(d\omega^k) = d(f^*\omega^k)$

The third and fourth property are the most noteworthy. Applying  $d$  two times in a row always leads to zero (as you can check by simply writing out  $dd$ ). And the exterior derivative commutes with pullbacks. This means that you can freely choose where and in what map you want to work and calculate derivatives; just pull everything to a space where you want to have it.

### 4.1.3. The Exterior Derivative in Euclidean Coordinates

We consider the exterior derivative on  $\mathbb{R}^n$  with the standard basis. The differential forms are interpreted as functions and vectorfields, as described in the last chapter in Section 3.1.5.

#### 0-Forms

If we have a differential 0-form on  $\mathbb{R}^n$  given by  $f : \mathbb{R}^n \rightarrow \mathbb{R}$ , then the exterior derivative is by definition the 1-form

$$df = \sum_{\alpha=1}^n \frac{\partial f}{\partial x_\alpha} dx_\alpha.$$

Therefore, applying  $df$  at any point  $p$  to a vector  $v$  is

$$df_p(v) = \langle \nabla f, v \rangle,$$

where  $\nabla f = (\frac{\partial f}{\partial x_1}, \dots, \frac{\partial f}{\partial x_n})$  is the gradient in euclidean coordinates. This means that  $d$  acts on 0-forms like the gradient operator.

#### 1-Forms

A vector field

$$\begin{aligned} \mathcal{V} &: \mathbb{R}^n \rightarrow \mathbb{R}^n, \\ \mathcal{V}(x) &= (v_1(x), \dots, v_n(x)), \end{aligned}$$

interpreted as a differential 1-form is given by

$$\omega_p^1 = \sum_{i=1}^n v_i(p) dx_i.$$

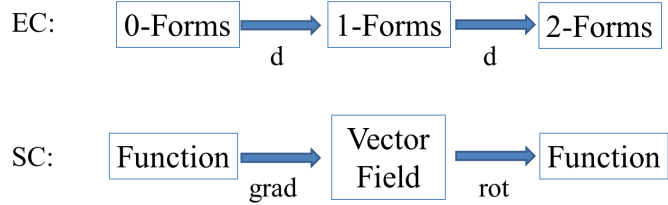


Figure 4.2.: This figure depicts how EC objects relate to standard calculus (SC) objects on a 2-manifold, namely to what SC differential operators the exterior derivative  $d$  relates.

To apply the exterior derivative to  $\omega^1$  yields

$$d\omega^1 = \sum_{i=1}^n \sum_{j=1}^n \frac{\partial v_i(p)}{\partial x_j} dx_j \wedge dx_i.$$

If we reorder these terms and use that  $dx_i \wedge dx_i = 0$ , we get

$$= \sum_{1 \leq i < j \leq n} \left( \frac{\partial v_j(p)}{\partial x_i} - \frac{\partial v_i(p)}{\partial x_j} \right) dx_i \wedge dx_j.$$

On  $\mathbb{R}^3$  this is exactly the *rot* or *curl* operator: the exterior derivative of a 3-form is

$$\begin{aligned} d(v_1 dx_1 + v_2 dx_2 + v_3 dx_3) = \\ \left( \frac{\partial v_3(x)}{\partial x_2} - \frac{\partial v_2(x)}{\partial x_3} \right) dx_2 \wedge dx_3 + \left( \frac{\partial v_1(x)}{\partial x_3} - \frac{\partial v_3(x)}{\partial x_1} \right) dx_3 \wedge dx_1 + \left( \frac{\partial v_2(x)}{\partial x_1} - \frac{\partial v_1(x)}{\partial x_2} \right) dx_1 \wedge dx_2. \end{aligned}$$

If we represent the arising 1-form and 2-form as vectors, the exterior derivative is

$$d \begin{pmatrix} v_1(x) \\ v_2(x) \\ v_3(x) \end{pmatrix} = \begin{pmatrix} \frac{\partial v_3(x)}{\partial x_2} - \frac{\partial v_2(x)}{\partial x_3} \\ \frac{\partial v_1(x)}{\partial x_3} - \frac{\partial v_3(x)}{\partial x_1} \\ \frac{\partial v_2(x)}{\partial x_1} - \frac{\partial v_1(x)}{\partial x_2} \end{pmatrix},$$

which is exactly the *curl* operator.

### 2-Forms on $\mathbb{R}^3$

A differential 2-form can be represented by a vector field  $\mathcal{V} = (v_1, v_2, v_3)$  as a weighted sum of basis elements:

$$\omega^2 = v_1 \cdot dx_2 \wedge dx_3 + v_2 \cdot dx_3 \wedge dx_1 + v_3 \cdot dx_1 \wedge dx_2.$$

The exterior derivative then is

$$d\omega^2 = \left( \frac{\partial v_1}{\partial x_1} + \frac{\partial v_2}{\partial x_2} + \frac{\partial v_3}{\partial x_3} \right) dx_1 \wedge dx_2 \wedge dx_3,$$

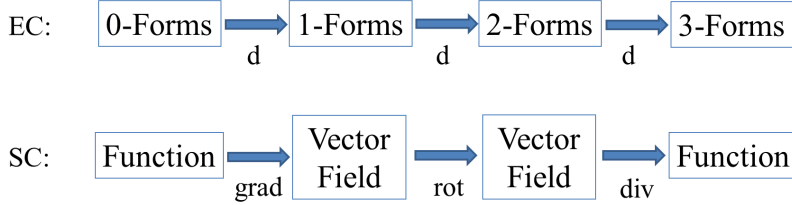


Figure 4.3.: This figure depicts how EC objects relate to standard calculus (SC) objects on a 3-manifold, namely to what SC differential operators the exterior derivative  $d$  is related.

which means that  $d$  is exactly the divergence operator.

The Figures 4.2 and 4.3 summarize the relation between differential forms and standard calculus on 2-manifolds and on 3-manifolds.

## 4.2. Stokes' Theorem

Now we can explain Stokes' theorem

$$\int_{\delta\Omega} \omega = \int_{\Omega} d\omega.$$

Stokes' theorem is a generalization of and follows from the fundamental theorem of calculus: if  $f : \mathbb{R} \rightarrow \mathbb{R}$  has an antiderivative  $F$ , i.e.  $F' = f$ , then

$$\int_a^b f(x)dx = F(b) - F(a).$$

The fundamental theorem of calculus can be rewritten in differential form notation: say  $\Omega = [a, b]$  is an oriented line with border  $\delta\Omega = -\{a\} + \{b\}$ . If we identify  $F$  with a 0-form  $\omega^0 = F$ , then  $dF = F' = f$  is a 1-form. As  $dF$  is a 1-form defined on a 1-manifold it can also be represented as a function. The fundamental theorem then becomes:

$$\int_{[a,b]} d\omega^0 = \int_{\delta[a,b]} \omega^0 = \int_{-\{a\}} \omega^0 + \int_{\{b\}} \omega^0 = -\omega^0(a) + \omega^0(b).$$

So the fundamental theorem is Stokes' theorem applied to 0-forms. Note how it is important that  $\omega^0$  respects the orientation of the points it is applied to.

We will only sketch a proof for Stokes' theorem. There are a few technical difficulties that are omitted. A clean proof can for example be found in [AF01] or [Fra11].

### 4.2.1. Proof Sketch

This sketch is following strongly the reasoning made in [AF01]. It is enough to show the theorem for so called singular cubes. A  $k$ -dimensional singular cube  $c^k$  is a manifold  $C^k$

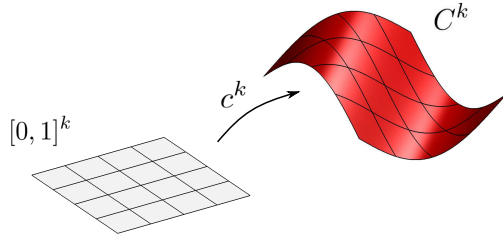


Figure 4.4.: A singular cube: a  $k$ -dimensional patch that can be parametrized by the cube  $[0, 1]^k$  using a single map.

together with a global parametrisation (see Figure 4.4)

$$c^k : [0, 1]^k \rightarrow C^k \subset \mathbb{R}^n.$$

We show

$$\int_{\delta C^{k+1}} \omega^k = \int_{C^{k+1}} d\omega^k.$$

To extend the theorem to arbitrary manifolds consider the Figure 4.5; the basic idea is that the theorem holds if a manifold is the union of a set of disjoint cubes  $\Omega = \bigcup c_i^k$ , as

$$\int_{\Omega} d\omega = \sum_i \int_{c_i^k} d\omega = \sum_i \int_{\delta c_i^k} \omega = \int_{\delta \Omega} \omega,$$

where the second step is the Stokes' theorem for singular cubes and the last step holds because internal boundaries cancel out, as motivated in Figure 4.5.

### Proof (sketch)

Given a singular cube  $C^{k+1}$  with parametrisation  $c^{k+1}$  we can pull the whole problem back to  $[0, 1]^{k+1}$ . We will show Stokes' theorem for the cube  $[0, 1]^{k+1}$ , which is

$$\int_{[0,1]^{k+1}} d\omega^k = \int_{\delta[0,1]^{k+1}} \omega^k. \quad (4.1)$$

If Equation 4.1 is proven, Stokes' theorem also holds for arbitrary singular cubes  $C^{k+1}$ :

$$\begin{aligned} \int_{c([0,1]^{k+1})} d\omega &= \int_{[0,1]^{k+1}} c^*(d\omega) && \text{(definition of the integral)} \\ &= \int_{[0,1]^{k+1}} d(c^*(\omega)) && \text{(d and pull-backs commute)} \end{aligned}$$

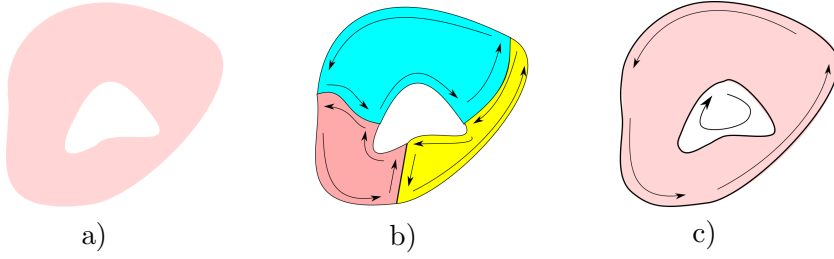


Figure 4.5.: The bordered manifold  $M$  (a) can be built out of 3 singular cubes (b). An integral  $\int_M$  equals the sum of integrals over the singular cubes. For every cube Stokes' theorem holds, so the integral  $\int_M$  is given by the sum of border integrals of the cubes:  $\int_M = \sum \int_{\delta c}$ . But integrals over inner edges cancel out because of their opposite orientations (c). Thus,  $\int_M d\omega = \sum \int_{\delta c} \omega = \int_{\delta M} \omega$ .

$$\begin{aligned}
 &= \int_{\delta[0,1]^{k+1}} c^*(\omega) && \text{(using Equation 4.1)} \\
 &= \int_{\delta(c([0,1]^{k+1}))} \omega && \text{(definition of the integral)}
 \end{aligned}$$

To prove Equation 4.1, we write an arbitrary  $k$ -form  $\omega^k$  on  $[0, 1]^{k+1} \subset \mathbb{R}^{k+1}$  as

$$\omega^k = \sum_{i=1}^{k+1} f_i(x_1, \dots, x_{k+1}) dx_1 \wedge \dots \wedge dx_{i-1} \wedge dx_{i+1} \dots \wedge dx_{k+1},$$

where in each term the  $i$ th  $dx_i$  is omitted. Then the exterior derivative of  $\omega^k$  is by definition

$$d\omega^k = \sum_{i=1}^{k+1} (-1)^{i-1} \frac{\partial f_i}{\partial x_i}(x_1, \dots, x_{k+1}) dx_1 \wedge \dots \wedge dx_{k+1}.$$

Substituting  $d\omega^k$  by the right side of the equation and using the linearity of the integral yields

$$\int_{[0,1]^{k+1}} d\omega^k = \sum_{i=1}^{k+1} (-1)^{i-1} \int_{[0,1]^{k+1}} \frac{\partial f_i}{\partial x_i}(x_1, \dots, x_{k+1}) dx_1 \wedge \dots \wedge dx_{k+1}.$$

Now we can use the known fundamental theorem to integrate the single terms in the sum relative to  $x_i$ ,

$$\int_0^1 \frac{\partial f_i}{\partial x_i}(x_1, \dots, x_{i-1}, t, x_{i+1}, \dots) dt = f(x_1, \dots, x_{i-1}, 1, x_{i+1}, \dots) - f(x_1, \dots, x_{i-1}, 0, x_{i+1}, \dots),$$

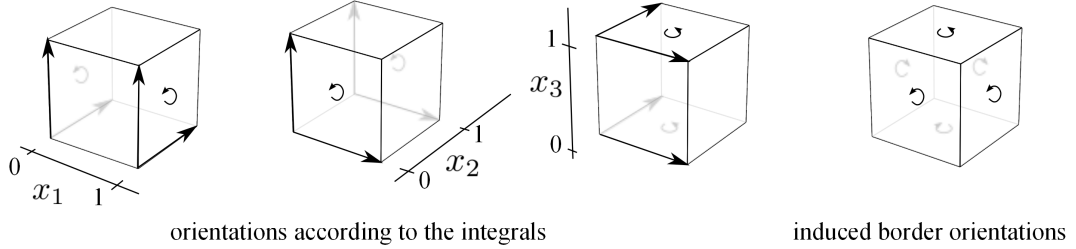


Figure 4.6.: On the left the orientations of the borders when computing the integrals  $\int_0^1 \int_0^1$  are depicted, on the right are the orientations induced by the border operator. The additional signs  $(-1)^{i-1}$  for the faces  $x_i = 1$  and  $(-1)^i$  for the faces  $x_i = 0$  lead to the induced border orientation.

such that one integral is dropped and we get

$$\begin{aligned}
 \int_{[0,1]^{k+1}} d\omega^k &= \sum_{i=1}^{k+1} (-1)^{i-1} \underbrace{\int_0^1 \dots \int_0^1}_{k+1 \text{ integrals}} \frac{\partial f_i}{\partial x_i}(x_1, \dots, x_{k+1}) dx_1 \dots dx_{k+1} \\
 &= \sum_{i=1}^{k+1} (-1)^{i-1} \left( \underbrace{\int_0^1 \dots \int_0^1}_{k \text{ integrals}} f_i(x_1, \dots, x_{i-1}, 1, x_{i+1}, \dots, x_{k+1}) dx_1 \dots dx_{i-1} dx_{i+1} \dots dx_{k+1} \right. \\
 &\quad \left. - \underbrace{\int_0^1 \dots \int_0^1}_{k \text{ integrals}} f_i(x_1, \dots, x_{i-1}, 0, x_{i+1}, \dots, x_{k+1}) dx_1 \dots dx_{i-1} dx_{i+1} \dots dx_{k+1} \right). \tag{4.2}
 \end{aligned}$$

Every term in the last sum integrates  $f_i$  over one side of the cube  $[0, 1]^{k+1}$ , because plugging in a 1 or a 0 for one parameter and integrating over the others has exactly that effect. The factors  $(-1)^{i-1}$  together with the minus from the fundamental theorem, result exactly in assigning to every term a sign matching the orientation of the respective cube side induced by the border operator applied to  $[0, 1]^{k+1}$ , see Figure 4.6. Also, the form  $f_i dx_1 \wedge \dots \wedge dx_{i-1} \wedge dx_{i+1} \wedge \dots \wedge dx_{k+1}$  vanish on all sides of the cube but on the sides  $x_i = 0$  and  $x_i = 1$ . Therefore, the sum in Equation 4.2 is exactly the integral  $\int_{\delta[0,1]^{k+1}} \omega^k$ , and we have proven

$$\int_{[0,1]^{k+1}} d\omega^k = \int_{\delta[0,1]^{k+1}} \omega^k.$$

□

### 4.2.2. The Geometry of $d$

Stokes' theorem is more than a valuable tool for calculations and for reformulations. It unmasks the geometric meaning of the exterior derivative  $d$ . It is difficult to get an understanding of what the exterior derivative does, only by looking at its definition. But Stokes' theorem helps you understand the exterior derivative. A first realization provided by Stokes is that the exterior derivative acts as a counterpart to the integral in the same way as the usual derivative for scalar functions  $f : \mathbb{R} \rightarrow \mathbb{R}$  does. If  $d\omega^k$  is integrated to  $\omega^k$ , the dimensionality of the integral is reduced by one, an integral dimension is ‘dropped’:

$$\int_{\Omega} d\omega = \int_{\delta\Omega} \omega.$$

But it goes further. Stokes' theorem explains the geometry of  $d$ . It binds the exterior derivative to the border operator, which is a purely geometric operation. Both operations are equivalent in some way, as you can choose either to apply the border operator to a region or to apply the exterior derivative to the differential form at hand. This can be made even clearer by using a bracket notation for the integral; the first argument is the manifold, the second argument is the differential form:

$$[\Omega, \omega] := \int_{\Omega} \omega.$$

Then Stokes' theorem can be formulated as

$$[\Omega, d\omega] = [\delta\Omega, \omega].$$

where the border operator and the exterior operator obviously play an equivalent role. That Stokes' theorem describes the geometric signification of the exterior derivative is maybe easiest to understand by looking at the classical differential operators, as done in the next section.

### 4.2.3. The Geometry of Classical Differential Operators

To highlight that Stokes' theorem captures the geometry of the exterior derivative, we focus on 3-manifolds and the standard calculus differential operators *div* and *curl*. We have seen in Section 4.1.3 that the exterior derivative on  $\mathbb{R}^3$  expressed in euclidean coordinates is the gradient *grad* for 0-forms, the curl  $\nabla \times$  for 1-forms and the divergence *div* for 2-forms. These standard calculus operators can be defined geometrically, they locally measure geometric properties of functions and vector fields.

We start with the curl. The geometric, coordinate free definition of the curl  $\nabla \times v$  of a vector field  $v$  is

$$(\nabla \times v) \cdot n = \lim_{diam(A) \rightarrow 0} \frac{\int_{\partial A} \langle v, t \rangle dx}{Area(A)},$$

where  $n$  is a normal vector,  $A$  is an area patch orthogonal to  $n$  and  $t$  is a tangent to the border of  $A$ , see Figure 4.7. This expresses that the curl measures how much a vector

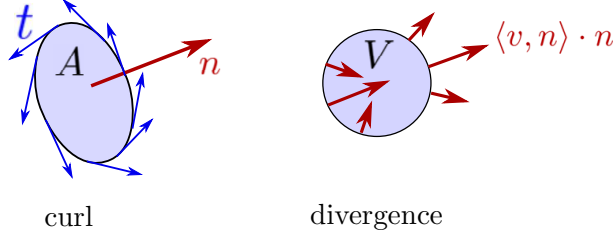


Figure 4.7.: The geometric definition of curl and divergence. Curl measures the flow around a infinitesimal patch orthogonal to a normal  $n$ . Divergence, here displayed in a 2D setting, measures the local netflow.

field rotates around some vector  $n$ . More precisely, the curl operator is an operator that takes a vector field and returns a linear mapping that measures how much the vector field curls around a point. That the exterior derivative  $d_1$  for 1-forms also measures this geometric property when forms are interpreted as in 3.1.5, is exactly captured by Stokes' theorem:

$$\lim_{diam(A) \rightarrow 0} \frac{\int_{\partial A} \omega^1}{Area(A)} = \lim_{diam(A) \rightarrow 0} \frac{\int_A d\omega^1}{Area(A)} = d\omega^1(a, b),$$

where  $a, b$  are vectors with  $a \times b = n$  and  $n$  normal to  $A$ .<sup>2</sup> The geometric interpretation of  $d\omega^1$  is really just stated by Stokes' theorem:  $d\omega^1$  averaged over an infinitesimal area is the same as integrating  $\omega^1$  around the infinitesimal boundary of the area.

The divergence measures the net flow in and out of a volume. The formal geometric definition of divergence is given by

$$div(v) = \lim_{diam(V) \rightarrow 0} \frac{\int_{\partial V} \langle v, n \rangle dx}{Vol(V)},$$

where  $n$  is the normal field on the border of the volume  $V$ , see Figure 4.7. As for  $d_1$ , Stokes' theorem explains that the exterior derivative  $d_2$  for 2-forms measures the same geometric property as the  $div$  operator:

$$\lim_{diam(V) \rightarrow 0} \frac{\int_{\partial V} \omega^2}{Vol(V)} = \lim_{diam(V) \rightarrow 0} \frac{\int_V d\omega^2}{Vol(V)} = d\omega^2.$$

---

<sup>2</sup>Stokes' theorem is used for the first equality. The second equality holds because  $\int_A d\omega^1 / Area(A)$  converges to  $d\omega^1(a, b) / area(a, b)$ , where  $a, b$  are arbitrary vectors lying in the tangential plane aligned to  $A$ . If we additionally require  $a \times b = n$  for a normal  $n$ , then  $area(a, b) = \|a \times b\| = 1$  can be dropped.

## 4.3. The Hodge Star

The exterior derivative can be used to describe all the operators that arise as its special cases, like *curl*, *div* etc (see Figures 4.2 and 4.3). But there is still an important element missing. For example we would like to apply the divergence operator to the gradient of a function  $\text{div}(\text{grad}(f))$  to get the Laplacian, as it is done in standard calculus:

$$\Delta = \text{div} \circ \text{grad}.$$

Figure 4.3 tells us that on 3-dimensional manifolds  $\text{grad}$  is  $d_0$  and  $\text{div}$  is  $d_2$ . This is a problem:  $d_0$  takes a 0-form and maps it to a 1-form, while  $d_2$  takes a 2-form and maps it to a 3-form. We can not apply  $d_2$  to  $d_0$ ! Nor are we able to describe any other higher order derivatives using  $d$ , as  $dd$  always is zero. The key to this ‘problem’ lies in the *duality* of forms.

We have seen that different forms have the same representation. In three dimensions differential 0-forms and differential 3-forms can be represented as real valued functions, 1-forms and 2-forms as vectorfields, so we should be able to naturally go from 1-forms to 2-forms and 0-forms to 3-forms. In  $n$ -dimensions you can generically switch between  $k$ -forms and  $n - k$ -forms. Every  $k$ -form has a dual  $n - k$ -form.

### 4.3.1. Intuition

The idea is to treat a differential  $k$ -form like a differential  $(n - k)$ -form. But while  $k$ -forms measure  $k$ -dimensional volumes,  $(n - k)$ -forms measure  $(n - k)$ -dimensional volumes. To get from one to the other we do the following: for a small  $k$ -dimensional cube  $c$  we let  $c^\perp$  be a  $n - k$ -dimensional cube perpendicular to  $c$  with a volume like  $c$ :

$$c \perp c^\perp,$$

$$\text{vol}_k(c) = \text{vol}_{n-k}(c^\perp).$$

Then, if we want to calculate an approximate integral of a  $k$ -form over a set of  $n - k$ -dimensional cubes  $\{c_1, \dots, c_l\}$ , thereby treating the  $k$ -form like an  $n - k$ -form, the sum

$$\sum_j " \omega^k(c_j) "$$

is instead calculated as

$$\sum_j \omega^k(c_j^\perp),$$

see the sketch in Figure 4.8. As the  $c_j$  are  $n - k$  dimensional, the  $c_j^\perp$  are  $k$ -dimensional and  $\omega^k$  can be used to measure them. To keep the notion of  $k$ -forms clean we associate a *dual*  $n - k$ -form  $\star \omega^k$  to a  $k$ -form  $\omega^k$ , that behaves like described, i.e., in a very dirty notation,

$$\star \omega^k(c) \approx \omega^k(c^\perp).$$

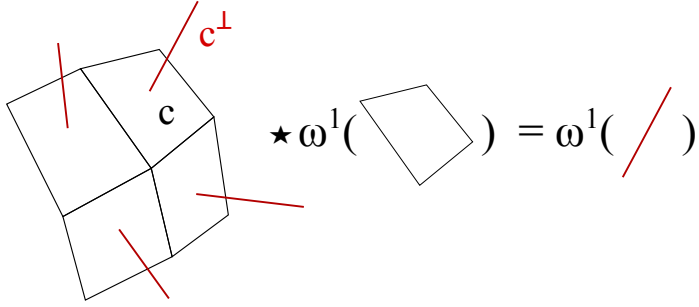


Figure 4.8.: Intuition for duality in  $\mathbb{R}^3$ : We have a one form  $\omega^1$  that can be evaluated on lines and would like a 2-Form  $\star\omega^1$  that can be evaluated on 2-dimensional regions. The dual form  $\star\omega$  evaluated on a small square should be the value of  $\omega^1$  evaluated on the orthogonal complement of the small square with equal volume, in this case an orthogonal line with length *area(square)*.

### 4.3.2. Dual Forms

We will now formally define the dual of a form and then examine how the definition fits the ‘intuition’ developed above.

#### Definition of $\star$

The spaces of forms  $\Lambda^k(\mathbb{R}^n)$  and  $\Lambda^{n-k}(\mathbb{R}^n)$  have the same dimension:

$$\dim(\Lambda^k(\mathbb{R}^n)) = \binom{n}{k} = \binom{n}{n-k} = \dim(\Lambda^{n-k}(\mathbb{R}^n)).$$

As they have the same dimension we can find a bijective linear mapping between these two spaces. Usually this mapping is defined by first defining a scalar product on the space of forms, and then using the scalar product to define the mapping.

In order to define a scalar product on the space  $\Lambda^k$  we select an orthonormal basis  $e_1, \dots, e_n$  of  $\mathbb{R}^n$  with respect to the Euclidean scalar product<sup>3</sup> and define the scalar product for two  $k$ -forms  $\omega^k, \nu^k$  as

$$\langle \omega^k, \nu^k \rangle = \sum_{i_1 < \dots < i_k} \omega^k(e_{i_1}, \dots, e_{i_k}) \cdot \nu^k(e_{i_1}, \dots, e_{i_k}).$$

This definition does *not* depend on the choice of the basis. If both forms are written in the base given by the  $de_i$ 's, the scalar product is:

$$\omega^k = \sum_{i_1 < \dots < i_k} w_{i_1, \dots, i_k} de_{i_1} \wedge \dots \wedge de_{i_k}$$

---

<sup>3</sup>Note that the Hodge duality is usually defined with respect to an arbitrary scalar product, but for us this will do

$$\nu^k = \sum_{i_1 < \dots < i_k} v_{i_1, \dots, i_k} de_{i_1} \wedge \dots \wedge de_{i_k}$$

$$\langle \omega^k, \nu^k \rangle = \sum_{i_1 < \dots < i_k} v_{i_1, \dots, i_k} \cdot w_{i_1, \dots, i_k},$$

i.e., the euclidean scalar product of the vectors describing  $v$  and  $w$ . This really is a scalar product: it is linear in both parameters and symmetric.

Duality is then defined using the volume form  $dVol$ , the form that computes the oriented volume of the input vectors, which in an orthonormal basis  $e_1, \dots, e_n$  is given by

$$dVol = de_1 \wedge \dots \wedge de_n.$$

The dual  $\star\omega^k$  of a  $k$ -form  $\omega^k$  is defined to be the  $n - k$ -form that fulfills

$$\langle \star\omega^k, \nu^{n-k} \rangle dVol = \omega^k \wedge \nu^{n-k} \text{ for all } (n - k)\text{-forms } \nu^{n-k}. \quad (4.3)$$

In the next Section we will try to match this definition to the intuition for the  $\star$ -operator developed above. The operator  $\star$  is called the Hodge star and  $\star\omega^k$  the Hodge star dual of  $\omega^k$ . The Hodge star describes a *linear* mapping from  $\Lambda^k$  to  $\Lambda^{n-k}$ :

$$\star(\omega_1^k + \lambda\omega_2^k) = \star\omega_1^k + \lambda\star\omega_2^k. \quad (4.4)$$

### Understanding $\star$

We can understand the definition of the Hodge operator by looking at how  $\star$  acts on basis elements  $de_{i_1} \wedge \dots \wedge de_{i_k}$  for a positively oriented orthonormal basis  $e_1, \dots, e_n$ . Following the definition of the  $\star$  operator in Equation 4.3, we need to find a form

$$\omega = \star(de_{i_1} \wedge \dots \wedge de_{i_k}),$$

such that

$$\langle \omega, \nu^{n-k} \rangle = (de_{i_1} \wedge \dots \wedge de_{i_k}) \wedge \nu^{n-k} \quad (4.5)$$

for all  $n - k$  forms  $\nu^{n-k}$ . It is enough to ensure that Equation 4.5 holds for basis  $n - k$ -forms  $\nu^{n-k} = de_{j_1} \wedge \dots \wedge de_{j_{n-k}}$ , as then, by linearity, it holds for arbitrary  $n - k$ -forms. Inserting basis forms  $\nu^{n-k} = de_{j_1} \wedge \dots \wedge de_{n-k}$  in the righthand side of Equation 4.5, we get

$$(de_{i_1} \wedge \dots \wedge de_{i_k}) \wedge (de_{j_1} \wedge \dots \wedge de_{j_{n-k}}) = \begin{cases} 0, & \text{if any } i_l \text{ and } j_m \text{ coincide,} \\ sign dVol, & \text{else.} \end{cases}$$

Here  $sign$  is the sign that comes from reordering the indices  $i_1, \dots, i_k, j_1, \dots, j_{n-k}$ , in the case that no  $i_l$  and  $j_m$  coincides, i.e.,  $j_1, \dots, j_{n-k}$  is the complement of the indices  $i_1, \dots, i_k$  in the set  $\{1, \dots, n\}$ . The  $sign$  is the sign in the equation

$$de_{i_1} \wedge \dots \wedge de_{i_k} \wedge de_{j_1} \wedge \dots \wedge de_{j_{n-k}} = sign \cdot de_1 \wedge de_2 \wedge \dots \wedge de_n.$$

But the only  $k$ -form  $\omega$  with

$$\langle \omega, (de_{j_1} \wedge \dots \wedge de_{j_{n-k}}) \rangle = \begin{cases} 0, & \text{if any } i_l \text{ and } j_m \text{ coincide,} \\ sign dVol, & \text{else,} \end{cases}$$

is the form

$$\omega = sign \cdot de_{j_1} \wedge \dots \wedge de_{j_{n-k}},$$

where the  $j_1, \dots, j_{n-k}$  are the complement of the indices  $i_1, \dots, i_k$  in the set  $\{1, \dots, n\}$ . Therefore, the dual of a basis element  $(de_{i_1} \wedge \dots \wedge de_{i_k})$ , following the definition in Equation 4.3 is

$$\star(de_{i_1} \wedge \dots \wedge de_{i_k}) = sign \cdot de_{j_1} \wedge \dots \wedge de_{j_{n-k}}, \quad (4.6)$$

with the  $j_1, \dots, j_{n-k}$  complementary to  $i_1, \dots, i_k$ , and the *sign* as discussed. Does this mean that the definition of Equation 4.3 matches the intuition for the Hodge  $\star$  developed earlier? It does. Consider the following example:

### Example

In a three dimensional setting with an orthonormal basis  $e_1, e_2, e_3$ , the Equation 4.6 results in

$$\star de_1 = de_2 \wedge de_3,$$

$$\star de_3 = de_1 \wedge de_2,$$

and

$$\star de_2 = -de_1 \wedge de_3 = de_3 \wedge de_1,$$

where we have a minus because

$$de_2 \wedge de_1 \wedge de_3 = -de_1 \wedge de_2 \wedge de_3.$$

This shows that the  $\star$  is close to the intuitive description in Section 4.3.1: suppose  $v = a \times b$  for vectors  $a, b$  and  $v$  in  $\mathbb{R}^3$ . The vectors  $a, b$  span a patch perpendicular to  $v$  with an area equal to the length of  $v$ . Furthermore,

$$de_1(v) = v_1 = (a_2 b_3 - a_3 b_2),$$

$$\star de_1(a, b) = (de_2 \wedge de_3)(a, b) = a_2 b_3 - a_3 b_2,$$

therefore,

$$\star de_1(a, b) = de_1(v),$$

so  $\star de_1$ ing the patch spanned by  $a, b$  is like  $de_1$ ing the ‘line’  $v$ , this is depicted in Figure 4.9. The same is true for  $de_2$  and  $de_3$ . And as the  $\star$  operator is linear and any one form is a sum  $\omega^1 = \lambda_1 de_1 + \lambda_2 de_2 + \lambda_3 de_3$  we get

$$\star \omega^1(a, b) = \omega^1(v).$$

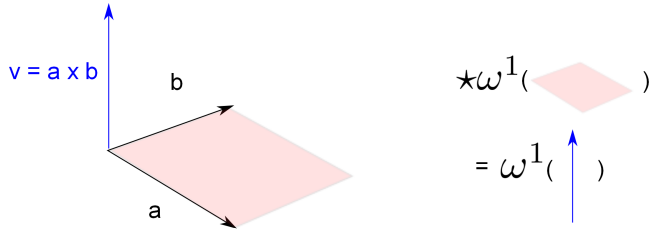


Figure 4.9.: Following the definition of the  $\star$  operator and Equation 4.6, we get in  $\mathbb{R}^3$  for  $v = a \times b \star \omega^1(a, b) = \omega^1(v)$  which is close to the intuition developed in Section 4.3.1. Compare this also to Figure 4.8

### 4.3.3. Realization of $\star$ in Standard Calculus

Differential forms relate to objects from standard calculus. We now determine how the  $\star$  operator acts on these presentations.

#### 0-forms and volume forms

The dual of a 0-form  $f$  is simply  $fdVol$  and the dual of an  $n$ -form  $fdVol$  is simply  $f$ - so the  $\star$  operator denotes only a change of interpretation of a function  $f$  as a 0-form or an  $n$ -form and is the identity in standard calculus:

$$\star f = f dVol,$$

$$\star f dVol = f.$$

#### 1-forms and 2-forms in $\mathbb{R}^3$

In three dimensions applying the Hodge operator to the 1-form associated to a vectorfield leads to the two form associated to the same vectorfield. The star operator again denotes only a change of interpretation:

$$\star(v_1de_1 + v_2de_2 + v_3de_3) = v_1(de_2 \wedge de_3) + v_2(de_3 \wedge de_1) + v_3(de_1 \wedge de_2),$$

$$\star(v_1(de_2 \wedge de_3) + v_2(de_3 \wedge de_1) + v_3(de_1 \wedge de_2)) = v_1de_1 + v_2de_2 + v_3de_3.$$

#### 1-forms in $\mathbb{R}^2$

For 1-forms on two dimensional manifolds something happens. The dual of a one form is again a one form, and

$$\star de_1 = de_2,$$

$$\star de_2 = -de_1,$$

$$\star(a de_1 + b de_2) = b de_1 - a de_2.$$

The operation equivalent to the Hodge  $\star$  for a two dimensional vector field is a rotation by  $90^\circ$ , in orthonormal coordinates this is simply

$$\begin{pmatrix} 0 & 1 \\ -1 & 0 \end{pmatrix}.$$

It also follows that  $\star\star\omega^1 = -\omega^1$  as rotating a vector twice by  $90^\circ$  changes its orientation. Note that this is directly related to the two sampling schemes for 1-forms described in Section 3.2.1. Once the vector field  $v$  is sampled and once the vectorfield rotated by  $90^\circ$  is sampled. This is like interpreting the sampled vector field once as  $\star\omega^1$  and once as  $\omega^1$ .

### The dual of the dual k-form

Differential 1-forms on 2-dimensional manifolds are not special, considering their behavior under the Hodge star. One can show with little effort that

$$\star\star\omega^k = (-1)^{k(n-k)}\omega^k.$$

Applying  $\star$  twice will switch the orientation of  $\omega^k$  exactly when  $k(n - k)$  is not even. But for  $n = 2, 3$ , the pair  $n = 2$  and  $k = 1$  is the only one where  $k(n - k)$  is not even and  $\star\star$  not the identity.

## 4.4. Exterior Calculus

The operators  $\star, d, \wedge$  build a very elegant and powerful language. This is the language of exterior calculus. In a 3 dimensional setting you additionally have the two operators  $\#$  and  ${}^\flat$  mentioned in Section 3.1.5, which formalize the relation between standard calculus and exterior calculus.

The operators  $\star, d$  can be used to describe higher order differential operators; for example  $d\star d$  is a second order operator. The operator  $\wedge$  concatenates differential forms and the operators  $\#$  and  ${}^\flat$  formalize the relation between 1-forms and vectorfields (see Section 3.1.5).

The most important operators of exterior calculus are the  $\star$  and  $d$  operator. They form the so-called de Rham complex, depicted in Figure 4.10. This complex summarizes how the operators of exterior calculus can be used to express standard calculus operators. We will meet important relations on this conglomerate of differential-form spaces and the operators  $d$  and  $\star$ . Note that the de Rham complex is a so called chain complex and has very interesting properties; these properties are maintained by the discrete de Rham complex, but this goes beyond the scope of this thesis.

One strength of exterior calculus is that differential operators can be formulated independently of the maps chosen to parametrize a manifold. Also it does not matter what manifold you are on. The operator  $d$  always retains its geometric meaning. For example  $d_0$  is always the gradient operator.

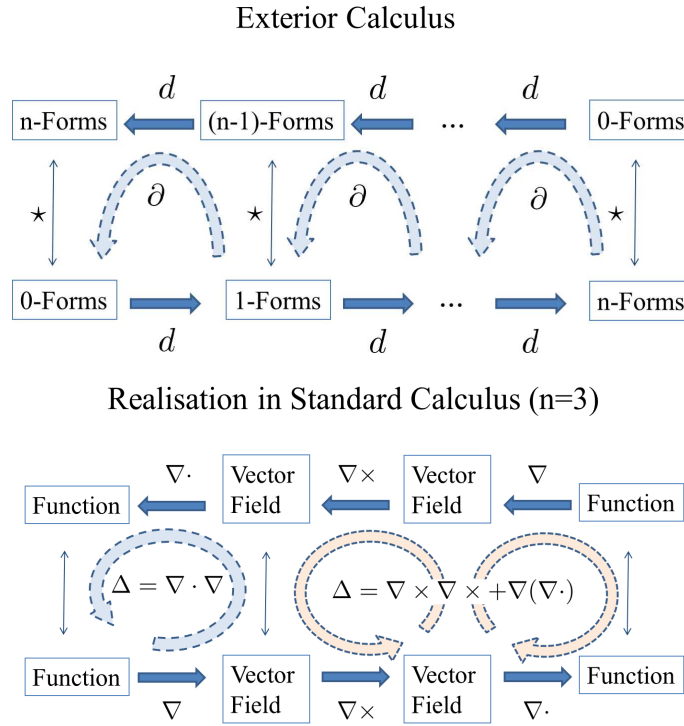


Figure 4.10.: Top: the de Rham complex for an  $n$ -dimensional manifold. The co-derivative  $\partial$  introduced in Section 4.4.1 is a concatenation of  $\star$  and  $d$ , for  $k$ -forms it is given by  $\partial_k = (-1)^k \star_{k+1}^{-1} d_{n-k} \star_k$ . Bottom: the realization of the de Rham complex in standard calculus. The dashed arrows represent Laplacians defined by concatenating operators.

The realization of the de Rham complex in 2 dimensions is depicted in Figure 4.11;  $\nabla \times$  in  $\mathbb{R}^2$  is

$$\nabla \times := \frac{\partial}{\partial x_2} - \frac{\partial}{\partial x_1}.$$

Using the star operator we can also describe the divergence operator in 2 dimensions. The realization of  $\star^{-1} d \star$  for 1-forms is minus the divergence operator  $\nabla \cdot$ .

#### 4.4.1. The Coderivative

It is useful to define an additional operator: the so called coderivative  $\partial_k$ , which is given by

$$\partial_k = (-1)^k \star_{k+1}^{-1} d_{n-k} \star_k.$$

It takes a differential  $k$ -form and returns a differential  $k-1$ -form. In two dimensions  $\partial_1$  is the divergence operator. Besides being a handy abbreviation, it is the adjoint to the

### Realisation in Standard Calculus (n=2)

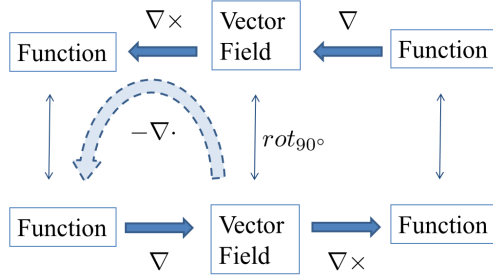


Figure 4.11.: The realization of the de Rham complex in two dimensions.

exterior derivative on borderless compact manifolds  $M$  or if one of the differential forms is zero on the border  $\delta M$ ,<sup>4</sup>

$$\langle d\omega, \nu \rangle = \langle \omega, \partial\nu \rangle, \quad (4.7)$$

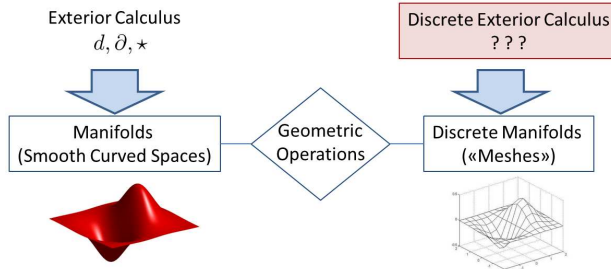
where the scalar product for forms is extended to differential forms via

$$\langle \omega, \nu \rangle = \int_M \langle \omega^k, \nu^k \rangle dVol = \int_M \omega \wedge \star \nu.$$

---

<sup>4</sup>The adjointness follows directly from Stokes' theorem and the behavior of  $d$  and  $\wedge$ :  $0 = \int_{\delta M} \omega^k \wedge \star \nu^{k+1} = \int_M (d\omega \wedge \star \nu - (-1)^{k+1} \omega \wedge d \star \nu)$  and then setting  $\omega \wedge d \star \nu = \omega \wedge \star \star^{-1} d \star \nu$  we end  $0 = \int_M \langle d_k \omega^k, \nu^{k+1} \rangle dVol - \int_M \langle \omega^k, \partial_{k+1} \nu^{k+1} \rangle dVol$

## 4.5. Discrete Exterior Calculus



We have introduced all ingredients needed to define Discrete Exterior Calculus. We use the common geometric features of smooth manifolds and discrete manifolds and exploit the acquired geometric understanding of the exterior derivative and the Hodge star, to introduce a Discrete Exterior Calculus that is geometrically close to Exterior Calculus.

This section is based on [Hir03] and [DKT08].

### 4.5.1. The Discrete Exterior Derivative

Both smooth and discrete manifolds have common geometric operations, namely the border operator. This can be used now to define a discrete exterior derivative on discrete manifolds, which preserves the geometry of the exterior derivative.

To conserve the geometry of  $d$  means to conserve Stokes' theorem. We can directly translate Stokes' theorem to the discrete setting. In the discrete setting the integral of a discrete form  $\mathbf{w}$  over a set of simplices  $\sigma$  is the scalar product  $\langle \sigma, \mathbf{w} \rangle$  and Stokes' theorem,

$$[\Omega, d\omega] = [\delta\Omega, \omega],$$

becomes

$$\langle \sigma, d_{\text{discrete}}^k \mathbf{w}^k \rangle = \langle \delta_{k+1} \sigma, \mathbf{w}^k \rangle, \quad (4.8)$$

where  $d_{\text{discrete}}$  is yet unknown. But this relation *defines* the unknown  $d_{\text{discrete}}$ , there is only one possible choice for  $d_{\text{discrete}}$  to meet 4.8. Using basic linear algebra we get

$$\langle \delta_{k+1} \sigma, \mathbf{w}^k \rangle = (\delta_{k+1} \sigma)^T \mathbf{w}^k = \sigma^T (\delta_{k+1}^T \mathbf{w}^k) = \langle \sigma, \delta_{k+1}^T \mathbf{w}^k \rangle.$$

This means that  $d_{\text{discrete}}^k$  has to be the transposed of the border-operator matrix

$$d_{\text{discrete}}^k = \delta_{k+1}^T.$$

This short argument shows that in order to get a discrete derivative that preserves Stokes' theorem and that preserves the geometric properties of the exterior derivative,  $d_{\text{discrete}}$  has to be the transposed of the border operator. Here you see once more how closely related the boundary operator and the exterior derivative are. This is

$$\begin{pmatrix} h_1 \\ h_2 \\ \vdots \\ h_9 \end{pmatrix} = \underbrace{\begin{pmatrix} -1 & 1 & 1 \\ \vdots & & \vdots \\ 1 & 1 & 1 \end{pmatrix}}_{d^1_{discrete}} \underbrace{\begin{pmatrix} g_1 \\ g_2 \\ \vdots \\ g_{18} \end{pmatrix}}_{1\text{ Form}}$$

$$h_1 = g_3 + g_2 - g_1$$

Figure 4.12.: Curl is realized as the incidence matrix of the faces. By applying this matrix the values on the border edges of a face are summed up according to the orientation of the face (thus  $-g_1$ )

the main insight behind DEC: the geometric importance of Stokes' theorem, which ties the exterior derivative to the border operator, and that the discrete exterior derivative should be tied to the discrete border operator in the same way.

### Examples

For example we know that  $d_0$  applied to 0-forms is the gradient. Our discrete realization of the exterior derivative for 0-forms is the matrix

$$d^0_{discrete} = \delta_1^T,$$

i.e., the transposed of the discrete border operator matrix for 1-simplices. This is a matrix with dimension (*#edges*  $\times$  *#vertices*). Applying this matrix to a discrete 0-form yields a vector of dimension *#edges*, a discrete 1-form. As  $\delta_1^T$  is the incidence matrix of the edges, it assigns the value  $\mathbf{w}^0(v_1) - \mathbf{w}^0(v_0)$  to an edge  $(v_0, v_1)$ . The gradient is simply realized as a difference.

Another example is the curl operator, depicted in Figure 4.12. The curl operator is a realization of  $d$  applied to differential 1-forms. In the discrete setting curl therefore is realized as

$$d^1_{discrete} = \delta_2^T.$$

As this is the incidence matrix of faces, applying  $d_1$  to a 1-form sums up the values of the discrete 1-form on edges along a face and assigns the sum to the face.

### Correctness

The discrete exterior derivative  $d_{discrete}$  does not introduce any new errors. It is consistent with the way we interpret and sample discrete differential forms: taking the exterior derivative before sampling a form produces the same result as applying the discrete exterior derivative after sampling.

Suppose that  $\mathbf{w}^0$  samples  $\omega^0$ . Then  $d_{discrete}^0 \mathbf{w}^0$  exactly samples  $d\omega^0$ :

$$\int_{[v_0, v_1]} d\omega^0 = \omega^0(v_1) - \omega^0(v_0) = \mathbf{w}^0(v_1) - \mathbf{w}^0(v_0).$$

But, by design, this is true for  $d_{discrete}^k$  with any  $k$ : suppose  $\mathbf{w}^k$  samples  $\omega^k$ , then

$$\int_{\sigma^{k+1}} d\omega^k = \int_{\delta\sigma^{k+1}} \omega^k = \langle \delta_{k+1}(\sigma^{k+1}), \mathbf{w}^k \rangle = (d_{discrete}^k \mathbf{w}^k)(\sigma^{k+1}).$$

What is left to be done is finding a discrete star operator and finding a way to represent discrete dual forms  $\star\mathbf{w}$ . If  $\mathbf{w}^k$  is a discrete  $k$ -form associated to  $k$ -dimensional simplices, the dual should be a discrete  $n - k$ -form associated to  $n - k$ -dimensional objects. For this we use a **dual mesh**. We use Voronoi duality, because it facilitates the definition of a discrete  $\star$ .

### 4.5.2. The Dual Mesh

When reading on it is important to keep the intuition behind the Hodge star in mind. Remember that  $k$ -forms  $\omega^k$  can be used to measure things on  $k$ -dimensional sets, while their dual  $\star\omega^k$  is a  $n - k$  form, measuring  $n - k$ -dimensional sets. Furthermore, if a  $k$ -form measures something on an (infinitesimal)  $k$ -cell, its dual measures the same thing on a  $n - k$ -cell orthogonal to it. For details revisit Section 4.3.

We illustrate the problem with discrete dual forms and the reason why we a dual mesh is introduced with an example in two dimensions. Consider  $\mathbb{R}^2$  with the standard coordinates  $(x, y)$ . As an example form we choose the differential 1-form  $\omega^1 = dx + a \cdot dy$  with an arbitrary weight  $a \in \mathbb{R}$ ; its dual is the 1-form  $\star\omega^1 = -a \cdot dx + dy$ . Sampling  $\omega^1$  on a straight edge  $e$  connecting the points  $(x_{start}, y_{start})$ ,  $(x_{end}, y_{end})$  produces

$$\mathbf{w}(e) = (x_{end} - x_{start}) + a(y_{end} - y_{start}). \quad (4.9)$$

Sampling the dual form  $\star\omega^1$  on some edge  $e$  gives

$$\star\mathbf{w}(e) = (y_{end} - y_{start}) - a(x_{end} - x_{start}). \quad (4.10)$$

As the dual form is a 1-form, so associating the discrete dual form to 1-dimensional objects, i.e. edges, is the right thing to do. The question is which edges should be chosen and how the discrete dual form can be computed from the discrete primary form.

The first approach might be to associate  $\star\mathbf{w}$  to the same edges as  $\mathbf{w}$ . But how can  $\star\mathbf{w}(e)$  be computed from  $\mathbf{w}(e)$ ? Suppose that the edge  $e$  is aligned to the  $x$ -axis and has length  $l$ . In our example, following Equations 4.9 and 4.10,

$$\mathbf{w}(e) = l,$$

$$\star\mathbf{w}(e) = a \cdot l.$$

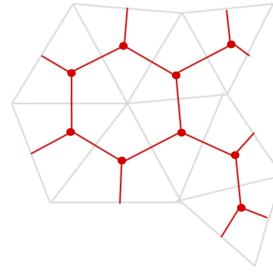


Figure 4.13.: The dual mesh (red) of a primary mesh (grey)

As for an arbitrary 1-form the value  $a$  can be arbitrary, there is no general relation between  $\star\mathbf{w}(e)$  and  $\mathbf{w}(e)$  for a fixed edge  $e$ . For a single edge  $e$ ,  $\mathbf{w}(e)$  does not carry any information about  $\star\mathbf{w}(e)$ , as  $a$  is unknown!

One possibility to overcome this would be to take edges around  $e$  into account to compute the value of the dual form on  $e$ , but this would loose information due to interpolation or would need additional assumptions. Still, this is a valid approach, and it will be used in Chapter 6 to compute the dual form on boundary edges. Another possibility is not to try to associate  $\star\mathbf{w}$  to the same edges as  $\mathbf{w}$ . While  $\omega$  measured on  $e$  does not carry information about  $\star\omega$  on  $e$ , we saw in Section 4.3 that there is a strong connection between  $\omega$  measured on  $e$  and  $\star\omega$  measured on an edge orthogonal to  $e$ ,  $e^\perp$ :

$$\omega(e) \approx \star\omega(e^\perp).$$

Indeed, if  $e^\perp$  is  $e$  rotated by  $90^\circ$ , then in our example (where the differential form is constant), the correct choice for  $\star\mathbf{w}(e^\perp)$  would be

$$\star\mathbf{w}(e^\perp) = \mathbf{w}(e).$$

This motivates the introduction of a dual mesh on top of the mesh, whose edges are orthogonal to the old edges. Or more generally to have a dual complex on top of the simplicial complex, whose ‘dual’ cells are orthogonal to the old ‘primary’ simplices.

### Voronoi Duality

In two dimensions, the dual mesh of a mesh is produced by replacing faces by vertices, edges by edges that connect the vertices dual to the faces the edge lies in between and vertices by faces, see Figure 4.13. The Voronoi dual of a mesh additionally has the property that dual edges are orthogonal to primary edges. The dual mesh in Figure 4.13 is a Voronoi dual.

The Voronoi dual of a simplicial complex is not a simplicial complex but a cell complex, just as the dual of the triangle mesh in Figure 4.13 is not again a triangle mesh. Instead of  $k$ -simplices, the dual consist of  $k$ -cells. The Voronoi dual of a discrete  $n$ -manifold is constructed as follows: the Voronoi dual of a  $n$ -simplex is its circumcenter. The Voronoi

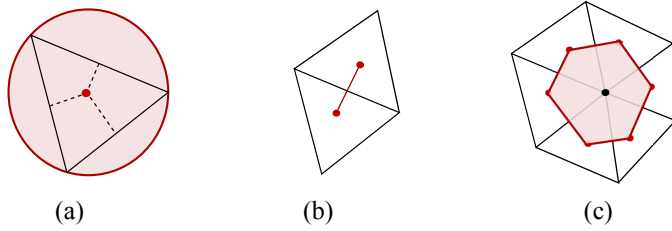


Figure 4.14.: The duals on a discrete 2-manifold: (a) The circumcenter of a triangle is the dual of the triangle. (b) The dual of an edge connects the dual vertices of the incident faces. (c) The dual of the central vertex is the 2-cell whose boundary vertices are again the dual of the incident faces. Here everything is depicted without orientation.

dual of a  $k$ -simplex is the  $n - k$  dimensional cell spanned by the circumcenters of the incident  $n$ -simplices, as depicted for  $n = 2$  in Figure 4.14.

From now on we will always make the difference the primal mesh consisting of primal vertices, edges, faces etc and the dual mesh consisting of dual vertices, edges and so on. If  $\sigma$  is a simplex, we will denote its dual cell by  $\star\sigma$ .

### Border Operator and Orientation of the Dual Mesh

A dual cell complex allows the definition of orientations, a border operator and finally an exterior derivative in the same way as simplicial complexes. But while we fix arbitrary reference orientations for primary simplices, the dual cells have an orientation that is induced by the orientation of the primary simplices. For discrete 2 and 3-manifolds the induced orientations are depicted in Figure 4.15. For more details see the Appendix A.2.

The border operator on the dual cell complex is very closely related to the border operator on the primary complex. A dual  $j$  cell  $\star\sigma^{n-j}$  is on the border of the dual  $j + 1$ -cell  $\star\sigma^{n-j-1}$  exactly if  $\sigma^{n-j-1}$  is on the border of  $\sigma^{n-j}$ . For example in  $n = 2$  a dual edge  $\star e$  is on the boundary of the dual face of a vertex  $\star v$ , exactly if the vertex  $v$  is on the boundary of the edge  $e$ .

The primary boundary matrix has an entry at the position  $(i, j)$ ,  $\delta(i, j) \neq 0$ , exactly if the implex  $i$  is on the boundary of the simplex  $j$ . But in that case the dual of the simplex  $j$  is on the boundary of the dual of the simplex  $i$ . Therefore, the border operator on the dual complex  $\delta^{\text{dual}}$  has  $\delta^{\text{dual}}(j, i) \neq 0$ . This means that

$$\delta_k(i, j) \neq 0 \Leftrightarrow \delta_{n-k+1}^{\text{dual}}(j, i) \neq 0.$$

But the dual border-matrix is not directly given by the transposed primary border matrix  $\delta^T$ ; we have to take care of orientations of the dual cells, as a dual cell  $\star\sigma$  on the dual mesh gets an orientation induced by the primary simplex  $\sigma$ , as depicted in Figure 4.15. The problem is that if a simplex  $\sigma$  lies on the border of an other simplex  $\tau$  and  $\sigma$  is positively oriented relative to  $\tau$ ,  $\star\tau$  lies on the border of  $\star\sigma$  but does *not* need to have

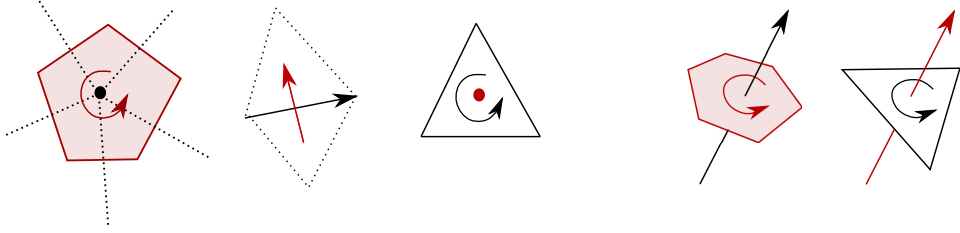


Figure 4.15.: The dual cells (red) with the orientations induced by the primary simplices. The first three sketches are in  $\mathbb{R}^2$ , the last two in  $\mathbb{R}^3$

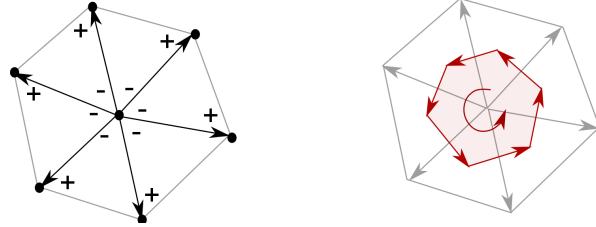


Figure 4.16.: The central vertex is negatively oriented with respect to the incident edges (left). The dual edges and the dual face have an induced orientation, drawn in red. The dual edges are oriented positively with respect to the dual face, while the center vertex was oriented negatively relative to the edges. Therefore  $\delta_2^{dual} = -(\delta_1^{primal})^T$  in the  $n = 2$  dimensional setting.

a positive orientation relative to  $\star\sigma$ , considering their induced orientations. An example of this for  $n = 2$  is given in Figure 4.16.

In the Appendix A.2 we show that the dual border operator  $\delta_k^{dual}$ , which maps  $k$ -cells to boundary  $k - 1$  cells is the transposed of the primary border matrix, but for a sign depending on the manifold dimension  $n$  and the order  $k$  of the forms:

$$\delta_k^{dual} = (-1)^{n-k+1} (\delta_{n-k+1}^{primal})^T. \quad (4.11)$$

### 4.5.3. Discrete Dual Forms

While in the continuous case the Hodge dual of a differential form is again a differential form, we make a strict distinction between discrete primary forms and discrete dual forms. While the discrete primary forms are defined on the simplices of the primary mesh, the discrete dual forms are defined on the dual mesh. The value of the discrete dual form  $\star\mathbf{w}$  on a dual simplex  $\star\sigma$  represents a sampled value of  $\star\omega$ :

$$\star\mathbf{w}(\star\sigma) = \int_{\star\sigma^k} \star\omega^k. \quad (4.12)$$

The discrete exterior derivative for dual forms on the dual mesh defined in the same way as the discrete exterior derivative on the primary mesh. In order to preserve the

geometry of  $d$  revealed by Stokes' theorem it is

$$d_{n-k}^{dual} = (\delta_{n-k+1}^{dual})^T.$$

Expressed with primal matrices, using Equation 4.11

$$d_{n-k}^{dual} = (-1)^k (\delta_k^{primal}) = (-1)^k (d_{k-1}^{primal})^T. \quad (4.13)$$

#### 4.5.4. The Discrete Hodge Star

A discrete Hodge operator has to describe the relation between a discrete form  $\mathbf{w}^k$  and its dual  $\star\mathbf{w}^k$ ,

$$\begin{aligned}\mathbf{w}^k &= (\mathbf{w}^k(\sigma_1^k), \dots, \mathbf{w}^k(\sigma_m^k)), \\ \star\mathbf{w}^k &= (\star\mathbf{w}^k(\star\sigma_1^k), \dots, \star\mathbf{w}^k(\star\sigma_m^k)).\end{aligned}$$

This amounts to considering how the integrals

$$\mathbf{w}^k(\sigma^k) = \int_{\sigma^k} \omega^k, \quad \star\mathbf{w}^k(\star\sigma^k) = \int_{\star\sigma^k} \star\omega^k$$

relate. As we use the Voronoi duality,  $\star\sigma$  is orthogonal to  $\sigma$ . If  $\omega^k$  is constant on  $\sigma^k$  and  $\star\sigma^k$ , we have, because of the way the Hodge star is designed

$$\int_{\star\sigma} \star\omega^k = \frac{\text{Vol}_{n-k}(\star\sigma^k)}{\text{Vol}_k(\sigma^k)} \int_{\sigma} \omega^k.$$

This motivates the use of the following diagonal matrix as a discrete version of the  $\star$  operator to relate the discrete dual and primary forms:

$$\star_k^{discrete} = \begin{pmatrix} \frac{\text{Vol}_{n-k}(\star\sigma_1^k)}{\text{Vol}_k(\sigma_1^k)} & & & \\ & \frac{\text{Vol}_{n-k}(\star\sigma_2^k)}{\text{Vol}_k(\sigma_2^k)} & & \\ & & \ddots & \\ & & & \frac{\text{Vol}_{n-k}(\star\sigma_m^k)}{\text{Vol}_k(\sigma_m^k)} \end{pmatrix}.$$

The dual of a discrete differential form is computed by

$$\star\mathbf{w}^k = \star_k^{discrete} \mathbf{w}^k.$$

#### Correctness

This discrete  $\star$  operator is *not* compatible with the sampling scheme; the dual of a discrete form  $\mathbf{w}^k$  sampling  $\omega^k$  only approximates a correctly sampled  $\star\omega^k$ . But if the size of the simplices gets smaller, the error of  $\star_k^{discrete}$  goes to zero, as  $\omega^k$  will be close to constant in small regions.

This simple  $\star_k^{discrete}$  operator still proves to be quite good. From a numerical point of view it is beneficial that the star operator is a diagonal matrix. By associating dual forms to dual Voronoi cells, the geometry of the Hodge star is captured quite well by this discrete Hodge star.

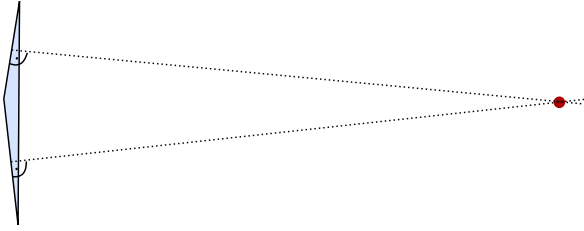


Figure 4.17.: The Voronoi dual of the obtuse simplex lies face away from the primary simplex. Here estimating the value of a dual form at the dual vertex by using the sampled value on the primary triangle can be arbitrarily bad.

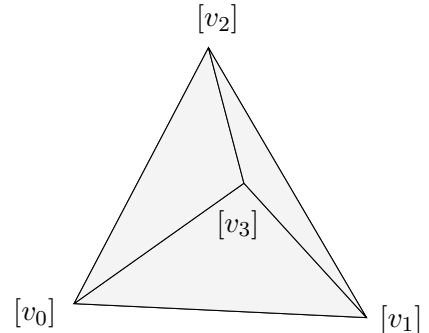
### Drawbacks of Voronoi Duality

Another drawback when choosing the dual mesh and discrete star as described is that Voronoi cells degenerate in the presence of obtuse simplices. The circumcenter of a simplex can lie arbitrarily far away from the simplex such that  $\star_{\text{discrete}} \mathbf{w}^k$  is not a good estimation for a sampled dual form, see Figure 4.17. Adapting the dual mesh and star matrices as done by Desbrun et Al. to derive a Laplacian in [MDSB02] or using a different dual mesh and star operator might be beneficial. But this was not investigated in this thesis.

#### 4.5.5. A Fully Formulated Example

With the discrete Hodge star we have now seen all basic DEC matrices. For illustration purposes we set up all DEC matrices occurring on the tetrahedra mesh depicted in the inlined Figure, considered as a discrete 2-manifold. Note that the faces are oriented consistently.

$$\begin{array}{ll}
 [e_0] = \{v_0, v_1\} & [f_0] = \{v_0, v_1, v_2\} \\
 [e_1] = \{v_0, v_2\} & [f_1] = \{v_1, v_3, v_2\} \\
 [e_2] = \{v_0, v_3\} & [f_2] = \{v_0, v_2, v_3\} \\
 [e_3] = \{v_1, v_2\} & [f_3] = \{v_0, v_3, v_1\} \\
 [e_4] = \{v_1, v_3\} & \\
 [e_5] = \{v_2, v_3\} &
 \end{array}$$



In the image, reference orientations for the simplices and a reference enumeration of the occurring simplices has been chosen. Next we set up the primary border matrices. The border matrix  $\delta_1$  stores the relative orientation of vertices and edges. It has dimension

$\#vertices \times \#edges$ , rows correspond to vertices and columns to edges.

$$\delta_1 = \begin{pmatrix} -1 & -1 & -1 & 0 & 0 & 0 \\ 1 & 0 & 0 & -1 & -1 & 0 \\ 0 & 1 & 0 & 1 & 0 & -1 \\ 0 & 0 & 1 & 0 & 1 & 1 \end{pmatrix}$$

The border operator  $\delta_2$  stores the relative orientation of faces and edges, it has dimension  $\#edges \times \#faces$ , rows correspond to edges and columns to faces:

$$\delta_2 = \begin{pmatrix} 1 & -1 & 0 & 1 & 0 & 0 \\ 0 & 0 & 0 & -1 & 1 & -1 \\ 0 & 1 & -1 & 0 & 0 & 1 \\ -1 & 0 & 1 & 0 & -1 & 0 \end{pmatrix}.$$

The primary exterior derivatives are given by the transposed of the border operators:

$$d_0 = \delta_1^T, \quad d_1 = \delta_2^T.$$

Now to the dual mesh. Most of the time we do not need to compute and keep the locations of the dual vertices explicitly, it is enough to set up the hodge star matrices and the dual exterior derivatives, where the later might not have to be stored explicitly, as they are, but for a factor, the transposed of the primary exterior derivatives. Yet for the sake of completeness: one closed formula for the circumcenter of a triangle  $p_0, p_1, p_2$  is

$$p_{circumcenter} = \alpha p_0 + \beta p_1 + \gamma p_2$$

with

$$\alpha = \frac{|p_1 - p_2|^2 (p_0 - p_1) \cdot (p_0 - p_2)}{2 |(p_0 - p_1) \times (p_1 - p_2)|^2}, \quad \beta = \frac{|p_0 - p_2|^2 (p_1 - p_0) \cdot (p_1 - p_2)}{2 |(p_0 - p_1) \times (p_1 - p_2)|^2},$$

$$\gamma = \frac{|p_0 - p_1|^2 (p_2 - p_0) \cdot (p_2 - p_1)}{2 |(p_0 - p_1) \times (p_1 - p_2)|^2}.$$

Note that there exist a variety of alternative formulas. The dual mesh is sketched in Figure 4.18.

The Hodge star matrices consist of dual-primal ratios. The matrix  $\star_0$  stores the ratios  $\frac{Vol(\star v)}{Vol(v)}$ . As the 0-dimensional volume of a vertex is 1,  $\star_0$  simply consists of the volumes of the Voronoi cells, i.e. the Voronoi areas. Voronoi areas can be computed directly, without computing the circumcenters first, see e.g. [MDSB02] for details and refinements. The contribution of one triangle  $(p_0, p_1, p_2)$  to a Voronoi area around  $p_0$ , as depicted in Figure 4.19 (a), is

$$\frac{1}{8} \left( |p_1 - p_0|^2 \cot(\angle p_2) + |p_2 - p_0|^2 \cot(\angle p_1) \right),$$

where  $\angle p$  denotes the angle of the triangle at  $p$ . For simplicity we assume that all sides of the tetrahedron are 1 and all angles  $\pi/3$ . Then all Voronoi cells have area  $\frac{\sqrt{3}}{4}$ , as can

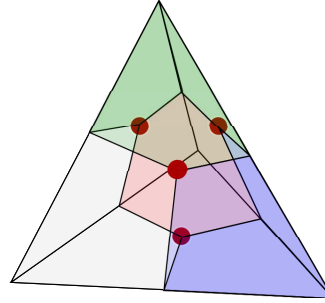


Figure 4.18.: The dual mesh on the tetrahedral, the red dots are the dual vertices and the dual faces are highlighted in different colors.

be computed by summing up the contribution of all incident triangles. Therefore, the discrete Hodge operator for 0-forms is

$$\star_0 = \begin{pmatrix} \frac{\sqrt{3}}{4} & & & \\ & \frac{\sqrt{3}}{4} & & \\ & & \frac{\sqrt{3}}{4} & \\ & & & \frac{\sqrt{3}}{4} \end{pmatrix}.$$

The  $\star_1$  matrix stores dual-edge edge ratios, i.e. the ratios  $\frac{\text{length}(\star e)}{\text{length}(e)}$ . These weights can also be computed without explicitly computing a circumcenter. The part of a dual edge  $p_0, p_1$  lying in a triangle  $p_0, p_1, p_2$ , as depicted in Figure 4.19 (b), is given by  $\frac{1}{2} \cot(\angle p_2) \cdot |p_1 - p_0|$ , and therefore the dual-edge edge ratio is

$$\frac{1}{2} (\cot(\angle p_2) + \cot(\angle p'_2)),$$

where  $p_2$  and  $p'_2$  are the third triangle vertices of the triangles neighboring the edge  $p_0, p_1$ , again see Figure 4.18. In our example all angles are  $\pi/3$ , and the dual-edge edge ratio is always  $\frac{1}{\sqrt{3}}$ . The discrete Hodge operator for 1-forms is given by

$$\star_1 = \begin{pmatrix} \frac{1}{\sqrt{3}} & & & \\ & \frac{1}{\sqrt{3}} & & \\ & & \ddots & \\ & & & \frac{1}{\sqrt{3}} \end{pmatrix}.$$

The  $\star_2$  matrix stores the weights  $\frac{\text{Vol}(\star f)}{\text{Vol}(f)}$  for faces  $f$ . The dual of a face is a vertex and its volume by definition 1. That is the weights are given by  $\frac{1}{\text{Area}(f)}$ . The area of an equilateral triangle with side length 1 is  $\frac{\sqrt{3}}{4}$ . Therefore, the Hodge operator for discrete

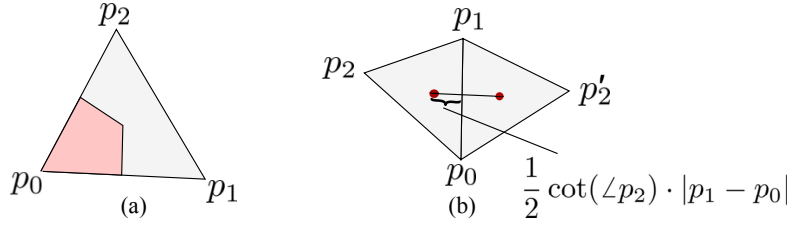


Figure 4.19.: (a) The area contributed by the triangle to the Voronoi area around  $p_0$ .  
(b) The edge dual to the edge  $p_0, p_1$ , its length gets a contribution from the two neighboring triangles.

2-forms is given by

$$\star_2 = \begin{pmatrix} \frac{4}{\sqrt{3}} & & \\ & \frac{4}{\sqrt{3}} & \\ & & \frac{4}{\sqrt{3}} \end{pmatrix}.$$

Note that it is a pure coincidence that  $\star_2 = \star_0^{-1}$ .

The last missing matrices are the dual exterior derivatives. But these require no additional work. By equation 4.13,  $d_{n-k}^{dual} = (-1)^k (\delta_k^{primal})^T$ . So the dual derivative  $d_0^{dual}$ , i.e. the derivative for dual 0-forms defined per dual vertex, and the dual derivative  $d_1^{dual}$ , i.e. the derivative for dual 1-forms defined per dual edge, are given by:

$$\begin{aligned} d_{2-2}^{dual} &= d_0^{dual} = \delta_2, \\ d_{2-1}^{dual} &= d_1^{dual} = -\delta_1. \end{aligned}$$

#### 4.5.6. The Discrete Coderivative

The coderivative is given by

$$\partial_k = (-1)^k \star_{k+1}^{-1} d_{n-k} \star_k.$$

Accordingly the discrete coderivative is

$$\partial_k^{discrete} = (-1)^k (\star_{k+1}^{discrete})^{-1} d_{n-k}^{dual} \star_k^{discrete}.$$

But by Equation 4.13

$$d_{n-k}^{dual} = (-1)^k (d_{k-1}^{primal})^T,$$

therefore, all signs cancel out and the discrete coderivative is given by

$$\partial_k^{discrete} = (\star_{k+1}^{discrete})^{-1} (d_{k-1}^{primal})^T \star_k^{discrete}. \quad (4.14)$$

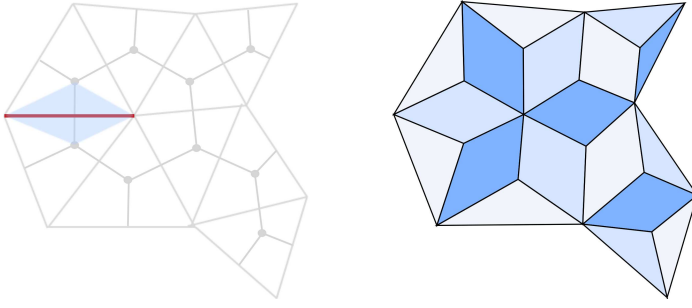


Figure 4.20.: Using the  $\star^1$ -matrix as a scalar product for discrete 1-forms weights the value associated to an edge according to the diamond shaped area spanned by the edge and its dual. These diamond shapes are disjoint and cover the whole manifold.

### Discrete Scalarproduct and Adjointness

We define the scalar product for discrete differential forms such that the discrete coderivative is adjoint to the discrete exterior derivative.

$$\langle d\mathbf{v}, \mathbf{w} \rangle_{discrete} = \langle \mathbf{v}, \partial\mathbf{w} \rangle_{discrete}$$

But a scalar product on a finite dimensional vector space can be described by a symmetric matrix  $S$ :

$$\langle \mathbf{v}, \mathbf{w} \rangle_{discrete} = \mathbf{v}^T S \mathbf{w}.$$

The discrete exterior derivative and the discrete coderivative are adjoint exactly if the scalarproduct for discrete forms is defined by

$$\langle \mathbf{v}, \mathbf{w} \rangle_{discrete} := \mathbf{v}^T \star_{discrete} \mathbf{w}, \quad (4.15)$$

as then

$$\langle d\mathbf{v}, \mathbf{w} \rangle_{discrete} = (d\mathbf{v})^T \star \mathbf{w} = (\mathbf{v})^T d^T \star \mathbf{w} = (\mathbf{v})^T \star (\star^{-1} d^T \star \mathbf{w}) = \langle \mathbf{v}, \partial\mathbf{w} \rangle_{discrete}.$$

The  $\star$  matrix does not only guarantee adjointness of the discrete  $d$  and  $\partial$ , it also approximate the scalar product for smooth  $k$ -forms: for 0-forms

$$\begin{aligned} \int_M \langle \omega^0, \nu^0 \rangle &= \sum \int_{\star\sigma^0} \omega^0 \cdot \nu^0 dVol \approx \sum \mathbf{v}(\sigma^0) \cdot \mathbf{w}(\sigma^0) \cdot Vol(\star\sigma^0) \\ &= \mathbf{v}^T \star_{discrete}^0 \mathbf{w}, \end{aligned}$$

as the matrix  $\star^0$  stores the volumes of the dual cells of vertices  $\sigma^0$ . Generally using the star matrix as scalar product scales the values of the discrete form such that they represent values scaled to the diamond shaped areas spanned by a simplex and its dual, see Figure 4.20; the smooth scalar product is approximated by

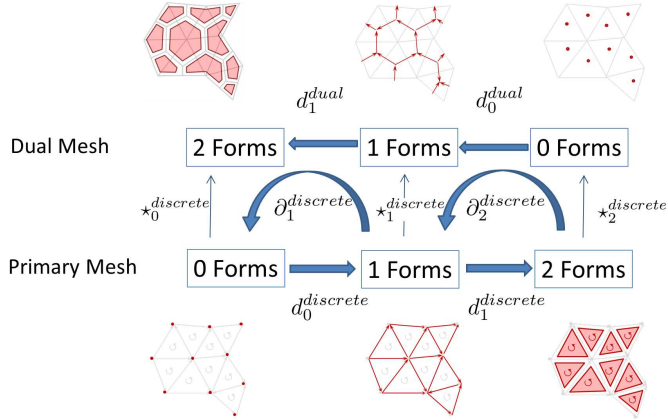
$$\langle \omega^k, \nu^k \rangle = \int_M \langle \omega^k, \nu^k \rangle = \sum \int_{hull(\sigma, \star\sigma)} \omega^k \wedge \star\nu^k \approx \mathbf{v}^T \star_{discrete}^k \mathbf{w}.$$

#### 4.5.7. This is Discrete Exterior Calculus

With the discrete star, forms, dual forms and the discrete exterior derivatives for dual and primal forms we can build a ‘discrete de Rham’ complex. The discrete de Rham complex captures the essence of discrete exterior calculus and keeps many properties from the continuous one.

The discrete scalar product for  $k$ -forms and the coderivative as an adjoint of the discrete derivative round off the picture of the DEC machinery. The discrete scalar product also defines a norm on the space of discrete  $k$ -forms - this norm is useful to formulate minimization problems for  $k$ -forms. An overview of the discrete exterior calculus operators and the de Rham complex for discrete 2-manifolds is depicted in Figure 4.21.

In DEC all discrete operators are simple sparse matrices and they can be used directly to discretize differential equations formulated using differential forms and exterior calculus. These linear equations are then easy to solve using standard methods. Discretizing a differential equation using DEC also preserves the *geometry* of the differential equation to some degree, as the discrete operators are designed to be geometrically close to the smooth operators.



### Discrete k Forms

$$\begin{aligned} &\cong \mathbb{R}^{\#k\text{-simplices}} \\ &\langle \mathbf{v}^k, \mathbf{w}^k \rangle_{\text{discrete}} = \mathbf{v}^T \star_k \mathbf{w} \quad (\text{scalar product}) \\ &\|\mathbf{w}^k\|_{\text{discrete}}^2 = \langle \mathbf{w}^k, \mathbf{w}^k \rangle_{\text{discrete}} \quad (\text{norm}) \end{aligned}$$

$$\text{dd} = 0$$

$$\begin{aligned} d^{\text{discrete}} d^{\text{discrete}} &= 0 \\ d^{\text{dual}} d^{\text{dual}} &= 0 \end{aligned}$$

### Codervative

$$\begin{aligned} \partial_k^{\text{discrete}} &= (-1)^k (\star_{k+1}^{\text{discrete}})^{-1} d_{n-k}^{\text{dual}} \star_k^{\text{discrete}} \\ \partial^{\text{discrete}} \partial^{\text{discrete}} &= 0 \\ \langle d^{\text{discrete}} \mathbf{w}^k, \mathbf{v}^{k+1} \rangle_{\text{discrete}} &= \langle \mathbf{w}^k, \partial^{k+1} \mathbf{v}^{k+1} \rangle_{\text{discrete}} \quad (\text{adjointness}) \end{aligned}$$

### Stokes Theorem

$$\begin{aligned} &\text{(adjointness of } d \text{ and the border operator)} \\ &\langle \delta^{\text{discrete}} \sigma, \mathbf{w}^k \rangle = \langle \sigma, d_k^{\text{discrete}} \mathbf{v}^k \rangle \end{aligned}$$

### The Matrices

#### Border Operator



#### Dual Border Operator

$$\delta_k^{\text{dual}} = (-1)^{n-k+1} (\delta_{n-k+1})^T$$

#### Hodge Star

$$\star_k^{\text{discrete}} = \begin{pmatrix} \frac{\text{Vol}_{n-1}(\star \sigma_1^k)}{\text{Vol}_k(\sigma_1^k)} & & & \\ & \frac{\text{Vol}_{n-k}(\star \sigma_2^k)}{\text{Vol}_k(\sigma_2^k)} & & \\ & & \ddots & \\ & & & \frac{\text{Vol}_{n-k}(\star \sigma_m^k)}{\text{Vol}_k(\sigma_m^k)} \end{pmatrix}.$$

#### Exterior Derivative

$$d_k^{\text{discrete}} = \delta_{k+1}^T$$

#### Codervative

$$\partial_k^{\text{discrete}} = (\star_{k+1}^{\text{discrete}})^{-1} \delta_k \star_k^{\text{discrete}}$$

#### Dual Exterior Derivative

$$d_{n-k}^{\text{dual}} = (-1)^k (\delta_k)$$

Figure 4.21.: A summary of the DEC operators and their most important properties.

## 5. Conformal Mesh Parametrization

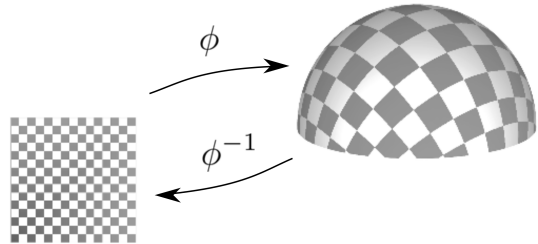


Figure 5.1.: A conformal map  $\phi$ , it preserves angles. A map is angle preserving exactly if its inverse  $\phi^{-1}$  is angle preserving too.

With the machinery of discrete and non discrete exterior calculus at hand we can solve various problems elegantly . The way to use this machinery is always similar. The first step is to formulate a problem using exterior calculus, then to translate it to the discrete exterior calculus setting and use the sparse matrix formulation to solve the given problem computationally.

The problem under consideration in this chapter is two dimensional surface parametrization as it happens for example with texture mapping. The goal is to find a parametrization of a mesh, i.e. texture coordinates for all its vertices, such that the parametrization has some nice properties, here conformality. This chapter is based on [GGT06] and [DMA02].

This chapter highlights the connection of discrete exterior calculus and conformal maps. The deduced algorithms are simple and fast and involve only the solving of linear systems; but there are more refined non linear methods closely related to the approach given that achieve better results, for example by developing border constraints more carefully as in [DMA02], [MTAD08].

### 5.1. Problem Statement

Given a smooth two dimensional surface  $M$ , we try to find a map  $\phi$  that parametrizes the whole surface,  $\phi : U \subset [0, 1] \times [0, 1] \rightarrow M$ . Such a global map exists if the surface  $M$  has the shape of a deformed disk. Therefore, we assume that the mesh  $M$  has the topology of a disk, later we will also allow the disk to have holes.

In the setting of texture mapping we would like the map  $\phi$  to distort the texture  $[0, 1] \times [0, 1]$  as little as possible. In general there is no perfect map. As soon as  $M$  has

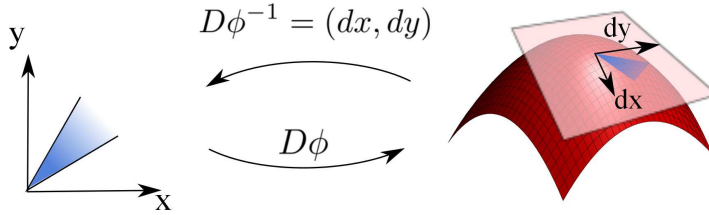


Figure 5.2.: Because  $dx$  and  $dy$  (depicted by their related vectors) are orthogonal and of the same length, the linear mapping given by the total derivative  $D\phi$  has to be angle preserving. Then  $\phi$  is also angle preserving.

points where both principle curvatures are non-zero the surface is non-developable; there exists no map that preserves angles and areas at once (see e.g. [Car92] on developable surfaces). As distortion freeness is not an option, the goal is to minimize distortion. There are various distortion measures that can be minimized. One possibility is to ask the map  $\phi$  to be conformal: angles should be preserved under the map. Conformality can be expressed very well in terms of exterior calculus. The downside of preserving angles is that areas can get distorted and compressed arbitrarily.

### Conformal Parameterizations

A map is conformal exactly if its inverse is conformal, see Figure 5.1. Rather than to express conformality for a map  $\phi : [0, 1]^2 \rightarrow M$ , we express conformality for its inverse, the coordinate functions

$$(x, y) : M \rightarrow [0, 1]^2,$$

$$x : M \rightarrow [0, 1],$$

$$y : M \rightarrow [0, 1].$$

The two coordinate functions  $x, y$  are 0-forms. In terms of exterior calculus conformality is ensured by

$$\star dx = dy. \quad (5.1)$$

As the exterior derivative  $d$  is the gradient operator and the star operator represents a rotation by  $90^\circ$  (compare with Figure 4.11), Equation 5.1 expresses that the gradients of the coordinate functions are orthogonal and of the same length. This ensures angle preservation compare with Figure 5.2.<sup>1</sup>

<sup>1</sup>Interpreting  $\tilde{\phi}(x, y, z) = \phi(x, y) + z \cdot N(x, y)$  where  $N$  is the surface normal,  $D\tilde{\phi}^{-1} = (dx, dy, N)^T$  is a linear mapping represented by an orthogonal matrix, where  $dx, dy$  are identified with the gradient vectors. Its inverse is  $D\tilde{\phi} = (1/\lambda dx, 1/\lambda dy, DN)$ . This leads to  $D\phi^T D\phi$  being the multiple of the identity matrix, therefore  $\text{angle}(D\phi v, D\phi w) = \text{angle}(v, w)$

### Conformality and Harmonicity

One important property of conformal maps is that their coordinate functions  $x$  and  $y$  are both *harmonic*. Harmonicity is a very telltale property for a function or differential form to have. Harmonicity arises naturally in a wide range of contexts and harmonic forms and functions have many useful properties. In every application covered in this thesis the harmonicity of forms plays a crucial role. Covering the properties of harmonic forms could fill a book—we will cover some properties of harmonic forms as we go along, mainly in the Sections 6.3 and 7.2.5.

The formal definition of harmonicity for differential  $k$ -forms uses the coderivative  $\partial$ . A differential form  $\omega$  is harmonic iff

$$\underbrace{(\partial d + d\partial)}_{\Delta} \omega = 0.$$

The operator  $\Delta = \partial d + d\partial$  is called the *Laplace-Beltrami operator*. It generalized the Laplace operator for functions  $f : \mathbb{R}^n \rightarrow \mathbb{R}$ , which you might already have met. In Euclidean coordinates the Laplace operator for functions is given by:

$$\Delta f(x_1, \dots, x_n) = \sum_{i=1}^n \frac{\partial^2}{\partial x_i^2} f(x_1, \dots, x_n).$$

It can also be defined as concatenation of the divergence and gradient operator,

$$\Delta = \text{div} \circ \text{grad}.$$

The Laplace-Beltrami operator for 0-forms simplifies to  $\partial d$ , as you cannot apply the co-differential operator to 0-forms. But  $\partial d$  is exactly  $\text{div} \circ \text{grad}$ , as  $d$  for 0-forms corresponds to the *grad* operator and  $\partial$  for 1-forms corresponds to the *div* operator, see Sections 4.2.3 and 4.4. This means that the Laplace-Beltrami operator really generalizes the Laplace operator.

A simple and for now sufficient way to approach harmonicity is to understand it as a smoothness constraint. But as a very strong one. It is so strong that, on patches with a disc topology, a harmonic 0-form is uniquely determined by the values it assumes on the boundary of the patch. That is to say that if we prescribe that a harmonic form should have fixed values on a patch boundary, there is at most one harmonic 0-form that can meet the constraint. And this is what we exploit when we compute conformal parameterizations.

From Equation 5.1 one can directly deduce that the coordinate functions  $x$  and  $y$  of a conformal map are harmonic 0-forms, that is, they fulfill

$$\Delta x = -\star^{-1} d \star dx = 0,$$

$$\Delta y = -\star^{-1} d \star dy = 0.$$

The harmonicity of  $x$  is proven by:

$$\begin{aligned} \star dx &= dy && (\text{Equation 5.1}) \\ d \star dx &= ddy && (\text{apply } d) \\ d \star dx &= 0 && (dd = 0) \\ \star^{-1} d \star dx &= 0 && (\text{apply } \star^{-1}). \end{aligned}$$

For the harmonicity of  $y$  we do the same but apply  $\star$  first on both sides of Equation 5.1, such that in the first step we have

$$-dx = \star dy.$$

### Final Problem Statement

As mentioned above, a harmonic function on a patch  $M$  is uniquely determined by the values it assumes on the border. If  $M$  is a smooth bordered orientable 2-manifold with disk topology,  $g$  describes fixed constraints on the border and all participating functions are sufficiently smooth, the following system of equations, called Dirichelet problem, has a unique solution:

$$\left. \begin{array}{ll} \Delta f = 0 & \text{inside } M, \\ f = g & \text{on } \delta M. \end{array} \right\}$$

Therefore, in order to find a conformal parametrization, it is enough to find two harmonic 0-forms  $x$  and  $y$  and choose the border constraint such that the conformality holds. I.e.,

$$\left. \begin{array}{ll} \Delta x = 0 & \text{inside } M, \\ \Delta y = 0 & \text{inside } M, \\ \text{Border Constraint for } x, y & \text{on } \delta M. \end{array} \right\} \quad (5.2)$$

where the border constraint uniquely determines the values of  $x$  and  $y$  on the border and should be chosen such that  $\star dx = dy$  inside the mesh. This is an important point to understand, we rely on the boundary constraint alone to ensure that Equation 5.1 is met.  $\Delta x = 0$  and  $\Delta y = 0$  are smoothness constraints that are independent form each other. They do not enforce that the gradient  $dx$  is orthonormal to  $dy$  in any way. The choice of good border constraints is problematic, but at least in principle a conformal parametrization can be found only by finding an optimal mapping for the border.

## 5.2. Conformal Embeddings with DEC

We can directly express the problem statement 5.2 in discrete exterior calculus. To begin with we assume that the mesh we want to parametrize is a discrete 2-manifold with the topology of a disk and *no* holes. We solve for two discrete 0-forms  $x$  and  $y$ , i.e., two vectors of per vertex texture coordinates. Using the discrete star and  $d$  operator the harmonicity constraint is given by the two linear equations

$$\begin{aligned} \star_0^{-1} d_1^{dual} \star_1 d_0^{primal} x &= 0, \\ \star_0^{-1} d_1^{dual} \star_1 d_0^{primal} y &= 0. \end{aligned} \quad (5.3)$$

Note that in the last section we made EC arguments and did not have to worry if a form or operator is dual or primal. In DEC we need to make this distinction. While it is implicitly clear which operators are meant, we did add subscripts and superscripts in 5.3 for clarity.

The border constraints are handled separately: we compute  $x$  and  $y$  coordinates for border vertices, leading to some coordinate vectors  $b_x, b_y$  and, for border vertices, replace the equation above by

$$x = b_x$$

$$y = b_y.$$

Obviously you can not choose arbitrary functions  $x, y$  if you want the map  $p \in M \rightarrow (x(p), y(p))$  to be a bijective mapping; you have to ensure that  $(x(p), y(p)) \neq (x(q), y(q))$  for  $p \neq q$ . The Tutte theorem and its generalization by Gortler et Al. [GGT06] presented in the following Section explain appropriate conditions.

### 5.2.1. Graph Theory

It is not clear when solving the linear system 5.3 with some border constraints leads to a valid parametrization. A parametrization  $p \in M \mapsto (x, y)$  has to be bijective, without any overlaps. It should *embed* the mesh  $M$  in  $\mathbb{R}^2$ .

Tutte's theorem gives simple constraints that guarantee that a mesh with a single border component is embedded correctly in  $\mathbb{R}^2$ . It applies to *3-connected planar graphs*. A graph is *planar* if it can be embedded in a plane, and a graph is *3-connected*, if removing any two edges does not split the graph into two non-connected components. For example discrete 2-manifolds with disk topology are planar and 3-connected. Tutte stated that if the border of any such graph is mapped to an arbitrary convex polygon and every vertex is mapped to convex combination of its neighbors, then this mapping is an embedding. Tutte's theorem, stated as in [GGT06]:

**Theorem 1.** (Tutte)[GGT06] *Let  $G$  be a 3-connected graph and  $\delta G$  be its border component. If  $\delta G$  is embedded in the plane as a convex polygon and every vertex is positioned as a strictly convex combination of its neighbors, then the drawing of  $G$  with these vertex positions is an embedding.*

This result means that mapping the boundary vertices of a mesh to any convex polygon  $b_x, b_y$  and solving a linear system

$$\begin{aligned} Ax &= 0 & x_{\text{border}} &= b_x \\ Ay &= 0 & y_{\text{border}} &= b_y \end{aligned} \tag{5.4}$$

leads to an embedding without self intersections, if  $A$  enforces that mapped vertices lie in the convex hull of their neighbors. This is the case if every line  $i$  of the matrix  $A$  fulfills

$$a_{ij} = 0 \text{ if } v_i \text{ and } v_j \text{ are not neighbors,} \tag{5.5}$$

$$\sum_j a_{ij} = 0, \quad (5.6)$$

$$a_{ii} < 0, a_{ij} \geq 0 \text{ for } i \neq j. \quad (5.7)$$

Enforcing the equation given by such a matrix row means enforcing

$$\sum_{j \neq i} a_{ij} v_j = -a_{ii} v_i.$$

Dividing by  $-a_{ii}$  on both sides normalizes the weights  $a_{ij}$ : it leads to positive weights  $w_j$  with  $\sum_j w_j = 1$  and

$$w_j := -\frac{a_{ij}}{a_{ii}}$$

$$v_i = \sum_{j \neq i} w_j v_j.$$

This expresses exactly that  $v_i$  lies in the convex hull of its neighbors. So Tutte's theorem does apply to the linear system 5.4 if Equations 5.5, 5.6 and 5.7 hold for  $A$ .

Tutte's theorem does not completely apply to our setting. Having only convex polygons as borders is too restrictive and the matrix from the linear system 5.3,

$$\star_0^{-1} d_1^{dual} \star_1 d_0,$$

does not fulfill Equation 5.7 when there are obtuse angles, that is angles  $> \pi/2$ , in the mesh. With obtuse angles the cotangent weights in the  $\star_1$  matrix (see Section 4.5.5) can be negative. But the Equations 5.5 and 5.6 are always met. To also meet Equation 5.7, we can either forbid obtuse triangles or use better weights. For example the improved mixed area weights from [MDSB02] which differ only very slightly from the cotangent weights, or the very similar mean value weights [Flo03]. Both weights are guaranteed to be non-negative.

In [GGT06] Gortler et al. proved an extension of Tutte's theorem, which relaxes the conditions needed to get embeddings and also is applicable when multiple borders are present and they are mapped to non-convex polygons:

**Theorem 2.** (*Gortler et al.*) *Under the following conditions a parametrization describes an embedding without self intersection:*

1.  *$G$  is an oriented 2-manifold with disc topology and multiple exterior faces (one exterior boundary and additional holes)*
2. *The exterior boundary is mapped to a polygon with winding number  $2\pi$  and no self intersections.*
3. *The interior boundaries are mapped to non intersecting polygons with winding numbers  $-2\pi$*
4. *Every mapped non boundary vertex lies in the convex hull of its neighbors*
5. *The reflex (i.e. non-convex) vertices on boundaries of the mapped graph lie in the convex hull of their neighbors*

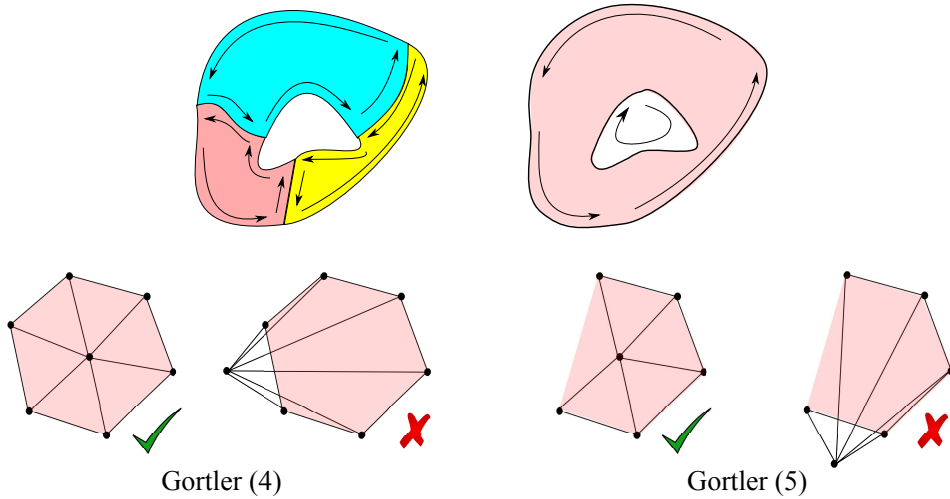


Figure 5.3.: Top: Inner borders of an embedded surface have an orientation opposite of the outer border. Bottom: The conditions (4) for inner vertices and (5) for reflex boundary vertices of Gortler's theorem. The center vertex has to lie in the marked area, i.e., the convex hull of its neighbors, else the map is not an embedding.

For proofs of both theorems we refer to [GGT06]. We do not reproduce any proof, as most concepts needed for the proof would not be needed anywhere else in this thesis.

Consider the five conditions of Theorem 2. The first condition ensures that the problem is solvable from a topological point of view and that there exist global parameterizations of the mesh. Conditions 2 and 3 are needed because the mapped oriented manifold is still an oriented manifold, now embedded in  $[0, 1]^2$  and therefore the interior borders have to be oriented negatively relative to the exterior border, see Figure 5.3.

The fourth condition is the same as in the Tutte theorem. The last property is the additional property to guarantee a map to be an embedding when you map multiple borders to possibly non-convex polygons. Border vertices that are mapped to reflex vertices have to be treated separately and have to fulfill the same constraint like inner vertices: to lie in the convex hull of its neighbors. Note also that inner borders always have reflex vertices and can consist only of reflex vertices.

While Tutte's theorem can be used directly to construct an embedding by choosing any convex weights and any convex polygon as mapped border, the extension of Gortler et al. is not as straight forward to use. The fifth property is not easy to guarantee. If a parametrization is given, it is easy to check, but before the mapping is giving, you do not know which border vertices are mapped to reflex border vertices and on which you therefore have to enforce (5).

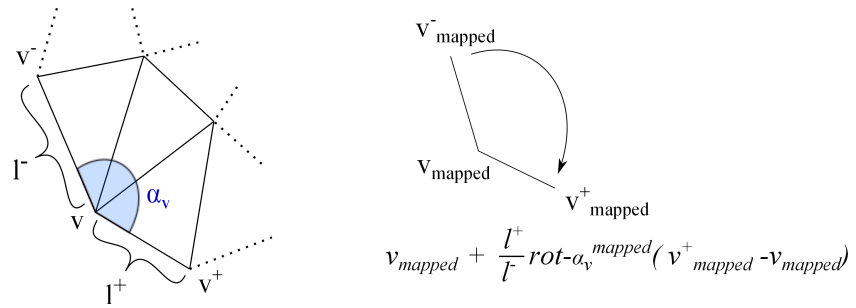


Figure 5.4.: The linear equation to preserve the border angle.

### 5.2.2. Fixed Border Constraints

The quality of a solution depends strongly on the quality of the border constraint. In the following we give some simple options. Note that we still assume that the mesh only has one border component.

#### Convex Polygon

A very simple, robust approach is to force the  $x$  and  $y$  coordinates of the border component to form some convex polygon, for example a circle. If the border component has  $n$  vertices, then for the  $k$ th border vertex  $b_x$  and  $b_y$  are simply set to

$$(b_x, b_y) = (\sin((2k/n)\pi), \cos((2k/n)\pi)).$$

You can get a slight improvement by spacing the values on the circle as they are spaced on the border of the mesh, i.e., by using the factor

$$(borderDist(v_k, v_0)/length(border)),$$

instead of the factor  $k/n$ . By Tutte's theorem solving Equation 5.3 with these border constraints always leads to an embedding. On the other hand this border constraint does not enforce conformality of the parametrization.

#### Conformal Border Constraint

Conformality means preserving angles. We now formulate a simple linear border constraint that tries to preserve the angles of border triangles.

Let  $v$  be a border vertex and  $v^+$  and  $v^-$  its predecessor and successor on the border (Figure 5.4.). Then the angle  $\alpha_v$  between the edges  $(v^-, v)$  and  $(v, v^+)$  measured on the mesh should be preserved. When mapped to the plane, the total angle of the image of the border has to be  $(n - 2)\pi$ , so we choose

$$\alpha_v^{mapped} = \alpha_v \frac{(n - 2)\pi}{\sum_{v \in border} \alpha_v} \quad (5.8)$$

as target angle. To get a simple linear system for the mapped border vertices  $v_{mapped}^*$  we constrain

$$(v_{mapped}^+ - v_{mapped}) + \frac{|v^+ - v|}{|v^- - v|} \text{rot}_{\alpha_v^{mapped}} \cdot (v_{mapped} - v_{mapped}^-) = 0, \quad (5.9)$$

which takes into account the relative distances between neighboring border vertices in addition to the angle  $\alpha_v$ , see Figure 5.4. This linear equation for the mapped vertex positions is described by the following matrix:

$$\begin{pmatrix} -\frac{l^+}{l^-} \cos(\alpha_m) & \frac{l^+}{l^-} \cos(\alpha_m) - 1 & 1 & \frac{l^+}{l^-} \sin(\alpha_m) & -\frac{l^+}{l^-} \sin(\alpha_m) & 0 \\ -\frac{l^+}{l^-} \sin(\alpha_m) & \frac{l^+}{l^-} \sin(\alpha_m) & 0 & -\frac{l^+}{l^-} \cos(\alpha_m) & \frac{l^+}{l^-} \cos(\alpha_m) - 1 & 1 \end{pmatrix} \begin{pmatrix} v_m^- \cdot x \\ v_m^- \cdot x \\ v_m^+ \cdot x \\ v_m^- \cdot y \\ v_m \cdot y \\ v_m^+ \cdot y \end{pmatrix} = \begin{pmatrix} 0 \\ 0 \end{pmatrix}.$$

The set of equations for the border positions has two degrees of freedom: the scale and the orientation of the mapped border. To get a solution we can fix two arbitrary boundary vertices to be mapped to  $(1,0)$  and  $(0,0)$ . The resulting values for border positions are rescaled and translated to  $[0, 1]^2$ . While this constraint will ensure better conformality if the overall Gaussian curvature is low and the border is not too exotic, i.e., the outer angles can be preserved very well, there is in general no guaranty that the conditions of Gortler's theorem are met and this border constraint might not produce embeddings.

### 5.2.3. Multiple Borders

Using Gortler's generalized Tutte theorem we can refine the boundary constraints above and consider the case of having multiple borders. Gortler's theorem suggests to treat reflex border vertices differently, enforcing a convexity constraint on them as well. Note that inner boundaries always have reflex vertices and can consist only of reflex vertices.

We will treat the exterior and the interior borders differently, as well as reflex and convex border vertices.

#### Exterior Border

On exterior borders Gortler's theorem suggests a slight improvement. We compute border positions  $b_x$  and  $b_y$  for the exterior border in any described way, but we enforce  $x = b_x$  and  $y = b_y$  only for border vertices that are not reflex according to the estimated target angles  $\alpha^{mapped}$ . For those that are reflex we replace this constraint by some convexity constraint. We propose to simply treat them like all interior vertices and take the convexity constraint given by Equation 5.3:

$$\star_0^{-1} d_1^{dual} \star_1 d_0^{primal} = 0.$$

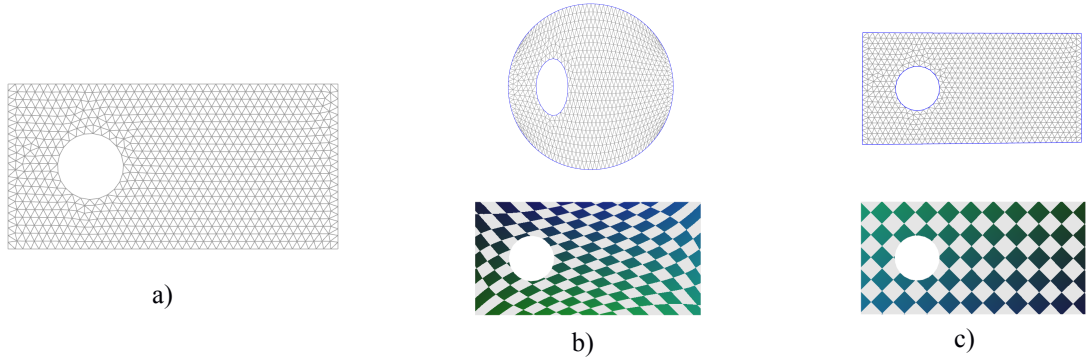


Figure 5.5.: A mesh that is trivial to parametrize with an inner boundary (a). Using the circle constraint obviously has to induce distortion (b), while the conformal constraint leads to a perfect embedding (c).

If the conformal border constraint leads to a good border, meaning that it allows a close to conformal map at the border, and replacing  $x = b_x, y = b_y$  by a convex constraint leads to no new reflex vertices, Gortler's theorem ensures that the calculated solution is an embedding.

### Interior Borders

For interior borders we proceed similarly; we choose to enforce a conformal constraint on the inner borders but without precomputing any border positions.

We start by computing target angle sizes at all vertex positions, as with the exterior border, using Equation 5.9. Again we treat all vertices that would be reflex vertices after this guess like inner vertices, choosing the convex constraint given by Equation 5.3 for these vertices. For the vertices estimated to be non reflex we enforce the linear equation derived for the conformal border constraint, i.e., Equation 5.9:

$$(v_{mapped}^+ - v_{mapped}) + \frac{|v^+ - v|}{|v^- - v|} rot_{\alpha_v^{mapped}} \cdot (v_{mapped} - v_{mapped}^-) = 0.$$

### Overall linear equation

The linear equation to get a conformal parametrization for a mesh with disk topology and multiple holes then is the following. There is one equation for each vertex  $x$  and  $y$  coordinate. Let  $b_x$  and  $b_y$  be some precomputed exterior border positions and  $\alpha_v^{mapped}$  be the target angle for a border vertex  $v$ . We then fix convex vertices ( $\alpha < \pi$ ) of the outer border,

$$\begin{aligned} x &= b_x, \\ y &= b_y, \end{aligned}$$

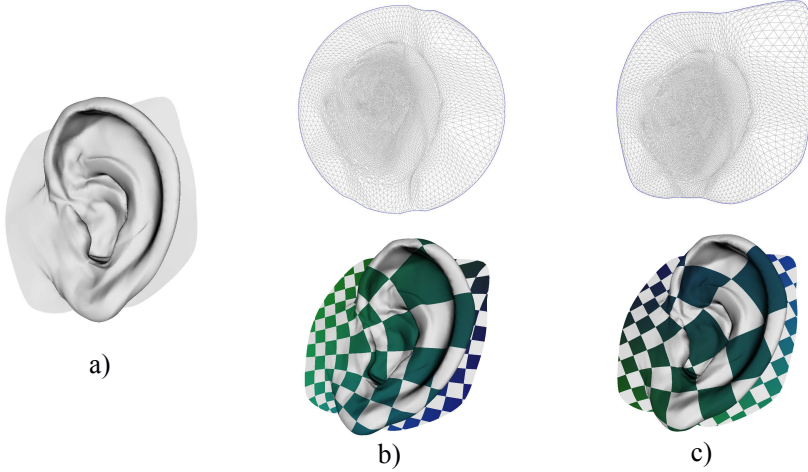


Figure 5.6.: The mesh of an ear (a). The circle constraint induces only little distortion (b). The ear boundary is nearly flat so the conformal constraint (c) gives a nearly perfect conformal parametrization.

choose the conformal border constraint 5.9 for convex vertices on inner borders,

$$(v_{mapped}^+ - v_{mapped}) + \frac{|v^+ - v|}{|v^- - v|} \text{rot}_{\alpha_v^{mapped}} \cdot (v_{mapped} - v_{mapped}^-) = 0,$$

and for all reflex border vertices and inner vertices we choose the constraint deduced using DEC:

$$\star_0^{-1} d_1^{dual} \star_1 d_0^{primal} x = 0,$$

$$\star_0^{-1} d_1^{dual} \star_1 d_0^{primal} y = 0.$$

#### 5.2.4. Results

As is to be expected the conformal border constraint has the potential to give the best results, but for some borders this constraint fails to meet the requirements of the extended Tutte theorem and does not produce an embedding. It may even produce boundary polygons with self intersections. But as long as the sum of the inner angles are close to the sum of angles of a planar polygon the approach works well.

The meshes in Figures 5.5 to 5.7 have boundaries that can easily be mapped to flat polygon, the conformal constraint presented works well. Multiple boundaries, as in Figures 5.5 and 5.7 are handled well, the inner boundaries are positioned automatically, as the convexity constraint on the reflex vertices is enforced.

The mesh in Figure 5.8 on the other hand has a boundary with an inner angle sum much greater than  $2\pi$  and the conformality constraint, which aims to conserve the angles on the boundary, fails. The precomputed boundary has self intersections and vertices

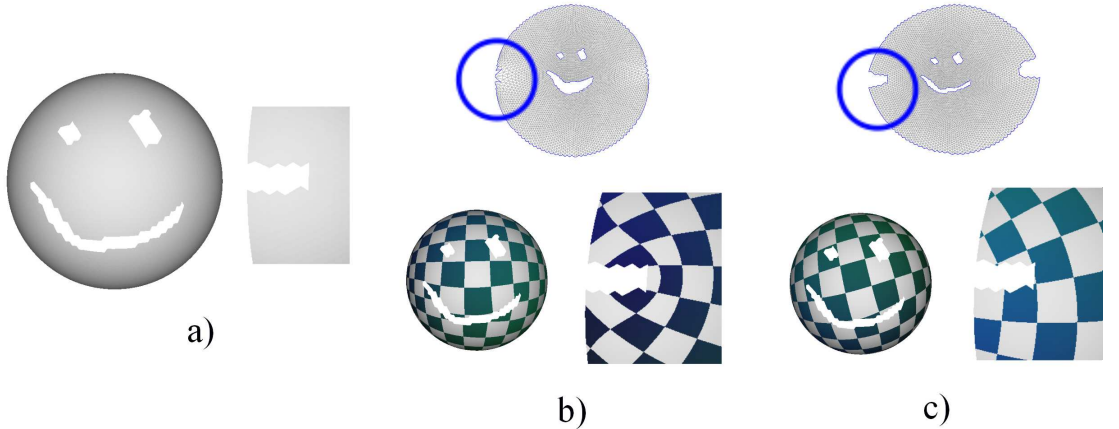


Figure 5.7.: A half sphere with multiple boundaries; a smile two eyes and ‘ears’ were cut out (a). As the boundary is nearly circular shaped the circle constraint works well (b) with pronounced distortion only around the ears. The conformal constraint gives a very similar embedding, but the ear area has less angular distortion.

assumed to be convex are reflex - so two of the conditions given by Gortler’s theorem fail and no embedding is produced.

Choosing a convex polygon as a border on the other hand is guaranteed to lead to embeddings; and in all examples the found parametrization is an embedding. But angles may not be preserved very well. The embedding is only conformal if the border of the original mesh is close to a circle, like in Figures 5.6 and 5.7.

Bottom line: for conformal parametrizations of patches with borders that are reasonably shaped, the simple approach described in this chapter works well and is easy to implement. More refined border conditions are described e.g. in [DMA02] where it is proposed to start with a convex border polygon and let the border evolve in a way to minimize an angle-distortion energy.

Nevertheless DEC proves to apply very well to this problem - DEC directly suggests the use of the discrete laplacian, i.e. cotan weights, which are well established in this setting. Besides this DEC explains that the key to finding a conformal mapping lies in finding a good boundary constraint that enforces conformality. But choosing the boundary constraint only by looking at the boundary might fail, for optimal solutions the boundary would need to be chosen depending on the rest of the mesh.

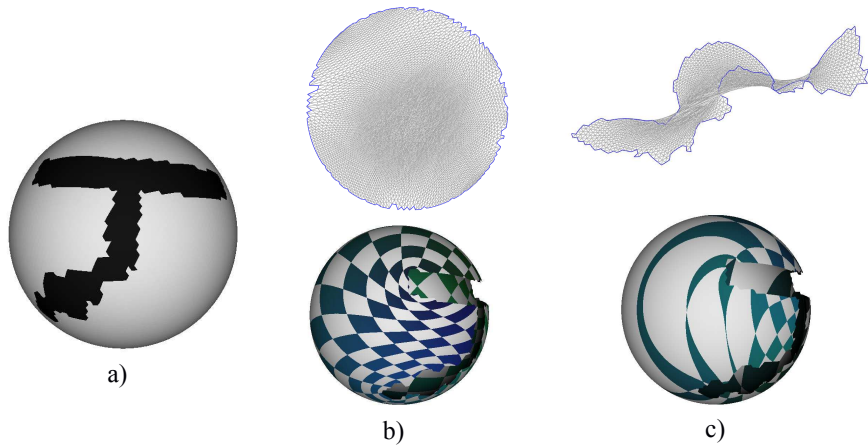


Figure 5.8.: (a) A sphere with a T shaped hole cut out. (b) The circular constraint still leads to an embedding, as guaranteed by Gortler's theorem. (c) In contrast, several conditions of Gortler fail when using the conformal embedding.



## 6. Vector Field Design and the General Laplacian

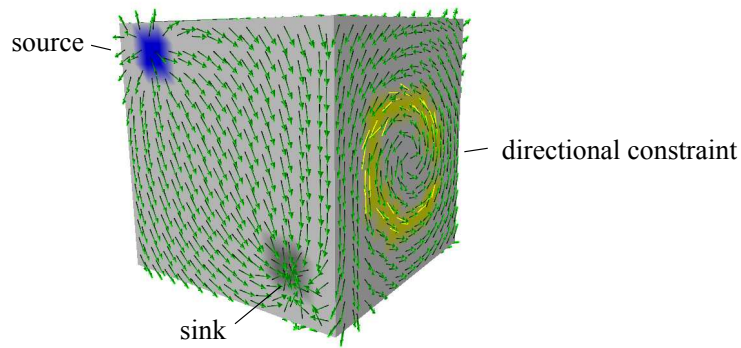


Figure 6.1.: A generated vector field, generated with a user given source sink and directional constraint.

The goal of this chapter is to generate natural looking tangential vector fields on two dimensional meshes, using a few intuitive, user-provided constraints, following the approach from Matthew Fisher et al. [FSDH07]. Possible constraints are the positions of sources and sinks or painted general flow directions. Tangential vector fields are naturally described by 1-forms and therefore the use of exterior and discrete exterior calculus suggests itself.

This chapter is divided in four sections. In the first (short) section the problem statement is formulated with exterior calculus. The problem statement naturally leads to the formulation of harmonicity for 1-forms. The second and third section give the theoretical background for a better understanding of the harmonicity of forms and of the topological constraints connected to vector field design. In this context we describe the following exterior calculus and differential topology results:

1. The Hopf Index Theorem, which describes the possible vector fields on a surface, based on its topology.
2. The Poincaré Lemma, which answers the question when a differential form  $\omega$  can be ‘integrated’, i.e., when there exist differential forms  $\nu$  with  $d\nu = \omega$ .
3. The Hodge Decomposition, which allows to split any differential form in three

‘orthogonal’ parts that can be treated somewhat independently, one of them harmonic.

4. A result from Hodge theory, which describes the dimension of the spaces of harmonic forms, solely depending on the topology of the surface.

In the third section we use the continuous theory to exactly formulate the properties of designed vector fields and translate this directly to DEC. And we consider vector field design on meshes with borders or holes.

## 6.1. Problem Statement

To produce a nice looking vector field, its visually prominent features need to be controlled. These are general flow directions and singularities. Singularities are points where the vector field vanishes. These can be sources, sinks, vortices or of a more exotic nature, see Figure 6.2. The Hopf index theorem described in the next section states that depending on the topology of the mesh such singularities are unavoidable. Therefore we want to control their type and positions.

We can do so by controlling the curl and the divergence of a vector field. We want to allow divergence and curl only on small, chosen areas. In terms of exterior calculus, curl can be expressed as  $d\omega^1$  and divergence as  $\partial\omega^1$ , see the schematic in Figure 4.11. This means that we want to design a 1-form with  $d\omega^1 = 0$  and  $\partial\omega^1 = 0$  everywhere, but on user specified areas, where the curl is non-zero  $d\omega^1 = c_{curl}$  or the divergence is non-zero  $\partial\omega^1 = c_{div}$ . As the manifold we are treating is two dimensional,  $d\omega^1$  and  $\partial\omega^1$  are scalar functions. So  $c_{div}$  and  $c_{curl}$  are scalar values. A positive  $c$  produces either a source or a vortex rotating in positive direction, a negative  $c$  produces a sink or a negatively rotating vortex, respectively.

To better control the look of the designed vector field, we want to constrain the vector field to follow some painted strokes. This amounts to constraining the vector field to fixed vectors on user provided strokes. But constraining the field to fixed vectors can introduce unavoidable curl and divergence. Thus the zero curl and divergence condition need to be relaxed, as they are potentially impossible to meet. Instead of requiring  $d\omega = 0$  and  $\partial\omega = 0$ , we require the 1-form to have a minimal exterior (co)-derivative:

$$\begin{aligned} \langle d\omega^1, d\omega^1 \rangle &\text{ minimal,} \\ \langle \partial\omega^1, \partial\omega^1 \rangle &\text{ minimal.} \end{aligned}$$

As explained in Section 6.3.4, minimizing the derivative and co-derivative separately is equivalent to minimizing the sum  $\langle d\omega^1, d\omega^1 \rangle + \langle \partial\omega^1, \partial\omega^1 \rangle$ . In summary, the problem statement we try to solve, expressed in EC terms is:

$\omega^1 = v_{fixed}$	on strokes,
$d\omega^1 = c_{curl}$	for vortices,
$\partial\omega^1 = c_{div}$	for source / sink vertices,
$\langle d\omega^1, d\omega^1 \rangle + \langle \partial\omega^1, \partial\omega^1 \rangle$ minimal	else.

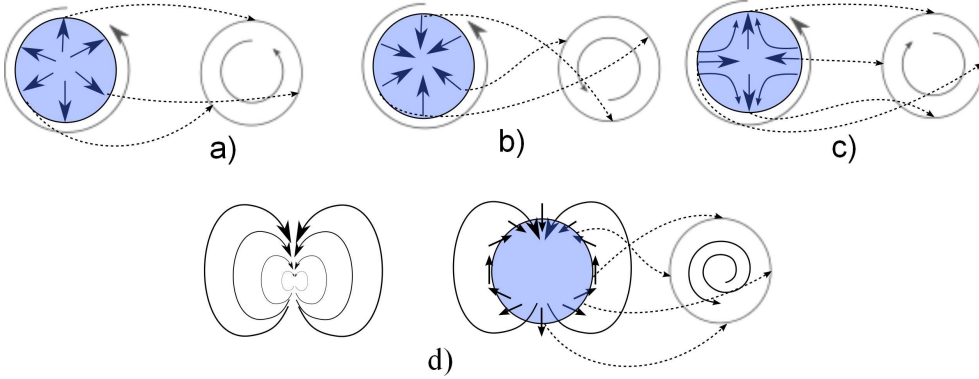


Figure 6.2.: The computation of the index of some singularities, which is the winding number of  $f = v / |v|$ .  $f$  is depicted by the dashed arrows. Sources (a) and sinks (b) have index 1, saddles (c) have index -1 and (d) is a singularity with index 2.

## 6.2. The Hopf Index Theorem

The Hopf index theorem describes the composition of the singularities of a smooth vector field. For a proof and an introduction to differential topology see for example [GP74]. Singularities are isolated points where the vector field vanishes. Hopf states that, depending only on the topology, singularities can not be avoided. Additionally, an invariant is described that gives a hint on what kind or combination of singularities to expect. The formulation of the Hopf index theorem is the following:

**Theorem 3. (Poincaré-Hopf Index Theorem)** *Let  $M$  be a compact orientable smooth manifold. Let  $v$  be a smooth tangential vector field (i.e. a 1-form) on  $M$  with isolated zeros. If  $M$  has a boundary  $v$  has to point in the outward normal direction on the border. Then*

$$\sum_{x_i: v(x_i)=0} \text{index}_v(x_i) = \chi(M),$$

where  $\chi(M)$  is the Euler characteristic of  $M$ .

Let's clarify the different ingredients of this theorem. The Euler characteristic on a  $k$ -dimensional manifold is similar as for 2 dimensions. In two dimensions, the manifold is triangulated in order to compute the Euler characteristic and is given by:

$$\chi(M) = \#\text{vertices} - \#\text{edges} + \#\text{faces}.$$

In higher dimensions you don't triangulate the manifold but you 'draw' a simplicial  $k$ -complex on the manifold; the Euler characteristic then is:

$$\chi(M) = \#\text{0-cells} - \#\text{1-cells} + \#\text{2-cells} - \#\text{3-cells} + \#\text{4-cells} \dots$$

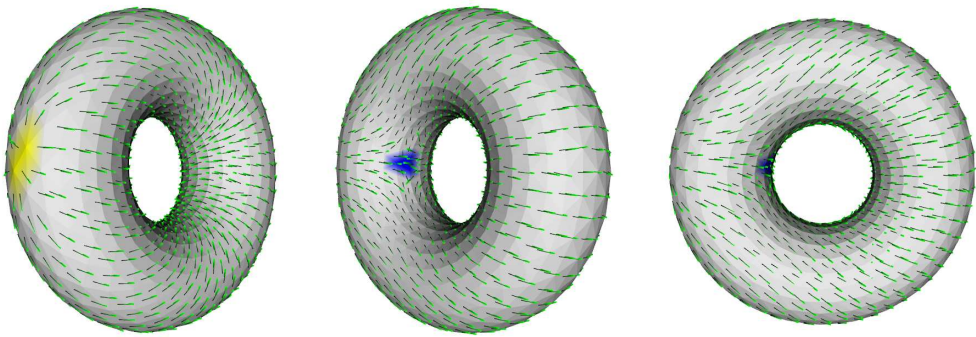


Figure 6.3.: An example for the Hopf index theorem: a torus with a vector field that has one source (yellow) and one saddle (blue). The torus has Euler characteristic 0, a source index +1 and a saddle index -1.

The index of a singularity  $x_i$ , that is a point  $x_i$  with  $v(x_i) = 0$ , is the *degree* of the map  $\frac{v}{|v|}$  at  $x_i$ . Sometimes the index is also called turning number. If  $M$  is two dimensional, the index basically counts the number of times

$$f : x \mapsto \frac{v(x)}{|v(x)|}$$

rotates when you follow a small circle around  $x_i$ . In Figure 6.2 you find some images to develop an intuition for the index. For example sources and sinks have index +1.

So what is the meaning of the Poincaré-Hopf index theorem? The theorem ties the existence of vanishing points of a vector field to the topology of the surface. By tying the sum of indices to the Euler characteristic, it gives a constraint on the composition of the singularities that depends only on the topology of the surface.

For example, by the Poincaré-Hopf theorem, all vector fields on borderless compact manifolds with non zero Euler characteristic have singularities. A sphere has Euler characteristic 2. This means that any smooth vector field has to have one vanishing point with index two or two vanishing points with index one (e.g. sources and sinks). If there are two sources and one sink then there has to be at least one additional vanishing point with characteristic -1 e.g. a saddle.

A torus has characteristic 0- it is possible to have vector fields without sources and sinks. It is not possible to have a field with exactly one source and one sink (giving a total index 2), but you could have one source and one saddle as in Figure 6.3.

### 6.3. Harmonic, Closed and Coclosed Forms

The formulation of vector field design in Section 6.1 actually aims to find nearly *harmonic* 1-forms with the additional constraint on  $d$  and  $\partial$  of the form. Here we give some background for the operators  $d$ ,  $\partial$  and  $\Delta$ . The space of  $k$ -forms on closed manifolds can

be split into three orthogonal spaces: the image of  $d$ , the image of  $\partial$  and the kernel of  $\Delta$  which is the space of harmonic forms. The kernel of the Laplacian  $\Delta$  also turns out to be the intersection of the kernels of  $d$  and  $\partial$ .

### 6.3.1. General Laplacian

For  $k$ -forms the Laplacian is defined as

$$\Delta_k = (-1)^{n-k+1} \star_k d_{n-k+1}^{\text{dual}} \star_{k+1} d_k + (-1)^{n-k} d_{k-1} \star_{k-1} d_{n-k}^{\text{dual}} \star_k.$$

Ignoring the implicitly clear sub-indices, and using the covariant derivative  $\partial_k = (-1)^{n-k} \star^{-1} d\star$  introduced in Section 4.4.1, we get

$$\Delta = \partial d + d\partial.$$

As mentioned in Section 5.1, this generalizes the usual Laplacian. We are interested in harmonic  $k$ -forms, i.e.,

$$\Delta_k \omega^k = 0,$$

and want to understand what it means for a form to be harmonic.

### 6.3.2. Curl- and Divergence-Freeness

First of all remember that the coderivative is adjoint to the derivative with respect to the scalar product for  $k$ -forms, as seen in Section 4.4.1. Being the adjoint means that for borderless Manifolds or when the involved forms are zero on the borders of the Manifold

$$\langle d\omega^k, \nu^{k+1} \rangle = \langle \omega^k, \partial\nu^{k+1} \rangle.$$

Therefore, for harmonic  $k$ -forms,

$$\begin{aligned} 0 &= \langle \Delta\omega^k, \omega^k \rangle = \langle \partial d\omega^k + d\partial\omega^k, \omega^k \rangle \\ &= \langle \partial d\omega^k, \omega^k \rangle + \langle d\partial\omega^k, \omega^k \rangle \\ &= \langle d\omega^k, d\omega^k \rangle + \langle \partial\omega^k, \partial\omega^k \rangle. \end{aligned}$$

Because the scalar product is non-degenerated, meaning that  $\langle \nu, \nu \rangle \geq 0$  with  $\langle \nu, \nu \rangle = 0$  iff  $\nu = 0$ , it follows that

$$\begin{aligned} d\omega^k &= 0, \\ \partial\omega^k &= 0. \end{aligned}$$

Therefore we get on borderless manifolds, or if  $\omega^k = 0$  on the border:

$$\Delta\omega^k = 0 \Leftrightarrow \begin{cases} d\omega^k = 0 \\ \partial\omega^k = 0 \end{cases}$$

For 1-forms,  $d$  is the curl operator and  $\partial$  is the divergence operator. Therefore, on compact borderless manifolds, harmonic vector fields are curl and divergence free. Harmonic forms are  $d$  and  $\partial$  free. In the vector field design set up the aim is to minimize

$$\langle d\omega^1, d\omega^1 \rangle + \langle \partial\omega^1, \partial\omega^1 \rangle.$$

So we solve for vector fields that are as harmonic as possible. Minimality under  $\langle d\omega^1, d\omega^1 \rangle + \langle \partial\omega^1, \partial\omega^1 \rangle$  is also called weak formulation of harmonicity.

### 6.3.3. Poincaré-Lemma

The Poincaré-Lemma describes when a differential form  $\omega$  is the derivative of some other form  $\nu$ , i.e., when there exists a  $\nu$  such that

$$d\nu = \omega. \quad (6.1)$$

The Poincaré-Lemma states that if a manifold  $M$  can be parametrized by one open contractible subset<sup>1</sup> of  $\mathbb{R}^n$ , this is exactly the case if

$$d\omega = 0. \quad (6.2)$$

A differential form  $\omega$  for which there exists a  $\nu$  such that Equation 6.1 holds is called *exact*, while an  $\omega$  fulfilling Equation 6.2 is called *closed*. The Poincaré Lemma is also true for the codifferential operator  $\partial$ . Under the same conditions as above a form is co-exact, exactly if it is co-closed:

$$\exists \nu : \partial\nu = \omega$$

$\Leftrightarrow$

$$\partial\omega = 0.$$

This means that, for general manifolds at least locally, a form is the exterior derivative of another form, exactly if it is  $d$ -free. The same is true for the coderivative  $\partial$ .

The lemma also answers the question how unique a  $\nu^k$  is, when you require  $d\nu^k = \omega^{k+1}$ . If  $\nu_1$  and  $\nu_2$  are solutions to Equation 6.1, then  $d(\nu_1 - \nu_2) = 0$ . By the Pointcaré-Lemma the difference  $\nu_1 - \nu_2$  is again the exterior derivative of a  $(k-1)$ -form  $\xi^{k-1}$ , therefore

$$\nu_2 = \nu_1 + d\xi^{k-1}.$$

This means that given one special solution  $\nu$  you get all solutions by adding the exterior derivative of arbitrary  $k-1$  forms.

#### Example

On any disc shaped manifold a 1-form  $\omega^1$  is the  $d$  of a 0-form exactly if  $d\omega^1 = 0$ . In vector calculus terms this means that a vector field is the gradient of a function exactly if the vector field is curl free. Or in 3 dimensions a vector field is the curl of another vector field exactly if it is divergence free.

### 6.3.4. Hodge Decomposition

We have seen three kinds of differential forms: exact forms, co-exact forms and harmonic forms. The Hodge decomposition theorem states that any  $k$ -form can be split in three orthogonal complements: a harmonic part  $\gamma : \Delta\gamma = 0$ , an exact part  $d\alpha^{k-1}$  and a co-exact part  $\partial\beta^{k+1}$ :

---

<sup>1</sup>For example a ball-shaped region

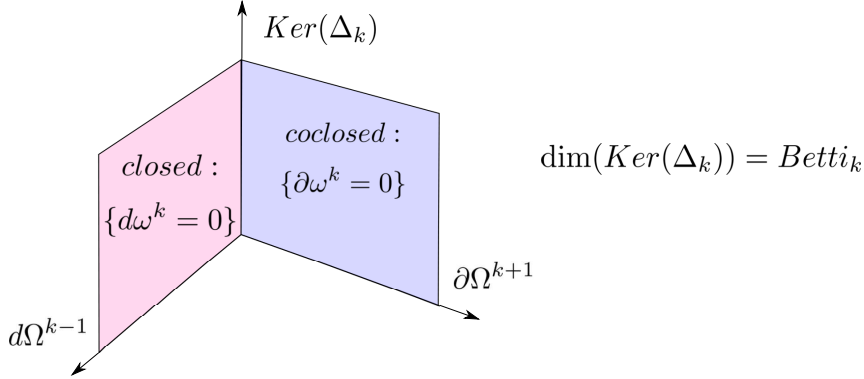


Figure 6.4.: By the Hodge decomposition theorem the space of  $k$ -forms on a closed manifold can be decomposed in the three spaces of exact forms  $d\Omega^{k-1}$ , coexact forms  $\partial\Omega^{k+1}$  and harmonic forms  $Ker(\Delta_k)$ . In general, closedness is not enough for a form to be exact, its harmonic component has to vanish too.

**Theorem 4. (Hodge Decomposition)(p372 in [Fra11])** On borderless, compact manifolds  $M$  any differential  $k$ -form can be expressed as

$$\omega^k = d\alpha^{k-1} + \partial\beta^{k+1} + \gamma.$$

Exact forms, co-exact forms and harmonic forms are mutually orthogonal to each other:

$$\langle d\alpha^{k-1}, \partial\beta^{k+1} \rangle = \langle d\alpha^{k-1}, \gamma \rangle = \langle \gamma, \partial\beta^{k+1} \rangle = 0.$$

The idea behind this result is that the spaces of exact and co-exact differential forms are orthogonal to each other and their orthogonal complement is the space of harmonic forms (Figure 6.4). The actual proof is complicated and technical. We show that the Hodge decomposition works in Discrete Exterior Calculus. And in DEC the proof is very simple, because all involved spaces have finite dimensions.

Realizing that these three spaces are orthogonal to each other simplifies the vector field design problem: vorticity constraints can be met independently of divergence constraints. Also, if there exist harmonic 1-forms on a manifold, then specifying only divergence and curl constraints does not uniquely determine a vector field, as there is no constraint on the harmonic component  $\gamma$ .

The Hodge decomposition also generalized the Pointcaré lemma to arbitrary closed manifolds. The closedness of a form  $d\omega = 0$  is not enough for the form to be exact, i.e., to be the exterior derivative of another form  $d\nu = \omega$ . But additionally the harmonic part of  $\omega$  needs to be zero too. Or put differently:

$$d\omega = 0$$

$\Leftrightarrow$

$$\omega = d\nu + h,$$

where  $h$  is a harmonic form, see also Figure 6.4.

### 6.3.5. Discrete Hodge Decomposition

In DEC the discrete version of the Hodge Decomposition holds. This means that in practice, when using DEC, constraints on  $d\omega$  and  $\partial\omega$  can be enforced independently from each other. As we have seen with conformal maps, when border constraints are enforced, some DEC matrices have to be adapted. To be able to use the Hodge decomposition also when using adapted matrices, we formulate the discrete Hodge theorem generally. We state fundamental properties for the matrices  $d$ ,  $\star$  and  $\partial$  that need to hold for the Hodge decomposition to hold.

**Theorem 5.** (*Discrete Hodge Decomposition*) *If the matrices  $d_k, \partial_k, \star_k$  and the scalar product  $\langle \cdot, \cdot \rangle_k$  on the space of discrete  $k$ -forms fulfill*

$$d_{k-1}d_k = 0, \quad (6.3)$$

$$\langle d_k \mathbf{v}^k, \mathbf{w}^{k+1} \rangle_{k+1} = \langle \mathbf{v}^k, \delta_{k+1} \mathbf{w}^{k+1} \rangle_k, \quad (6.4)$$

*then the following three subspaces are orthogonal to each other, with respect to the scalar product  $\langle \cdot, \cdot \rangle_k$ , and span the space of all discrete  $k$ -forms:*

$$\text{Img}(d_{k-1}) \perp \text{Img}(\partial_{k+1}) \perp (\text{Ker}(d_k) \cap \text{Ker}(\delta_k))$$

*This means that any discrete  $k$ -form can be written uniquely as a sum*

$$\mathbf{w}^k = d_{k-1} \mathbf{a}^{k-1} + \partial_{k+1} \mathbf{b}^{k+1} + \mathbf{c}^k,$$

*where  $\mathbf{c}^k$  is a discrete harmonic  $k$ -form.*

To see this we just need to use the adjointness 6.4:  $\text{Img}(d_{k-1}) \perp \text{Img}(\partial_{k+1})$  is true, as

$$\langle d\mathbf{w}, \partial\mathbf{v} \rangle = \underbrace{\langle dd\mathbf{w}, \mathbf{v} \rangle}_0 = 0 \quad \forall \mathbf{v}, \mathbf{w}.$$

Furthermore,  $(\text{Img}(d_{k-1}) \perp \text{Img}(\partial_{k+1}))^\perp = (\text{Ker}(d_k) \cap \text{Ker}(\delta_k))$ , because

$$\begin{aligned} (\text{Img}(d_{k-1}) \perp \text{Img}(\partial_{k+1}))^\perp &= \mathbf{w}^k : \begin{cases} \langle \partial_{k+1} \mathbf{v}^{k+1}, \mathbf{w}^k \rangle = 0 & \forall \mathbf{v}^{k+1} \\ \langle d_{k-1} \mathbf{v}^{k-1}, \mathbf{w}^k \rangle = 0 & \forall \mathbf{v}^{k-1} \end{cases} \\ &= \mathbf{w}^k : \begin{cases} \langle \mathbf{v}^{k+1}, d_k \mathbf{w}^k \rangle = 0 & \forall \mathbf{v}^{k+1} \\ \langle \mathbf{v}^{k-1}, \partial_k \mathbf{w}^k \rangle = 0 & \forall \mathbf{v}^{k-1} \end{cases} \\ &= \mathbf{w}^k : \begin{cases} d_k \mathbf{w}^k = 0 \\ \partial_k \mathbf{w}^k = 0 \end{cases} \\ &= \text{Ker}(d_k) \cap \text{Ker}(\delta_k). \end{aligned}$$

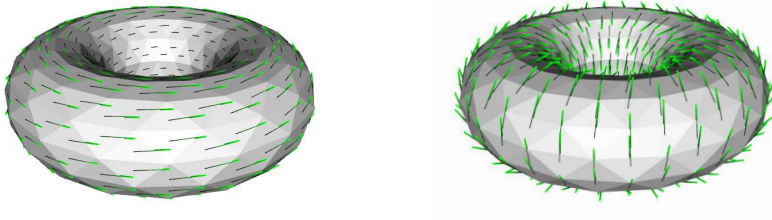


Figure 6.5.: The first Bettinumber for the torus is 2, as it consists of one loop. Therefore the space of harmonic vectorfields on the torus has dimension 2, every harmonic vector field is a combination of the two fields depicted here.

### 6.3.6. Dimension of Harmonic Spaces

To round off the description of harmonic forms we want to mention the following reformulation of a theorem by de Rham. The result we are interested in states (p373 in [Fra11])

*The dimension of the kernel of the Laplacian on the space of  $k$ -forms on a compact borderless manifold is equal to the dimension of the de Rham cohomology group of degree  $k$ , the dimension of which is the  $k$ -th Bettinumber.*

We mention cohomology groups here because if you look into this matter, you will unavoidably come across cohomology groups at once. The cohomology group is an algebraic group that can be defined for manifolds and which only depends on the topology of the manifold. Cohomology groups also have a direct relation to harmonic forms, see Chapter 8 for introductory literature. Despite their importance we will ignore cohomology groups in this thesis, as this would go beyond the scope of this thesis. In the above we are interested only in the statement that the dimension of the kernel of the Laplacian on the space of  $k$ -forms is given by the  $k$ -th Bettinumber:

$$\dim \ker(\Delta_k) = \text{Betti}_k.$$

Remember that the kernel  $\ker(\Delta_k)$  is the space of the forms  $\omega^k$  with  $\Delta_k \omega^k = 0$ , that is the space of harmonic  $k$ -forms.

The Bettinumbers are finite natural numbers that depend only on the topology of the manifold. The zeroth and the first Bettinumber capture the following properties on two dimensional compact Riemannian manifolds: the 0-Bettinumber is the number of connected components of the manifold. The first Bettinumber is two times the number of "handles" or "loops" the manifold has. Here "handle" is meant in its plainest sense. A coffee cup usually has exactly one loop-like handle, therefore the first Betti number of its surface is 2. A donut consists of exactly one loop-like handle, so its first Bettinumber is 2 as well. It is also merely a deformation of a classical coffee cup. A pretzel consist

of three handles so its surface has Bettinumber 6. And a sphere has no handles at all, therefore it has Betti number 0.

The result therefore states not only that the space of harmonic forms always has a finite dimension, but that the dimension also only depends on the topology of the manifold, and this, again, is very nice. Figure 6.5 shows the result on the torus for vector fields. The overview over the different  $k$ -form subspaces on closed manifold is depicted in Figure 6.4.

The theory about harmonic forms, closed forms and co-closed forms on closed (i.e. compact and borderless) manifolds is rich and beautiful but also deep. To see more of it I recommend the book 'The Geometry of Physics' [Fra11], Chapters 13 and 14 which describes the theory and its backgrounds in a concise, yet intuitive way, mentioning also the technical problems that would arise in a thorough treatment.

## 6.4. Application: Vector Field Design

By the Hodge decomposition theorem, constraints on the divergence of a vector field are independent of constraints on the curl of a vector field. We solve for a 1-form  $\mathbf{w}^1$  with prescribed divergence and curl and additional directional constraints. First of all we note that in DEC the divergence of a discrete vector field  $d\mathbf{w}^1$  is a discrete 0-form, therefore divergence constraints are given per vertex on a mesh. Rotational constraints are given by triangle, as the curl  $d\mathbf{w}^1$  is a discrete 2-form. Finally directional constraints constrain specific values of the discrete 1-form  $\mathbf{w}^1$  and therefore are given on selected edges.

All the constraints can be compiled easily in one linear system:

$$\begin{pmatrix} d \\ \partial \\ Z \end{pmatrix} \mathbf{w}^1 = \begin{pmatrix} r_t \\ s_v \\ c_z \end{pmatrix}, \quad (6.5)$$

where  $Z$  is the identity matrix, constrained to the edges affected by directional constraints,  $r_t$  is the vector of target rotation values of defined by triangle,  $s_v$  is the target divergence values, defined by vertex, and  $c_z$  is the vector of constraints per edge, given by the directional constraints.

The constraints  $r_t$ ,  $s_v$  and  $c_z$  are provided by a user and are very likely to be contradictory. For example constraints on singularities as vortices given by the Hopf Index theorem are easily violated, if an impossible combination of singularities is prescribed. Or directional constraints might induce divergence or curl. Therefore the linear system is solved in a least square sense.

But the correct norm to for the least squares problem is not the Euclidean norm. For example we want to minimize  $d\mathbf{w}^1 - r_t$  as a discrete 2-form and as seen in Section 4.5.6 the correct norm for 0-forms is given by  $\star_0$ , meaning that

$$\langle d\mathbf{w}^1, d\mathbf{w}^1 \rangle_2 = (d\mathbf{w}^1)^T \star_2 (d\mathbf{w}^1)$$

should be minimal, and analogously

$$\langle \partial \mathbf{w}^1, \partial \mathbf{w}^1 \rangle_0 = (\partial \mathbf{w}^1)^T \star_0 (\partial \mathbf{w}^1).$$

Therefore, the linear equation 6.5 should be minimized relative to the scalar product or norm given by the diagonal matrix

$$L = \begin{pmatrix} \star_2 & & \\ & \star_0 & \\ & & W \end{pmatrix},$$

$$\langle \cdot, \cdot \rangle_{vfdesign} = (\cdot)^T L(\cdot),$$

$$\|\cdot\|_{vfdesign} = \langle \cdot, \cdot \rangle_{vfdesign}.$$

Here  $W$  is a diagonal weight matrix introduced to additionally control the influence of directional constraints. The least square solution  $\mathbf{w}^1$

$$\arg \min_{\mathbf{w}^1} \left\| \begin{pmatrix} d \\ \partial \\ Z \end{pmatrix} \mathbf{w}^1 - \begin{pmatrix} r_t \\ s_v \\ c_z \end{pmatrix} \right\|_{vfdesign}$$

is then the solution of the normal equation

$$(d^T \quad \partial^T \quad Z^T) L \begin{pmatrix} d \\ \partial \\ Z \end{pmatrix} \mathbf{w}^1 = (d^T \quad \partial^T \quad Z^T) L \begin{pmatrix} r_t \\ s_v \\ c_z \end{pmatrix}. \quad (6.6)$$

This linear system can be implemented directly and solved with any sparse solver.

Again note the elegance of DEC: the vector field design problem can be formulated directly in DEC and leads to a simple sparse linear system. But there are two points not yet answered: how to treat meshes with borders, and how to get a vector field on the triangle faces from a discrete 1-form, which is only a set of values stored on edges.

#### 6.4.1. 1-Form to Vector Field

Up to now we designed a discrete 1-form  $\mathbf{w}^1$ , without clarifying how the discrete 1-form can be used to generate a tangential vector field on the mesh. So given a discrete 1-form, i.e., a set of values defined per edge that represent values sampled as described in Section 3.2.1 how to generate a tangential vector field? In other words we want a discrete analogue to the continuous  $\#$  operator from Section 3.1.5.

The definition of sharp operators for discrete exterior calculus is not obvious and closely related to interpolation schemes. One approach is to interpolate the values of the discrete 1-forms to define a continuous differential 1-form on every triangle. The interpolated 1-forms integrated along an edge  $e$  has to lead to the value  $\mathbf{w}^1(e)$ . Then the non-discrete sharp operator can be applied to the interpolated 1-form to get a vector at any position on the mesh.

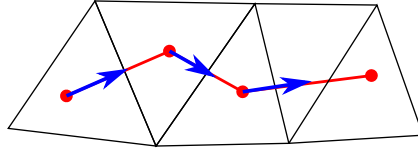


Figure 6.6.: Getting a directional constraint (the blue arrows) from the mouse stroke (red).

In [Hir03] it is argued that there are at least four different  $\#$  operators that can be gained from any single interpolation scheme. Also discrete dual forms need to be interpolated differently than discrete primary forms, as they are defined on different simplices or cells.

The authors of the vector field design paper [FSDH07] propose to use so called Whitney forms or Whitney elements for the interpolation step. This leads to differentiable 1-forms on every triangle, but with discontinuities on vertices and edges. We skip all details here and simply give the resulting  $\#$  operator. For any triangle  $t_{ijk}$  with vertices  $i, j, k$  and edges  $e_{ij}, e_{jk}, e_{ki}$  the proposed vector at a point with barycentric coordinates  $\alpha_i, \alpha_j, \alpha_k$  is

$$\begin{aligned} u(\alpha_i, \alpha_j, \alpha_k) = & \frac{1}{2\text{area}(t_{ijk})} ((\mathbf{w}_{ki}\alpha_k - \mathbf{w}_{ij}\alpha_j)e_{jk}^\perp) + \\ & (\mathbf{w}_{ij}\alpha_i - \mathbf{w}_{jk}\alpha_k)e_{ki}^\perp + \\ & (\mathbf{w}_{jk}\alpha_j - \mathbf{w}_{ki}\alpha_i)e_{ij}^\perp, \end{aligned} \quad (6.7)$$

where  $e^\perp$  denotes the edge  $e$  rotated by  $90^\circ$  in the plane of the triangle  $t_{ijk}$ , according to the orientation of  $t_{ijk}$ . We then have as a discrete sharp operator

$$\mathbf{w}_{ijk}^{1\#}(\alpha_i, \alpha_j, \alpha_k) = u(\alpha_i, \alpha_j, \alpha_k).$$

Note that in the context of fluid simulation in the next Chapter we will need to get a continuous vector field from discrete 1-form, such that this  $\#$  will not be suited. But the 1-form will be strictly divergence free and we will give a  $\#$  operator for this special case.

#### 6.4.2. Directional Constraints

The directional constraints  $Z\mathbf{w}^1 = c_z$  are provided by the user using strokes (Figure 6.6). The simplest way to translate a stroke into 1-form constraints is to capture the path of the mouse stroke and translate it to vectors that describe the direction of the mouse motion per triangle. A single vector  $v$  on a triangle  $t$  can then be interpreted as describing a constant vector field on the triangle. According to the sampling scheme described in Section 3.2.1, the target value for an edge  $e$  of the triangle  $t$  simply is the projection of  $v$  on  $e_t$ :

$$c_z = \langle v, (e.end - e.start) \rangle.$$

If an edge  $e$  is part of two triangles with different vector valued constraints  $v_1, v_2$ , simply taking the value

$$c_z = \frac{1}{2} (\langle v_1, (e.end - e.start) \rangle + \langle v_2, (e.end - e.start) \rangle)$$

works well.

For the magnitude of the directional constraints  $v$  we propose two schemes. The first is to norm all directional constraints to the same user-specified length  $\lambda$ , i.e.,

$$|v| = \lambda. \quad (6.8)$$

The second one is to solve Equation 6.6 once without any directional constraints to generate a first vector field  $\nu_{pre}$  and then to scale the directional constraints to have the same length as the precomputed vector field:

$$|v| = |\nu_{pre}|. \quad (6.9)$$

### 6.4.3. Results

Both directional constraint types have different properties. Specifying a constraint of the type in Equation 6.8 can introduce new divergence or influence the vector field globally in an unintuitive way. Especially if the constraint is drawn in an environment where the vector field nearly vanishes, the enforcement of the no divergence constraint might lead to a global change of the vector field flow, see Figure 6.7. On the other hand you can use the introduction of divergence to your advantage: you can directly draw sources or sinks or more complex singularities which then are enforced 6.8.

Constraints described by Equation 6.9 are less aggressive; the impact on divergence is less pronounced. The constraint makes the designed vector field follow the given stroke without affecting the global look of the vector field. But you can not use such a constraint to specify new singularities.

### 6.4.4. Border Constraints

Meshes with boundaries are not treated correctly or intuitively without further adaptations, see Figure 6.9. The problem is that the discrete zero divergence condition,

$$\partial \mathbf{w}^1 = 0,$$

is not enforced correctly on boundaries. The problem is that border vertices do not have a full 1-neighborhood of faces.

Let's look at the discrete co-derivative  $\partial_1 = \star_0^{-1} d^{dual} \star_1$ . The  $\star_1$  applied to the discrete 1-form  $\mathbf{w}^1$  leads to a dual 1-form; the values associated to the dual edges represent the flow of the vector field going through the dual edge. The dual discrete derivative  $d^{dual}$  sums up the values on the dual edges along the border of dual faces. At interior vertices the value  $d^{dual} \star_1 \mathbf{w}^1$  describes the overall flow in or out of the associated dual faces and is a correct approximation of divergence. But dual faces of border vertices are not

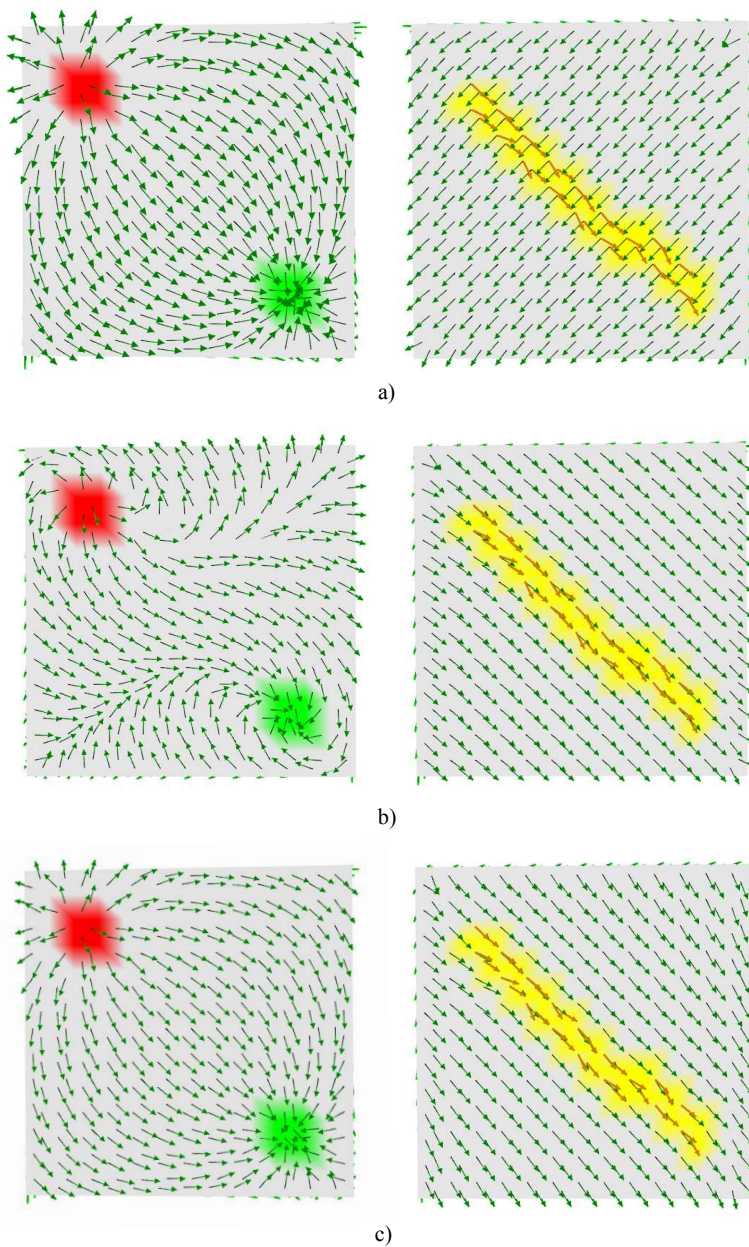


Figure 6.7.: (a) On the front of a cube a source and a sink have been set. On the back of the cube a directional constraint is given by a stroke but is not yet enforced. (b) The directional constraint is enforced following Equation 6.8. Because the length of the constraint is not well chosen the field is affected globally. (c) The directional constraint is enforced using precalculated vector lengths following Equation 6.9. This introduces no new divergence and the front of the cube stays unaffected.

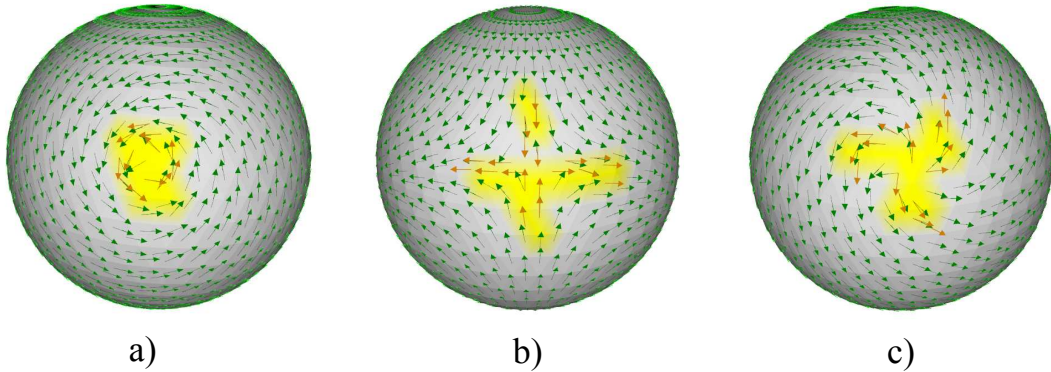


Figure 6.8.: The constraint from Equation 6.8 can be used to induce singularities, e.g. vortices (a), saddles (b) or spirals (c).

closed and no flow through the boundary is considered (see Figure 6.10). Therefore,  $\partial^{discrete} \mathbf{w}^1 = 0$  implicitly enforces that there is no flow through the boundary of meshes, and that the designed vector field is parallel to borders.

In order to compute the total divergence on a dual face of a border vertex we need to know the flow through primary border edges. But this is a problem. The value stored on primary edges is the flow along the edge. Put differently we would need to know the dual form on primary vertices.

The authors of [FSDH07] propose to use the zero curl condition  $d\mathbf{w}^1 = 0$  together with the Whitney based interpolation scheme to compute the flow through a primary border edge. The curl freeness on a triangle  $t_{ijk}$  means  $\mathbf{w}_{ij}^1 = -\mathbf{w}_{jk}^1 - \mathbf{w}_{ki}^1$  and using the interpolation scheme from Equation 6.7 they compute the flow  $f_{ij}$  through the edge  $e_{ij}$

$$f_{ij} = \int_{e_{ij}} \langle u(t, 1-t, 0), \frac{1}{|e_{ij}|} e_{ij}^T \rangle = \mathbf{w}_{jk}^1 \cot(\theta^i) - \mathbf{w}_{ki}^1 \cot(\theta^j). \quad (6.10)$$

The estimated flow through the border edges can be used to control the behaviour of the vector field on the boundaries. When computing  $\delta_1$ , we can adapt the matrix  $d_1^{dual} \star_1$  to use the estimated flux through the boundary edges as well (see Figure 6.10).

### Implementation

All that needs to be changed is that the matrix  $d_1^{dual} \star_1$  needs to be adapted on all rows corresponding to boundary vertices to take the estimated boundary flux into account. Supposing the edges  $e_{ij}$ ,  $e_{jk}$  are two boundary edges at the vertex  $v_j$ , then

$$(d_1^{dual} \star_1)_{adapted}(v_j) := d_1^{dual} \star_1(v_j) + 0.5f_{ij} + 0.5f_{jk}.$$

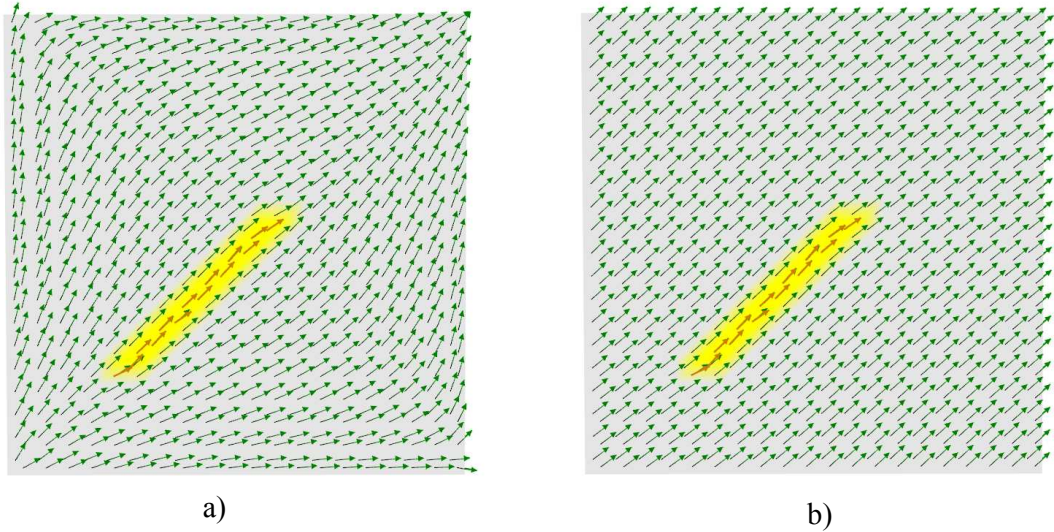


Figure 6.9.: A square with border. Without further adaptations of the DEC matrices the vector field is implicitly enforced to be tangential to the border (a). The adapted matrices allow the vector field to behave freely on the boundary (b).

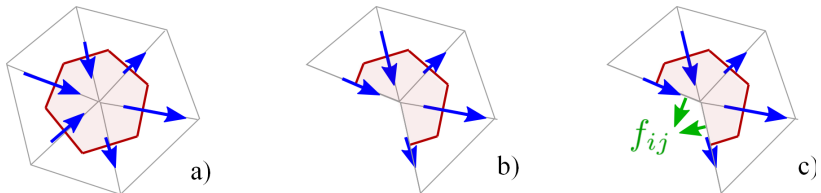


Figure 6.10.: A discrete dual 1-form  $\star_1 \mathbf{w}$  stores the flux through the edges (blue arrows) on the dual edges. Inner vertices have a full 1-neighborhood (a) and summing up the dual edges around a vertex is a correct estimation of divergence. Border vertices do not have a full neighborhood (b), summing up the dual edges around a vertex neglect any flow through the mesh boundary. Therefore  $\partial_1$  needs to be adapted to take the estimated flux over the boundary into account as well (c).

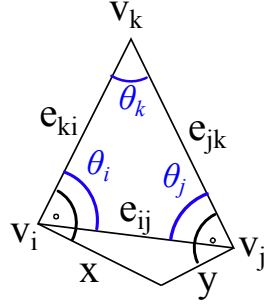


Figure 6.11.: The flow along the edges  $e_{ki} = (v_k, v_i)$  and  $e_{jk} = (v_j, v_k)$  is known. The flow through the edge  $e_{ij}$  can then be estimated as the flow through  $x$  plus the flow through  $y$ . Some basic trigonometry shows that the length of  $x$  is  $|e_{ki}| \cot(\theta_j)$  and the length of  $y$  is  $|e_{jk}| \cot(\theta_i)$ . As  $x$  and  $y$  are orthogonal to  $e_{ki}$  and  $e_{jk}$  respectively, the flow through  $x$  and  $y$  can be estimated as  $-\mathbf{w}_{ki}^1 \cot(\theta^j)$  and  $\mathbf{w}_{jk}^1 \cot(\theta^i)$  respectively, leading to Equation 6.10

The factor  $+0.5f_{ij} + 0.5f_{jk}$  for boundary vertices can be easily described as a matrix:

$$M_{borderdiff} = \begin{cases} \downarrow v \in e_1 \in border & \downarrow v \in e_2 \in border \\ v \notin border \rightarrow & \\ v \in border \rightarrow & \begin{pmatrix} 0 & 0 & \dots & 0 & 0 \\ 0 & 0.5 \cdot sgn(e_1, brdr) & \dots & 0.5 \cdot sgn(e_2, brdr) & 0 \\ 0 & & \dots & & 0 \\ 0 & & \dots & & 0 \end{pmatrix} \end{cases}.$$

$$\begin{cases} e \notin border & \\ e_{ij} \in border & \begin{pmatrix} 0 & 0 & \dots & 0 & 0 \\ & \cot(\theta^i) sgn(e_{jk}, t_{ijk}) & \dots & \cot(\theta^j) sgn(e_{ki}, t_{ijk}) & 0 \\ 0 & & \dots & & 0 \end{pmatrix} \end{cases}$$

The second matrix is a square matrix of size ( $\#edges \times \#edges$ ) that computes the flux for border edges following Equation 6.10 and is zero for all non border edges. The first matrix computes the border flux relevant for border vertices and is of size ( $\#vertices \times \#edges$ ). The  $sgn$  denote the relative orientations of the edges to the border or the face they lie in.

### Pros and Cons of this approach

In the vector field design setting using the adapted matrix works very well. But to generally use the adapted  $(d_1^{dual} \star_1)_{adapted}$  on meshes with borders might not be a good idea. First of all the constraint works with the assumption that there is no curl on boundary triangles. Secondly with the adapted matrix, the property  $\partial_1^{dual} \partial_2^{dual} = 0$  does not hold any more and the adjointness of  $d_0$  and  $\delta_1$  also fails. And with it the discrete

Hodge theorem. From a theoretical standpoint where we want the DEC operators to have properties similar to the properties of the continuous operators the loss of adjointness and  $\partial_1^{dual} \partial_2^{dual} = 0$  is bad.

On the other hand it is natural for the Hodge decomposition theorem to fail on meshes with boundaries- only if the forms fulfill additional boundary constraints the Hodge decomposition holds. It is interesting that the unadapted DEC matrices lead to differential forms tangential to the mesh boundaries. This mirrors the smooth setting, where the Hodge decomposition can be shown to hold on arbitrary manifolds for forms tangential to the border [Fra11].

Finding good adaptations for DEC matrices to enforce boundary conditions seems to be highly application dependent. In the next Chapter where a fluid simulation using DEC is presented there will also be the need to solve for a harmonic 1-form with given boundary constraints. But instead of using the approach described here, the tangentiality of the 1-form searched is used and matrices are derived that are consistent with the discrete Hodge decomposition theorem, in order to achieve higher precision.

Nevertheless, in this vector design setting, or in any setting where the emphasis is on visually pleasant results rather than on optimal precision, the adapted  $d^{dual}$  operator is very suitable.

# 7. A Fluid Simulation with DEC

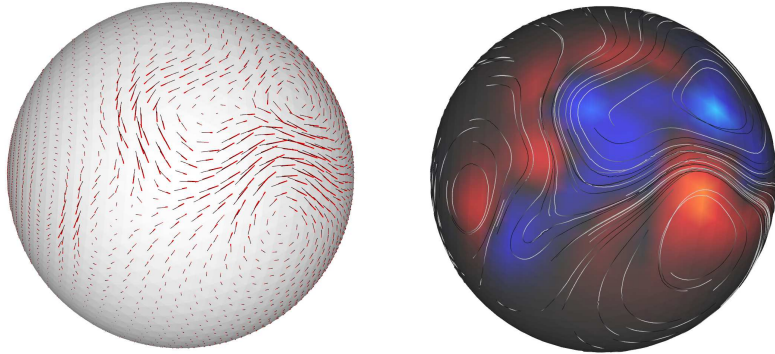


Figure 7.1.: The simulation of a viscous fluid on a sphere with 1920 triangles. Motion was induced by stirring.

In this chapter a fluid simulation using DEC is presented, following the approach from Elcott et al. [ETK<sup>+</sup>07]. All theory but fluid dynamics has been introduced, so this chapter is a demonstration of DEC in use.

One of the challenges when simulating fluids is to keep geometric features like incompressibility or vortices. Because of the geometric nature of DEC and because DEC conserves the geometry of the curl and divergence operator, these difficulties drop away. On the other hand simplifying assumptions are taken, and together with the interpolation scheme used, it is not clear how accurate the simulation is. The authors of [ETK<sup>+</sup>07] have taken the pragmatic point of view that their simulation is designed to preserve visually important features of fluids and left thoughts about accuracy for future work.

## 7.1. Problem Statement

The two features this simulation concentrates on are the viscosity and vorticity of fluids. Viscosity is a measure for the internal friction of a fluid. If a fluid parcel, that is a small, particle-like volume, moves with some speed, the neighboring fluid is affected by friction and dragged along to some extent, while the fluid parcel itself is slowed down. Vortices are fluid parcels that have picked up rotation. If a fluid parcel picked up some rotation it keeps rotating when moving along the flow. The rotation is only damped by the internal friction of the fluid.

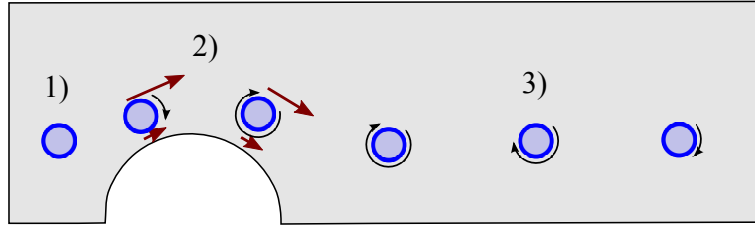


Figure 7.2.: A parcel without any rotation (1) moves along the border of an obstacle and picks up vorticity due to the viscosity of the fluid (2). The vorticity then is diffused and slowly decreases, again because of the viscosity of the fluid (3).

In combination with obstacles the viscosity of a fluid also induces new vorticities. If a fluid has internal friction, its velocity on the boundary of static, non-moving obstacle has to be zero. A parcel moving along an obstacle then picks up vorticity, as depicted in Figure 7.2.

Vorticity is measured by the curl of the velocity field. As seen in Section 4.2.3, curl measures how much rotation a velocity field induces locally.

### 7.1.1. Navier Stokes

The first step is to formulate the behaviour of fluids appropriately with vector calculus and exterior calculus. Physics provide the following description of incompressible viscous fluids, the Navier-Stokes equation:

$$\frac{\partial u}{\partial t} + Du \cdot u = -\nabla p + \nu \Delta u, \\ \operatorname{div}(u) = 0. \quad (7.1)$$

The single terms have the following meanings:

- $u(x, t)$  is a time and position dependent vector field of velocities. The velocities describe the speed and the direction of 'particles' at fixed positions
- The condition  $\operatorname{div}(u) = 0$  describes that the fluid is incompressible; at every point all incoming flow has to go out. This ensures that the total volume of the fluid is preserved.
- $\frac{\partial u}{\partial t} + Du \cdot u$  is the material derivative or derivative along the motion (see Figure 7.3). The material derivative is based on the idea that you track particles or parcels and compute the change of their velocity. The trajectory  $\alpha$  of a particle is defined by:

$$\frac{\partial \alpha(t)}{\partial t} = u(\alpha(t), t)$$

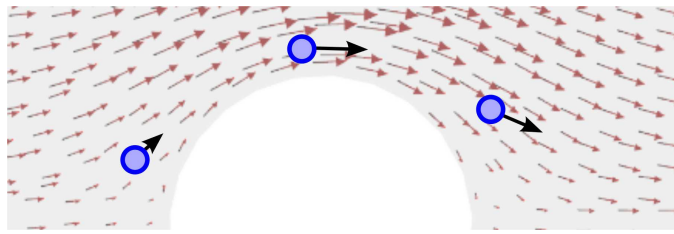


Figure 7.3.: A comparision of the derivative and the derivative along the motion: the velocity field is constant over time and its derivative  $\frac{\partial u}{\partial t}$  is zero. But the velocity of a tracked particle changes; the material derivative describes this change.

The change of velocity of such a particle can then simply be computed by using the chain rule,

$$\begin{aligned}\frac{\partial}{\partial t} u(\alpha(t), t) &= Du \cdot \frac{\partial}{\partial t} \begin{pmatrix} \alpha(t) \\ t \end{pmatrix} \\ &= \left( \frac{\partial u}{\partial x}, \frac{\partial u}{\partial y}, \frac{\partial u}{\partial z}, \frac{\partial}{\partial t} \right) \cdot \begin{pmatrix} u(\alpha(t), t) \\ 1 \end{pmatrix} \\ &= \frac{\partial u}{\partial t} + Du \cdot u.\end{aligned}$$

- $p(x, t)$  is a scalar field that describes the pressure at the position  $x$  at time  $t$ . The vectors  $-\nabla p$  therefore point in the direction of the largest pressure decrease.
- The factor  $\nu \Delta u$  is the diffusion factor and  $\nu$  is the viscosity, a real valued material dependent constant. The viscosity  $\nu$  describes how 'thick' the fluid is, how much internal friction it has. For example honey is thicker than water and its viscosity  $\nu$  is higher; water having a viscosity of 0.001. The term  $\nu \Delta u$  describes that the higher the friction is, the more the velocities get diffused.

The Navier-Stokes equation states that the movement of small parcels is influenced by pressure differences and a diffusion term. Every particle is pulled both in the direction of the largest pressure decrease and in a direction such that curl and divergence are decreased (diffusion), where the influence of the diffusion depends on the fluid's viscosity.

### Navier Stokes for Vorticities

To put an emphasis on the behavior of vortices in the fluid simulation, the authors of [ETK<sup>+</sup>07] reformulate the Navier Stokes equation in terms of vorticities. You get such a description by applying  $\nabla \times$  to both sides of Equation 7.1,

$$\nabla \times \frac{\partial u}{\partial t} + \nabla \times (u \cdot \nabla u) = - \underbrace{\nabla \times \nabla p}_{=0} + \nu \nabla \times \Delta u,$$

leading to<sup>1</sup>:

$$\frac{\partial w}{\partial t} + Dw \cdot u - Du \cdot w = \nu \Delta w, \\ w = \nabla \times u, \quad \operatorname{div}(u) = 0. \quad (7.2)$$

Simulating the curl  $\nabla \times u$  of the velocity field instead of the velocities  $u$  has benefits. The pressure term disappears. And simulating the curl leads to a better simulation of the vortices.

The left hand side of Equation 7.2 describes the derivative of curl along the motion, similarly to the derivative of  $u$  along the motion that appeared in Equation 7.1. Equation 7.2 therefore states that vorticity is carried along the flow while being diffused with time. The viscosity  $\nu$  controls how fast vorticities get diffused. The extreme is an inviscid fluid, a fluid with no internal friction. There the viscosity is  $\nu = 0$  and the derivative of the curl along the motion is 0. Therefore the curl along the motion is constant and vorticities are carried with the flow without ever being diminished.

### Stirring

To take account of additional forces  $F$ , for example induced by stirring, the Equations 7.1 and 7.2 need to be slightly adapted to

$$\frac{\partial u}{\partial t} + Du \cdot u = -\nabla p + \nu \Delta u + F,$$

such that the change of velocity also depends on  $F$ . The formulation for vorticities then becomes

$$\frac{\partial w}{\partial t} + Dw \cdot u - Du \cdot w = \nu \Delta w + \nabla \times F, \quad (7.3)$$

where  $F$  is a vector valued function.

#### 7.1.2. A Numerical Integration Scheme

The authors of [ETK<sup>+</sup>07] propose to solve the equation 7.3 for the simulation of the fluid, using what they call a geometric integration scheme. The scheme is a combination of implicit numerical integration and the tracking of particles and mimics the geometric behavior of the flow. Suppose a fluid parcel with space time position  $(p', t_{n+1})$  was at the position  $(p, t_n)$  in the timestep before. Then,

$$\frac{\partial w}{\partial t} + Dw \cdot u - Du \cdot w \approx \frac{(w(p', t_{n+1}) - w(p, t_n))}{t_{n+1} - t_n},$$

and inserting this in Equation 7.3 produces

$$w(p', t_{n+1}) \approx w(p, t_n) + (t_{n+1} - t_n) \cdot \nu \Delta w(p', t_{n+1}) \\ + (t_{n+1} - t_n) \cdot \nabla \times F_{t_{n+1}}, \quad (7.4)$$

---

<sup>1</sup>You need to use  $\nabla u = 0$  to show the identity  $\nabla \times (Du \cdot u) = Dw \cdot u - Du \cdot w$  where  $w = \nabla \times u$ . Also  $\nabla \times \Delta u = \Delta(\nabla \times u)$  is used. Both identities are easy to check by writing them out.

1. Velocities  $u_{t_n}$  are known at time  $t_n$
2. Compute vorticity  $w_{t_{n+1}}$  at time  $t_{n+1}$  at some positions  $p'$ :
  - a) Backtrack  $p'$  according to the velocity field  $u_{t_n}$  to the position  $p$  it was at time  $t_n$
  - b) Use  $u_{t_n}$  to compute  $w_{t_n}(p, t_n)$ .
  - c) Solve  $w_{t_{n+1}}(p', t_{n+1}) = w_{t_n}(p, t_n) + (t_{n+1} - t_n)\Delta w_{t_{n+1}}(p', t_{n+1})$  for  $w_{t_{n+1}}(p', t_{n+1})$  to add diffusion.
3. Add forces  $\omega_{t_{n+1}} = (t_{n+1} - t_n) \cdot \nabla \times F_{t_{n+1}}$
4. Recover the velocity field  $u_{t_{n+1}}$  from the vorticities  $w_{t_{n+1}}$ .

Figure 7.4.: The numerical integration scheme.

where  $F_{t_{n+1}}$  are the additional forces at the time  $t_{n+1}$ . Equation 7.4 can be used for numerical integration over time and directly leads to the integration procedure listed in Figure 7.4.

Before we go on describing each of the steps 2-4 in detail, we have to consider the theoretical feasibility of step 4. In step 4 a velocity field needs to be computed from vorticities alone. In general it is not possible to recover a form  $\omega$  only from its exterior derivative  $d\omega$ , as stated by the Poincaré Lemma in Section 6.3.3. But using the incompressibility of the fluid and making additional assumptions about the harmonic part of the flow, step 4 can be realized. As this is of a theoretical nature and sets the frame for the implementation of the integration scheme, we cover the background of step 4 in the next subsection, Section 7.1.3.

Once the background of step 4 is clarified, we turn to giving detailed descriptions of the single steps of the integration scheme in Section 7.2: the steps 2(a) and (b) of the integration scheme are treated in Section 7.2.3, and steps 2(c) and 3 are described in Section 7.2.4. Step 4 decays in two sub steps; the first is the computation of a harmonic flow component, and is treated in Section 7.2.5. The second is the recovery of the non-harmonic part of the velocity field, and is covered in Section 7.2.6.

### 7.1.3. From Vorticities to Velocities

Here we cover the theoretical background of the step 4 in the integration scheme from Figure 7.4, but without giving implementation details, cf. Sections 7.2.5 and 7.2.6.

In EC terms, velocities can be represented by a 1-form  $u$  and vorticities by a 2-form  $w$ . The problem statement from step 4 then is the following: given a 2-form  $w$  we want

to solve for a 1-form  $u$  such that

$$\left. \begin{array}{l} \partial u = 0 \text{ (incompressibility)} \\ du = w \end{array} \right\}$$

From the Pointcarré Lemma we know that in general the problem  $\partial u = w$  can not uniquely be solved for  $u$ . But by using the incompressibility of fluids and making additional assumptions about  $u$ ,  $u$  can be computed.

The first step is to apply the Hodge decomposition theorem to  $u$ :

$$u = \partial a + db + c,$$

where  $c$  is a harmonic 1-form. From the incompressibility condition  $\partial u = 0$ , we know that the non divergence free part  $db$  needs to be zero.<sup>2</sup> Therefore the Hodge decomposition simplifies to:

$$u = \partial a + c.$$

As the harmonic part  $c$  fulfils  $dc = 0$ ,

$$w = du = d\partial a. \quad (7.5)$$

There is no way to get the harmonic component  $c$  out of the vorticities  $w$ , as  $w$  depends only of  $a$ . This is not astonishing, as by the Hodge decomposition it is orthogonal to vorticities. The harmonic part  $c$  of  $u$  therefore needs to be computed separately. But from  $w = d\partial a$  not even  $a$  is well defined. But not all is lost. We are only interested in  $\partial a$ , and using the adjointness of  $d$  and  $\partial$  one can show<sup>3</sup>

$$d\partial a = d\partial b \Rightarrow \partial a = \partial b. \quad (7.6)$$

Equation 7.6 means that it does not matter what  $a$  with  $w = d\partial a$  is chosen, as, by Equation 7.6, the contribution  $\partial a$  to the velocities  $u$  is the same for all  $a$  with  $w = d\partial a$ . From the Hodge decomposition theorem we also know that we can constrain  $da$  independently from  $\partial a$ , so we can add the constraint  $da = 0$  to Equation 7.5 to pick a specific solution  $a$ . But if  $da = 0$ , then the term  $\partial da$  is zero too, and we can add  $\partial da$  to Equation 7.5, getting

$$w = d\partial a + \partial da = \Delta a. \quad (7.7)$$

But this is the Poisson problem, which we are able to solve for  $a$ .

So from the vorticities  $w$  we can get the vorticity part  $da$  of the velocity field  $u$ , but not the harmonic part  $c$ . The authors of [ETK<sup>+</sup>07] simply assume that the harmonic part  $c$  is not time dependent and can be computed once and for all from application dependent constraints. We can capture this section in a theorem:

---

<sup>2</sup>We can get this by the usual argument using the no divergence constraint:  $0 = \partial u = \partial \partial a + \partial db + \partial c = \partial db$  and then the adjointness of  $d$  and  $\partial$ :  $\partial db = 0 \Rightarrow \langle \partial db, b \rangle = 0 \Rightarrow \langle db, db \rangle = 0 \Rightarrow db = 0$

<sup>3</sup>If  $d\partial a = d\partial b$ , then  $d\partial(a - b) = 0$  and therefore, using the adjointness of  $d$  and  $\partial$ , we get  $\partial(a - b) = 0$ .

**Theorem 6.** (*Vorticity to Velocity*) If the harmonic component  $c$  of a 1-form  $u$  is given, the space of forms allows a Hodge decomposition and the operators  $d$  and  $\partial$  are adjoint, then the system

$$\left. \begin{array}{l} \partial u = 0 \text{ (incompressibility)} \\ du = w \end{array} \right\} \quad (7.8)$$

can be solved by finding a solution  $a$  of

$$\Delta a = w,$$

and setting

$$u = \partial a + c.$$

From Section 6.3.6 we know that, depending on the topology of the manifold, harmonic forms  $c$  do not need to exist. Namely on the surface of a sphere there are no harmonic 1-forms. A fluid simulation on the surface of a sphere therefore is less complicated than one on a plane with borders.

From the Section 4.4 where the coderivative was introduced, and the Section 6.3.4 about the Hodge decomposition, we know that on manifolds with borders, the operators  $d$  and  $\partial$  need not to be adjoint and the Hodge decomposition needs not to hold either. In [Fra11] (p377ff) more general results are mentioned. The Hodge decomposition does for example hold for ‘tangential’ forms, that is forms  $\omega$  for which  $\star\omega$  restricted to the border  $\delta M$  is 0. One example of a tangential form would be 1-forms represented by vector fields whose vectors are tangential to borders. Tangential forms arise naturally in the fluid simulation setting, as the boundary of the mesh often represents an impenetrable wall through which a fluid cannot flow.

## 7.2. Implementation

We restrict ourselves to simulations of fluids on two dimensional surfaces. There is no difference in the theory or the algorithm when working on three dimensions, but the display of flow that is restricted to two dimensions is simpler. And in two dimensions the fluid simulation can be demonstrated on curved manifolds.

In the following subsections we work out the details of the integration scheme presented in Figure 7.4. There are many details that need to be handled correctly for the fluid simulation to work properly.

In Section 7.2.1 we describe the sampling scheme used in this application. In comparison to the other applications the sampling schemes of primary forms and dual forms is reversed. This allows the correct enforcement of boundary constraints. In Section 7.2.2 we give a graphical overview of the simulation algorithm, and the Sections 7.2.3 to 7.2.6 explain the single steps of the simulation. Section 7.2.3 covers the computation of a *continuous* vector field from a discrete 1-form, as well as the back-tracing step, Section 7.2.4 covers the handling of diffusion and the addition of forces, and the Sections 7.2.5 and 7.2.6 treat the computation of the harmonic component of the flow, as well as the recovery of the velocity field from the vorticities.

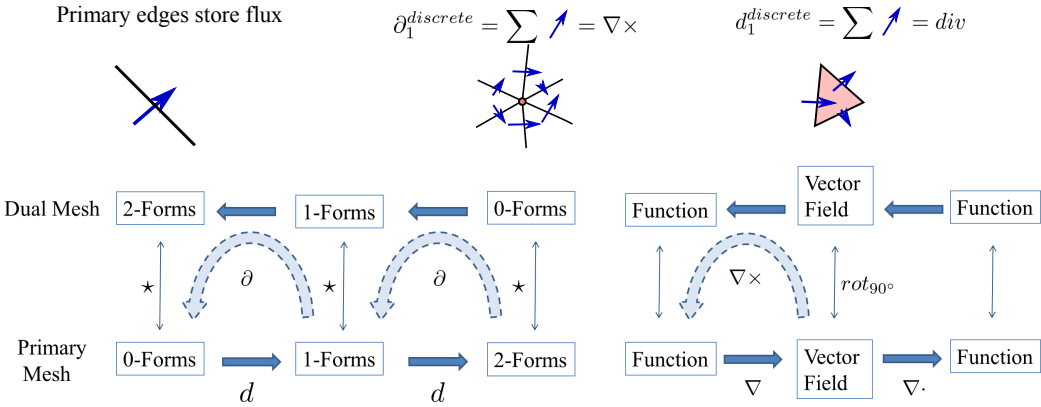


Figure 7.5.: By switching the roles of the dual and primal mesh vector fields are sampled differently, such that primary edges store *flux*, the flow through them, instead of the flow along them. This results in the operators  $d$  and  $\partial$  also changing their meaning.

### 7.2.1. Sampling Scheme

To simplify the specification of border constraints, the role of the dual mesh and the primary mesh are switched, such that what we interpreted so far as dual forms are stored on the primary mesh and vice versa. Primary edges then store the flow through them instead of the flow along them, see also the different sampling schemes from Section 3.2.1. As a result of the swap, the operators  $d$  and  $\partial$  also have different interpretation in vector calculus, see Figure 7.5. For this application vorticity is stored on vertices as a discrete 0-form, or equivalently as a discrete dual 2-forms on dual faces. Divergence is stored as a discrete 2-form on triangles.

The changed roles allow to constrain the flow through the boundaries of the mesh. For example the constraint on impenetrable obstacles and walls is that there is no flow across the boundary. If the discrete 1-form  $\mathbf{u}^1$  represents the velocity form, impenetrability is simply enforced by constraining the flux across the concerned edges to be 0,  $\mathbf{u}^1(e_{\text{boundary}}) = 0$ .

Note that changing the roles of the dual and primal mesh is consistent with the remark in Section 7.1.3, that tangential forms have the property  $\star w|_{\delta M} = 0$ . This can not be enforced on the dual mesh, as the border of the dual mesh is not the geometric border of the mesh.

### 7.2.2. Algorithm Overview

Figure 7.6 sketches one time step of the algorithm that implements the integration scheme (IS) from Figure 7.4 designed to solve the equation

$$\begin{aligned} w(p_{t_{n+1}}, t_{n+1}) \approx & w(p_{t_n}, t_n) + (t_{n+1} - t_n) \cdot \nu \Delta w(p_{t_{n+1}}, t_{n+1}) \\ & + (t_{n+1} - t_n) \cdot \nabla \times F_{t_{n+1}}. \end{aligned}$$

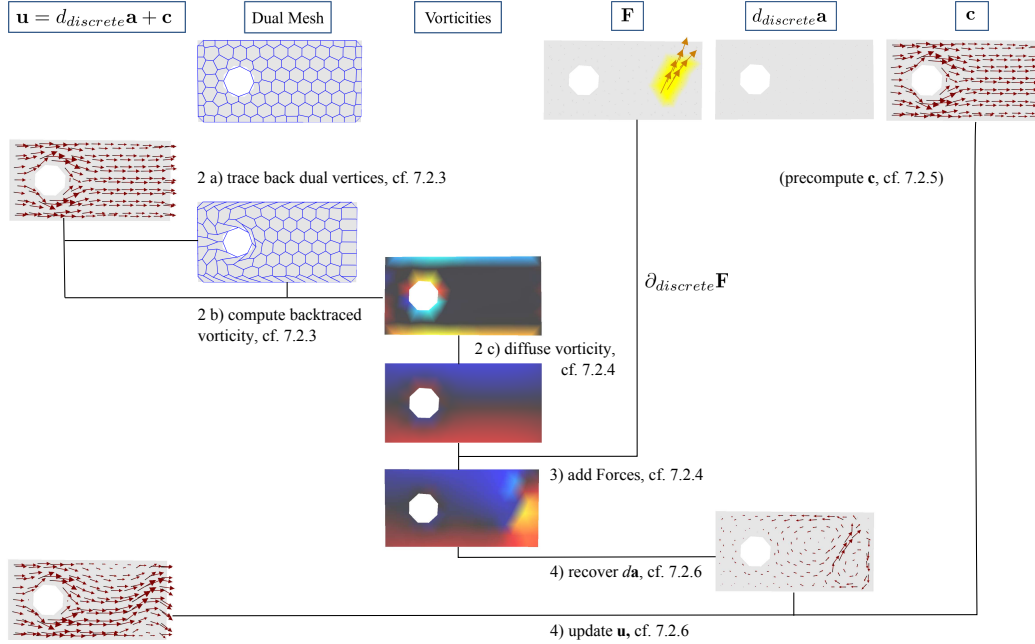


Figure 7.6.: A schematic representation of one time step of the fluid simulation. The labels refer to the corresponding steps in the integration scheme from Figure 7.4, and to the section the step is discussed. The harmonic component  $\mathbf{c}$  is computed separately during a set up stage.

On a high level, the Algorithm consists of the following elements:

During a set up step a harmonic component  $\mathbf{c}$  (see Section 7.2.5) and the dual mesh need to be computed explicitly. The non vorticity free part  $d\mathbf{a}$  of the velocity field  $\mathbf{u}$  is initially set to zero and  $\mathbf{u}$  is set to be the harmonic field  $\mathbf{c}$ . Forces  $\mathbf{F}$  induced by stirring are captured between time steps, in the same way as strokes are captured in the vector field design application.

A single integration time step consists of the following substeps: first the dual vertices are traced back, using a continuous interpolation of the velocity field  $\mathbf{u}$ , in order to compute the back traced vorticities (IS 2 (a), see Section 7.2.3). The back traced vorticity associated to some dual face is computed by first tracing back the dual face and then summing up the flow of  $\mathbf{u}$  around the back traced dual face (IS 2 (b), see Section 7.2.3). These vorticities are diffused and the vorticities  $\partial\mathbf{F}$  of the additional forces  $\mathbf{F}$  are added to the diffused vorticities (IS steps 2 (c) and 3, see Section 7.2.4). Finally the vorticity part  $d\mathbf{a}$  of the velocity field  $\mathbf{u}$  is recovered from the obtained vorticities, and  $\mathbf{u}$  is updated, using the precomputed harmonic component  $\mathbf{c}$  (IS step 4, see Section 7.2.6).

### 7.2.3. Interpolation and Pathtracing

The first step in the IS is to backtrace the vorticities. Vorticities are calculated by summing up the flow around dual faces. In order to compute the backtraced vorticities, the dual faces, or more specifically the dual vertices, are backtraced.

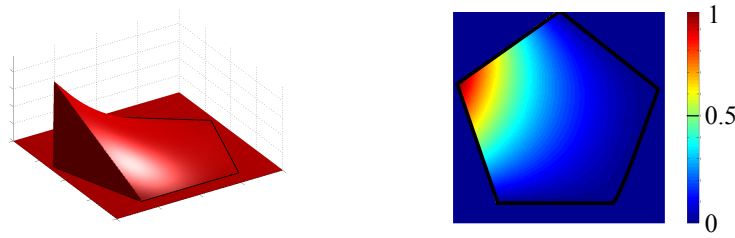


Figure 7.7.: The baricentric weight function for one vertex in a pentagon, once as shaded surface, once as color plot. Note that the weight is linear on the polygon edges.

To be able to trace the path of a vertex and to be able to compute the flow around a backtraced dual face, we need a continuous vector field defined on the mesh. Note that the interpolation scheme using Whitney forms described in Section 6.4.1 is not suited, as it does not produce a continuous vector field. Therefore, we first describe how to compute a continuous vector field from a discrete 1-form, then how this field can be used for tracing the path of a particle, and finally how the velocity field is used to compute the vorticity on a backtraced dual face. Logically these are the steps 2 a) and 2 b) of the integration scheme.

### A Continuous Vector Field on the Mesh

The authors of [ETK<sup>+</sup>07] propose the following interpolation scheme to get a continuous vector field. First, velocity vectors are computed at the positions of dual vertices; this can be done using the sharp operator from 6.4.1. A velocity vector at an arbitrary point  $p$  on the mesh is then computed by first identifying the dual face the  $p$  lies in, i.e. identifying the closest vertex, and then smoothly interpolating the velocity vectors given on the corners of the dual face.

The velocity vectors are interpolated over the dual faces using the weights described in [WSHD07]. To compute the interpolated velocity at some position  $x$  on a flat convex polygon with vertices  $p_1, \dots, p_k$ , every vertex is assigned a weight  $w_j$ , depending on  $x$ . The weight  $w_j$  for the vertex  $p_j$  is given by:

$$c_j(x) = \frac{|n_{j1} \times n_{j2}|}{\langle n_{j1}, p_j - x \rangle \cdot \langle n_{j2}, p_j - x \rangle},$$

$$w_j(x) = \frac{c_j}{\sum_{i=1}^k c_i},$$

where  $n_{j1}$  and  $n_{j2}$  are the normals on the edges incident to  $p_j$ . On the edges of the polygon, these weights are linear. Particularly the weights coincide for neighboring polygons, and therefore can be used to produce a vector field without discontinuities between neighboring dual faces. One weight function is depicted in Figure 7.7.

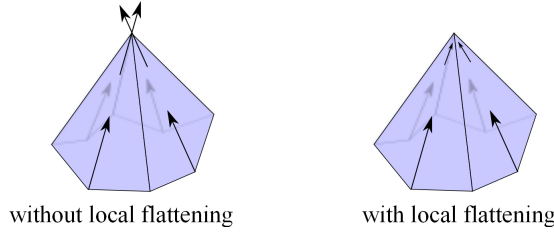


Figure 7.8.: On curved meshes dual faces are not flat, they need to be flattened in the interpolation step to get a continuous interpolation of the vector field.

On flat meshes these weights can be used directly to interpolated the velocities computed on dual vertices via

$$u(x) = \sum_j w_j(x) u_j.$$

On a curved mesh such an interpolation will not lead to a tangential vector. To simply reproject the interpolated vector on the appropriate triangle leads to a non continuous vector field, see Figure 7.8. Therefore, we propose to flatten the dual face and the velocities by projecting them along the curvature normal described in [MDSB02] associated to the dual face, do the interpolation with the projected vector field and then project the interpolated vector back to the appropriate triangle. The flattening is given by:

$$\begin{aligned} u_{flat}(x) &= \sum (u_j - N_{curv} \langle N_{curv}, u_j \rangle) w_j \\ &= (\sum u_j w_j) - N_{curv} (\sum \langle N_{curv}, w_j u_j \rangle). \end{aligned}$$

And the reprojection onto a triangle  $t$  with normal  $N_t$  along  $N_{curv}$  is given by

$$u(x) = u_{flat}(x) - N_{curv} \frac{\langle u_{flat}(x), N_t \rangle}{\langle N_{curv}, N_t \rangle}.$$

### Pathtracing on a mesh

Given a continuous vector field on the mesh, the pathtracing step (IS 2 a)) is straight forward to implement. Let  $u(x)$  be the interpolated velocity field, then this field can be pathtraced by doing small steps of size  $h$  according to  $u$ . A simple pathtracing algorithm is described in Figure 7.9.

### Backtracing Vorticities

When the dual vertices have been traced back, the vorticity is calculated on the back-traced dual mesh (IS 2 b)). Additional ‘dual vertices’ are introduced on the midpoints of primary border edges such that the dual border faces are complete. These dual vertices are treated separately: as viscous fluids have by definition zero velocity on borders, the

```
backtrace:
    t = T;
    while (t > 0) do
        backtrace(t, stepSize, pos, triangle);
    end while

backtrace(t,stepSize, pos, triangle):
    u = u(pos,triangle);
    maxT = maxt(pos,triangle,u);
    step = min(t,stepSize,maxT)
    if step < maxT then
        pos+ = step · u;
        t- = step;
    end if
    if triangle boundary reached then
        triangle = neighborTriangle;
    end if
```

Figure 7.9.: A straight forward algorithm to trace the trajectory of a particle.  $u(\dots)$  is the interpolated vector field and  $\text{maxt}$  is a helper function that computes the maximal possible time step before hitting the border of the current triangle.

midpoints of border edges don't need to be traced back, as they don't move. Their velocity is defined to be zero; this zero velocity is also used when interpolating the velocity field on boundary dual faces. Note that this separate treatment of the dual vertices on the boundary is the reason why obstacles induce vorticity in our simulation.

On the backtraced dual faces the vorticity is computed by integrating the velocity field along their boundary. If  $p_0, \dots, p_n$  are the boundary vertices of the backtraced dual face this is

$$\sum_{i=0}^n \langle u(p_i) + u(p_{i+1}), p_{i+1} - p_i \rangle / 2,$$

where  $u(p)$  denotes the interpolated velocity field  $u$  at the position  $p$ . A further improvement is to use the harmonic component  $\mathbf{c}$  of  $u$  only if at least one backtraced dual vertex lies on the boundary of the mesh. By definition a harmonic field has no vorticity and therefore is irrelevant for the vorticity calculation away from obstacle boundaries. But due to floating point errors the vorticity of the harmonic component will never totally vanish. This introduces artifacts, as vorticity erroneously induced by the harmonic field is accumulated over time. Therefore, the calculation of backtraced vorticity on dual boundary faces and dual inner faces is treated separately:

$$\begin{aligned} \sum_{i=0}^n \langle d\mathbf{a}(p_i) + d\mathbf{a}(p_{i+1}), p_{i+1} - p_i \rangle / 2 & \quad \text{for inner dual faces,} \\ \sum_{i=0}^n \langle u(p_i) + u(p_{i+1}), p_{i+1} - p_i \rangle / 2 & \quad \text{for boundary dual faces.} \end{aligned}$$

These are values defined on the dual faces and represent a *dual* 2-form. To get the vorticities as a primary 0-form they additionally need to be  $\star_0^{-1}$ -ed.

#### 7.2.4. Diffusion and Additional Forces

After tracing back the vorticities (IS steps 2 a) and b)), the obtained vorticities are diffused (IS step 2 c)) and additional forces are accounted for (IS step 3). Both, the diffusion of vorticities and addition of forces, are simple and can be implemented directly using the DEC operators. The diffusion of vorticity as described by Equation 7.4, i.e.

$$\mathbf{w}_{t_{n+1}} = \mathbf{w}^{backtraced} + \nu t \Delta \mathbf{w}_{t_{n+1}},$$

translates in DEC to solving the following sparse linear system for  $\mathbf{w}_{t_{n+1}}^0$ :

$$(Id - \nu(t_{n+1} - t_n) \star_0^{-1} d_0^{dual} \star_1 d_0) \mathbf{w}_{t_{n+1}} = \mathbf{w}^{backtraced}.$$

The addition of forces to the vorticities is given by

$$\mathbf{w}_{t_{n+1}}^{backtraced+} = (t_{n+1} - t_n) \cdot \partial_{discrete}^1 \mathbf{f}^l.$$

### 7.2.5. The Harmonic Component

What is left is the recovery of  $u$  from the vorticities, that is IS step 4. This involves the precomputation of a harmonic form and the recovery of the vorticity part  $da$ . Both computations are related to each other but they occur in different steps in the algorithm. The computation of the harmonic component occurs only once during a set up step and the recovery of  $da$  occurs once in every time step (IS step 4).

In the vector design chapter we already introduced methods to compute harmonic vector fields on meshes with boundaries. But the constraints derived here lead to solutions with a quality superior to the harmonic forms obtained using the adapted matrices from the vector design chapter.

#### Harmonic Forms and Cycles

In Section 6.3.6 we have seen that the problem statement ' $\omega^1$  is harmonic' has degrees of freedom depending only on the topology of the manifold. The following result mentioned in [Fra11] (p377) explains these degrees of freedom for 1-forms on borderless manifolds, and *tangential* 1-forms on manifolds with boundary. Note that the result is formulated more generally in [Fra11], treating harmonic  $k$ -forms and using the notion of  $k$ -cycles.

**Theorem 7.** *Let  $M$  be a compact manifold with boundary. Let  $z_1, \dots, z_\beta$  be a basis of 1-cycles on the manifold. Then there exists a unique tangent harmonic 1-form  $\alpha^1$  with prescribed periods  $p_1, \dots, p_\beta$*

$$\int_{z_1} \alpha^1 = p_1$$

$$\int_{z_2} \alpha^1 = p_2$$

...

$$\int_{z_\beta} \alpha^1 = p_\beta$$

For a correct definition of cycles see [Fra11]. A basis of 1-cycles is basically a set of closed curves from which you can build any closed curve on the manifold by concatenation. In Figure 7.10 a torus and a bordered manifold are depicted on which two cycles form the basis of 1-cycles. On these manifolds a harmonic tangential differential 1-form is well defined if the flow along the two cycles, i.e. the period on the two cycles, is fixed.

On manifolds without boundaries one additional constraint is needed for each 1-cycle in the basis of 1-cycles for the computation of a harmonic component. On objects with sphere topology there is no need to compute any harmonic component, as the space of harmonic 1-forms is zero dimensional—there are no harmonic 1-forms on spheres.

The only type of meshes with boundary we consider are flat meshes with one or more holes that describe impenetrable obstacles, like the one depicted in Figure 7.11.

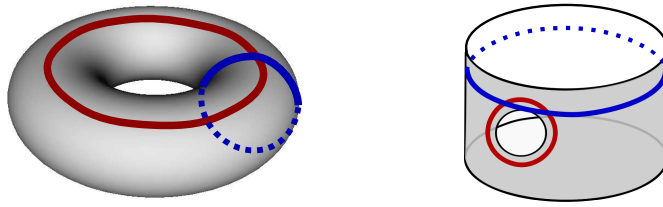


Figure 7.10.: Harmonicity for tangential 1-form on a 2-manifold has as many degrees of freedom as there are elements in a cycle basis of the manifold. On the torus and the bordered manifold depicted here cycle bases have two elements. A harmonic tangential 1-form is uniquely defined if the flow along the basis cycles is fixed.

### Computing the Harmonic Component on Flat Bordered Meshes

We assume that all inner boundaries describe obstacles and only the outer boundary has sections that allow flow to pass. We now design a set of constraints for the computation of the harmonic component of the flow. The goal is to find a harmonic 1-form with

$$\begin{aligned} \partial \mathbf{c} &= 0 && \text{(zero vorticity)} \\ d\mathbf{c} &= 0 && \text{(zero divergence)} \\ \mathbf{c} &= 0 && \text{on inner boundaries} \\ \mathbf{c} &= \mathbf{u} && \text{on the exterior boundary} \end{aligned} \quad (7.9)$$

The constraints  $\mathbf{u}$  on the exterior border can not be chosen arbitrarily. At the very least summing up the flux over the exterior border should be zero, else the zero divergence condition is impossible to fulfill. A simple consistent constraint can be obtained by choosing a fixed direction  $v$  and setting all edges of the exterior boundary to

$$\mathbf{c}(\text{edge}) = \langle \text{edge}^\perp, v \rangle =: \mathbf{u}(\text{edge}). \quad (7.10)$$

Constraining only the values on boundaries does not get rid of all degrees of freedom. For any two solutions  $v, w$  of the system 7.9, the difference  $v - w$  is a 1-form tangential on all boundaries. Therefore, the theorem described in the last section applies to the difference of solutions. In particular this means that if the system 7.9 has a solution, there exists a solution with arbitrary prescribed periods on a system of independent cycles.

Every inner border introduces one new cycle and an additional degree of freedom. Therefore for every obstacle one additional constraint has to be provided that fixes the period around the obstacles. We will constrain these periods to be zero. The overall constraints are depicted in Figure 7.11.

These constraints can be enforced by slightly changing the dual mesh and adapting the DEC matrices. The dual mesh is changed in the following way: the vertices on an

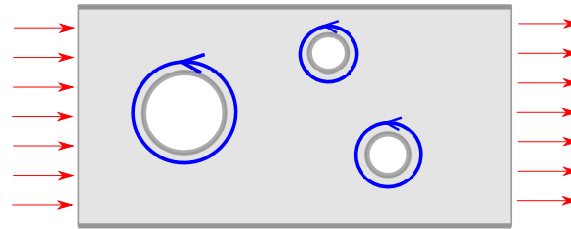


Figure 7.11.: Example constraints for a harmonic component. The period around every obstacle has to be fixed by fixing the flow along the blue circles. The exterior boundary allows incoming flow on one side and outgoing flow on the other, following Equation 7.10. All other boundaries allow no flux.

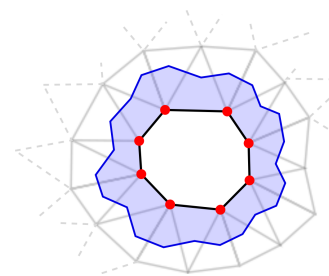


Figure 7.12.: The border vertices of the inner border (red) are interpreted as one vertex with a single dual face (blue).

inner border are interpreted as one vertex and their dual faces are combined to one single dual face, as depicted in Figure 7.12. The boundary of this dual face is the closed cycle on which the zero periodicity is enforced.

The dual derivative computes the flow around dual faces. Therefore, if it is adapted according to the changed dual mesh, the zero vorticity constraint for harmonic 1-forms,

$$\widetilde{d}_1^{dual} \star_1 \mathbf{c} = 0,$$

naturally enforces a zero period around inner borders. The dual derivative  $d_1^{dual}$  is adapted by adding one line per border component,

$$\widetilde{d}_1^{dual} = \begin{pmatrix} d_1^{dual} \\ (1_{border_1})^T \cdot d_1^{dual} \\ \vdots \\ (1_{border_k})^T \cdot d_1^{dual} \end{pmatrix},$$

and dropping the matrix columns corresponding to the dual faces of single boundary vertices. Equivalently the corresponding values of  $\star_0$  can be set to zero, as we only consider  $\widetilde{d}_1^{dual T} \star^0 \widetilde{d}_1^{dual}$ . Additionally some positive dual primal weights  $W$  for the newly composed dual faces have to be appended to  $\star_0$ . The weight  $W$  can be chosen to be the combined area of the dual faces of border vertices, but any positive weights will work. This leads to

$$\widetilde{\star}_0 = \begin{pmatrix} \star_0 & & & \\ & W & & \\ & & \ddots & \\ & & & W \end{pmatrix}.$$

With these adapted matrices and  $\widetilde{\partial}$  denoting  $\partial$  expressed with the adapted matrices, the system 7.9 can be solved by solving

$$\begin{pmatrix} d^T & \widetilde{\partial}^T & Id_{border}^T \end{pmatrix} \begin{pmatrix} \star_2 & & \\ & \widetilde{\star}_0 & \\ & & \lambda \end{pmatrix} \begin{pmatrix} d \\ \widetilde{\partial} \\ Id_{border} \end{pmatrix} \mathbf{c}^1 = \lambda \mathbf{u}. \quad (7.11)$$

Here  $\lambda$  is a positive weight for the boundary constraints and  $\mathbf{u}$  is zero on inner edges and the chosen constraint on the exterior boundary, for example given by Equation 7.10.

### 7.2.6. Recovering $da$

With the precomputed harmonic component  $\mathbf{c}$  in place, we can describe the last step of the integration scheme, step 4, the recovery of the velocity field from vorticities alone.

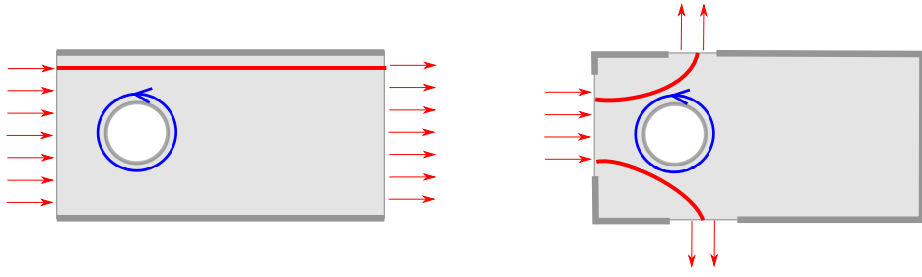


Figure 7.13.: The constraints on the exterior boundary induce new ‘cycles’ (red) on which the period of the harmonic form is non-zero. How these cycles look and how many there are depends on the boundary condition. A vorticity part  $d\mathbf{a}$  has to be constrained to have a zero period along these induced cycles, else it is not orthogonal to the harmonic form.

The last missing element, the reconstruction of the vorticity part  $d\mathbf{a}$  from the vorticities  $\mathbf{w}$  works as described in Theorem 6 in Section 7.1.3, by solving

$$\Delta \mathbf{a}^1 = \mathbf{w}_{t_{n+1}}^0, \quad (7.12)$$

and setting

$$\mathbf{v}_{updated}^1 = d_0 \mathbf{a}^1 + \mathbf{c}^1. \quad (7.13)$$

There is one hick up. The condition of the theorem is that consistent DEC matrices are used that allow a Hodge decomposition, such that the harmonic component  $\mathbf{c}$  is orthogonal to  $d\mathbf{a}$ .

The harmonic component is computed with adapted DEC matrices and by additionally enforcing some values on the outer border. These constraints on the exterior boundary actually introduce new ‘cycles’ and fix the additional periods of the harmonic form. These additional ‘cycles’ and their number depends on the boundary constraint, see Figure 7.13.

For  $d\mathbf{a}$  to be orthogonal to  $\mathbf{c}$ ,  $\partial d\mathbf{a} = 0$  should enforce that  $d\mathbf{a}$  has a zero period on all cycles where  $\mathbf{c}$  has a non zero period. Applying  $\partial$  to  $d\mathbf{a}$  sums up the flow of  $d\mathbf{a}$  around dual faces. As the cycles induced by the exterior boundary constraint are not accounted in the DEC matrix  $\partial$ ,  $\partial d\mathbf{a} = 0$  fails to enforce zero periodicity on them. While the correct thing would be to identify such induced cycles and add additional constraints on them, a much simpler approach is to add the constraint  $d\mathbf{a} = 0$  on *all* boundary edges, this seems also to be the approach taken in [ETK<sup>+</sup>07]. This constraint can be enforced by additionally minimizing  $\mu (d^T I d_{boundaryedges} d) \cdot a$  for some large weight  $\mu \in \mathbb{R}$ , which leads to the equation

$$(\Delta + \mu(d^T I d_{boundaryedges} d)) \mathbf{a}^1 = \mathbf{w}_{t_{n+1}}^0, \quad (7.14)$$

$$\mathbf{v}_{updated}^1 = d_0 \mathbf{a}^1 + \mathbf{c}^1. \quad (7.15)$$

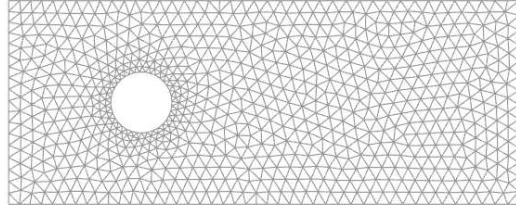


Figure 7.14.: An adaptive mesh generated with [PS04] in Matlab, with 1 400 faces.

This leads to a slightly incorrect behavior close to boundaries presumed to be permeable: in this vorticity reconstruction step they are treated like obstacle boundaries, they will reflect flow. But if the permeable boundaries are in regions with no vorticity or they are sufficiently far away from the areas of interest, this can be ignored.

### 7.3. Results

The algorithm gives plausible results if the meshes are of good quality. Because Voronoi duality is used and the dual mesh is used explicitly, all triangles have to be non-obtuse. The algorithm was tested on spheres and on flat meshes with one obstacle. Both were generated such that there are no obtuse triangles. The quality of the results is much increased if the meshes have a higher resolution around the obstacles, as the most complex processes happen there. All flat meshes used are adaptive meshes, generated with the Matlab tool described in [PS04], like the mesh displayed in Figure 7.14.

It is hard to tell how accurate the simulations are. The time step size and the sampling density of the mesh have a huge influence on the simulation. As in every step velocities are interpolated, each time step induces some unwanted diffusion. The sparser the mesh is, the more diffusion is introduced by the interpolation in every step. Choosing a larger time step reduces this effect but also leads to less exact numerical integration; and if the steps are too large, the simulation becomes unstable.

In Figure 7.15 the influence of the time step size and the mesh density are demonstrated. On meshes with a low sample density the result is governed by the diffusion introduced by the interpolation and higher time steps pay off; on meshes with a high vertex density the higher time steps already lead to unstable behavior. Figure 7.16 shows the influence of the time step size on a single mesh.

For an optimal solution the size of the time step would have to be adapted to the mesh resolution such that the two influences, additional diffusion and incorrect integration, are minimal. Independently the viscosity  $\nu$  can be varied and controls the diffusion rather well, as depicted in Figure 7.17.

Apart from the simulation being highly dependent on the mesh and time step, visually interesting results can be achieved by tweaking the parameters. And the simulation works well on curved meshes, as for example the simulation on the sphere in Figure 7.18.

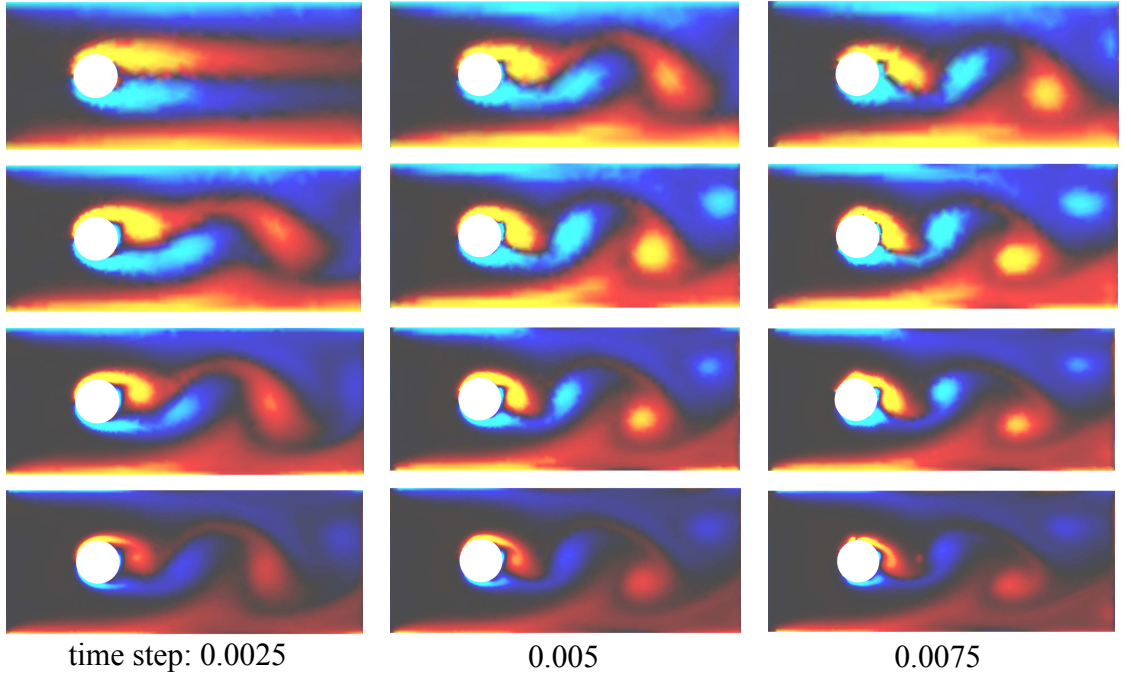


Figure 7.15.: The algorithm was run with different time step sizes on meshes with different densities, while keeping the vorticity fixed. The velocity from left to right is 10 units per second and the mesh is 2 units wide. The time step size, listed from left to right, was selected to be 0.025, 0.005 and 0.075. The meshes have, listed from top to bottom, 1 400, 2 800, 5 300 and 12 000 faces. All meshes are adaptive and were generated using the same vertex distribution as for the mesh in Figure 7.14. The meshes are colored with the vorticity of the flow. Gray is a low absolute vorticity, light blue denotes high counter clockwise vorticity and yellow denotes high clockwise velocity.

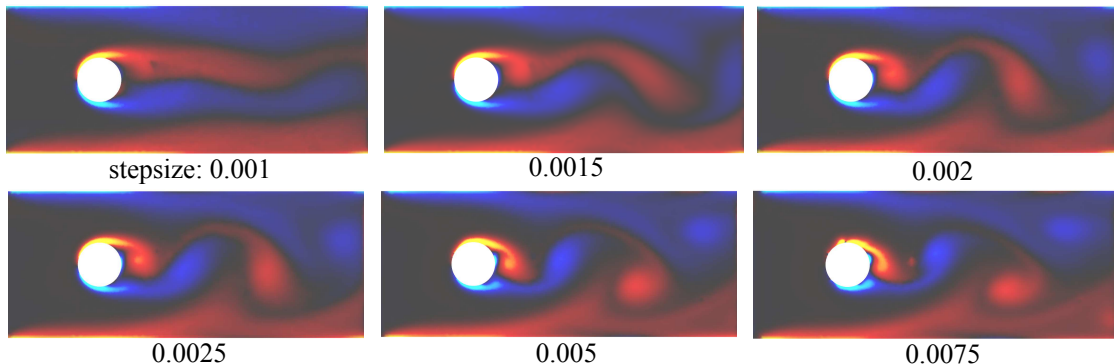


Figure 7.16.: On a mesh with 12 000 faces the time step was varied while keeping the viscosity at 0.02. Velocity and coloring are the same as in Figure 7.15. The behavior of the simulation depends on the time step; for the time step of 0.0075 the simulation begins to be unstable.

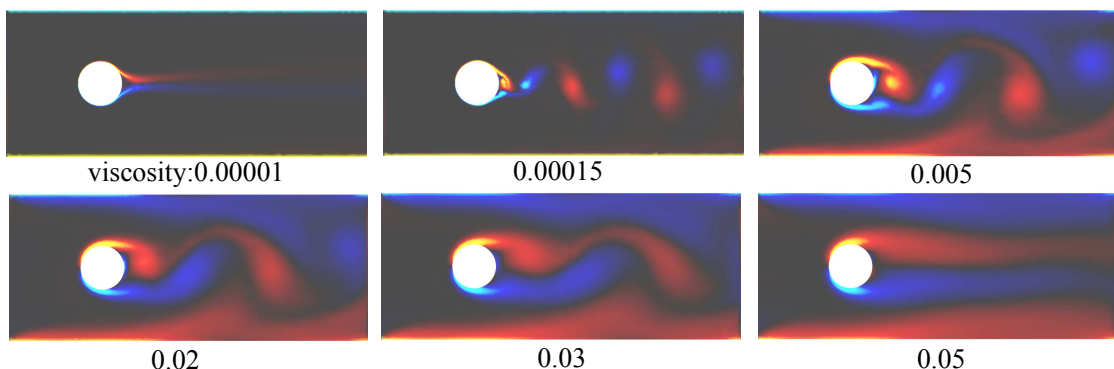


Figure 7.17.: On a mesh with 12 000 faces the viscosity was varied while keeping the time step at 0.02. Velocity and coloring are the same as in Figure 7.15.

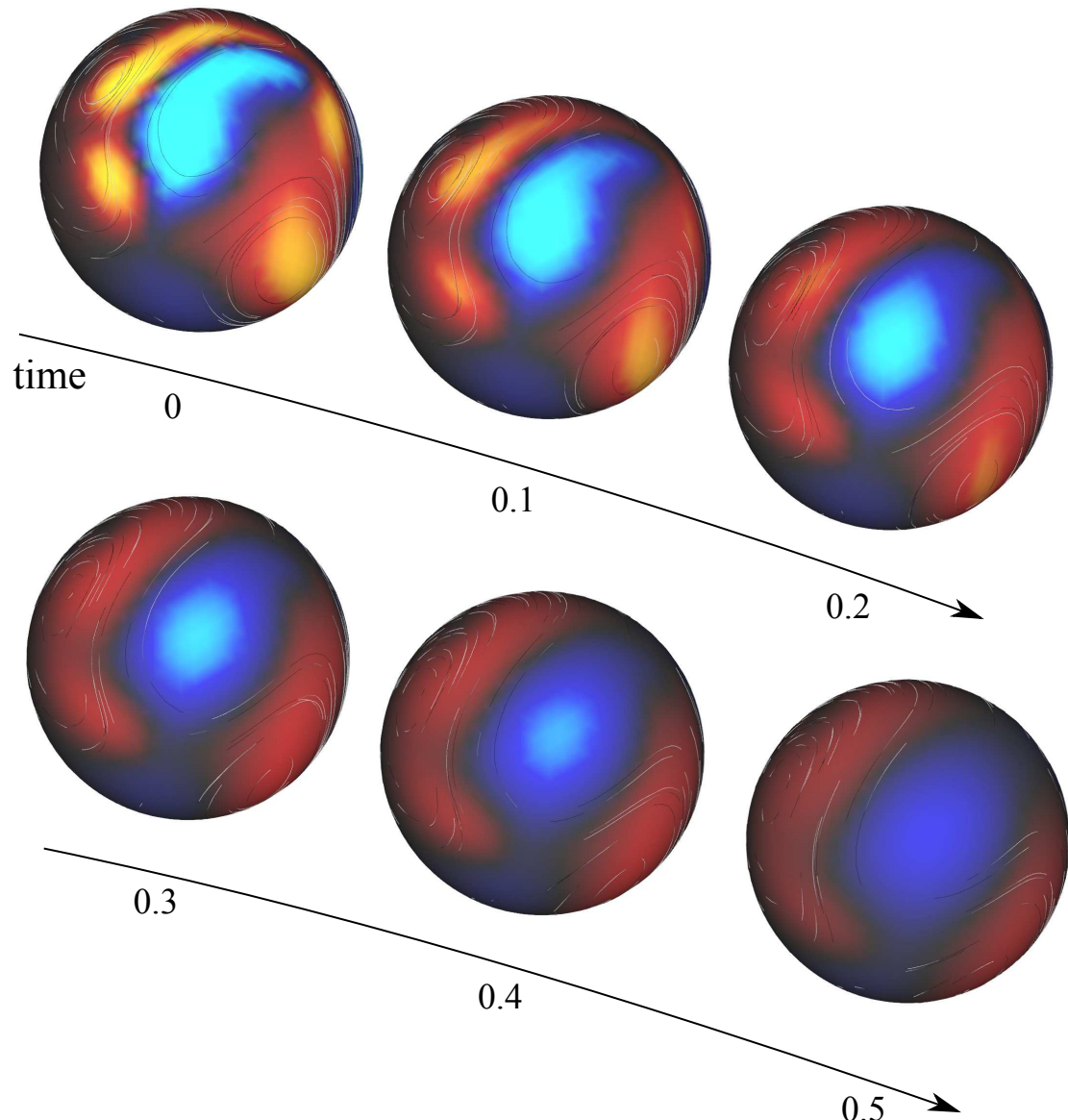


Figure 7.18.: A fluid simulation on a sphere with about 1500 faces. The timestep was selected to be 0.005 and motion was induced by stirring, the viscosity was set to 0.03.

## 8. Discussion and Further Literature

Discrete Exterior Calculus aims to discretize the operators of exterior calculus while staying close to their geometric nature. And it succeeds; the DEC operators can be a valuable tool in various applications on meshes. Like their continuous counter parts, the DEC operators are closely bound to geometric operations and are coordinate free: there is no need to introduce local coordinates on triangles or similar.

The strength of DEC lies in that some EC features are conserved exactly. The discrete operators form a discrete de Rham complex very similar to the continuous one. Stokes theorem is designed to be conserved, the adjointness of derivative and coderivative are preserved just as the exactness of the operators  $d$  and  $\delta$ , i.e.  $dd = 0$  and  $\delta\delta = 0$ . Keeping these fundamental properties allows elegant reasoning in DEC terms along the lines of the continuous reasonings, such that results like the hodge decomposition hold in DEC, not approximately, but exactly. This pays off in practice.

One might be tempted to see DEC as an automatism for the discretization of differential equations: just formulate a problem in EC and replace the operators by DEC operators. This approach will often fail. The different treatment of duality in the continuous and the discrete theory is a key issue. Because discrete dual forms are defined on a different geometric object, they can not be compared or mixed directly with primary forms. This implies that a problem must be carefully reformulated before DEC is applicable.

Furthermore, using DEC to solve a problem requires a clear understanding of the problem and of its geometry to correctly implement constraints and combine DEC with other methods. This is best demonstrated with the fluid simulation in Chapter 7, where the problem is first reformulated in terms of vorticities to develop an integration scheme that respects the geometry of the problem and combines well with DEC.

### Where to go from here

This thesis is designed to be an introductory text. It covers the basics on manifolds, forms, differential forms and exterior calculus, emphasizing geometric aspects. The goal is to show the huge potential of EC and DEC and also help building a strong intuition for the various operators and their relations. But covering that much ground with an emphasis on intuition has its costs; important aspects are only mentioned and most issues are not treated rigorously.

There are many rigorous introductions to Differential Forms, for example the the textbook 'Global Analysis' [AF01].

The texts [Hir03] and [DHLM05] introduce DEC rigorously as an independent theory, targeting an audience well acquainted with differential forms and possible applications

of differential forms. This thesis should give enough background to understand these texts.

A more rigorous study of chain complexes and co chain complexes will give a more abstract view on DEC, emphasizing the important common properties that EC and DEC share. Important in this context are also cohomology groups together with the de Rham complex, but the theory is rather involved. In '*The Geometry of Physics*' [Fra11], Chapters 13 and 14 you can find a nice introduction of the most important concepts. See also [DKT08], where a discrete result about cohomolgy groups is proven.

One important omission of this thesis is error analysis, variational calculus and finite element methods. Finite element methods are closely related to DEC and have a very developed error analysis. There is a wealth of literature on FEM; for example the text book [BS02].

## A. Further Details

### A.1. The Well-Definedness of the Integral for Differential Forms

That the integral definition of Section 3.1.6 really is independent of the chosen map  $\phi$  follows directly from the common transformation formula. Say we use a different map  $\psi : V \rightarrow \Omega \subset M$ , then  $\psi = \phi \circ h$  for some mapping  $h : U \subset \mathbb{R}^k \rightarrow V \subset \mathbb{R}^k$  and

$$\begin{aligned} \int_{\psi(V)} \omega^k &= \int_V \omega_{\psi(x_1, \dots, x_k)} \left( \frac{\partial \psi}{\partial x_1}, \dots, \frac{\partial \psi}{\partial x_k} \right) dx_1 \dots dx_k \\ &= \int_V \omega_{\psi(x_1, \dots, x_k)} \left( \frac{\partial \phi \circ h}{\partial x_1}, \dots, \frac{\partial \phi \circ h}{\partial x_k} \right) dx_1 \dots dx_k \\ &= \int_V \det(Dh) \omega_{\phi \circ h(x_1, \dots, x_k)} \left( \frac{\partial \phi}{\partial x_1}, \dots, \frac{\partial \phi}{\partial x_k} \right) dx_1 \dots dx_k \end{aligned}$$

and using the transformation formula

$$= \int_U \omega_{\phi(x_1, \dots, x_n)} \left( \frac{\partial \phi}{\partial x_1}, \dots, \frac{\partial \phi}{\partial x_k} \right) dx_1 \dots dx_k$$

#### Example

The integral of a  $k$ -form  $\omega^k = f(x) \cdot dVol$  over a  $k$ -dimensional set  $\phi(U)$  parametrized by the orientation preserving map  $\phi$  is the following:

$$\int_{\phi(U)} f dVol = \int_U f(\phi(x)) dVol \left( \frac{\partial \phi}{\partial x_1}, \dots, \frac{\partial \phi}{\partial x_k} \right) dx_1 \dots dx_k$$

And as  $dVol \left( \frac{\partial \phi}{\partial x_1}, \dots, \frac{\partial \phi}{\partial x_k} \right) = \sqrt{\det((D\phi)^T D\phi)}$  this is

$$\int_{\phi(U)} f dVol = \int_U f(\phi(x)) \sqrt{\det((D\phi)^T D\phi)} dx_1 \dots dx_k$$

## A.2. The Dual Discrete Border Operator

The setting is the following: we are on an  $n$ -dimensional (discrete) manifold and the  $n$ -simplex  $\sigma^n$  is oriented according to the orientation of the manifold.  $\sigma^k$  is some face on  $\sigma^n$  with an arbitrary orientation and  $\sigma^{k-1}$  is a face of  $\sigma^k$ . On the dual-mesh side we have the cell  $\star\sigma^k$  that lies on the border of  $\star\sigma^{k-1}$ ; both dual cells have an orientation induced by the primary cells. Our goal is to relate the primary border matrix  $\delta_k$  which stores the relative orientation of  $\sigma^k$  and  $\sigma^{k-1}$  and the dual border matrix  $\delta_{n-k+1}^{\text{dual}}$  that stores the relative orientation of the  $(n-k+1)$ -cell  $\star\sigma^{k-1}$  and  $\star\sigma^k$ .

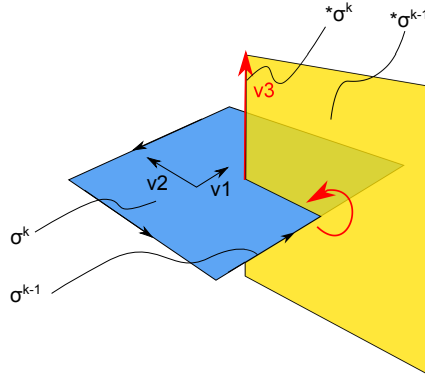


Figure A.1.:  $v_1, v_2$  defines the orientation of  $\sigma^k$  (here  $k = 2$ ) and  $v_1, v_2, v_3$  defines the orientation of the 3-manifold we are on;  $v_2 (v_k)$  is an inside pointing border normal for  $\sigma^{k-1}$  and outside normal for  $\star\sigma^k$ .  $\sigma^{k+1}$  is one border simplex, oriented according to  $\omega^k$ . The duals  $\star\omega^k$  and  $\star\omega^{k-1}$  have orientations induced by the primal cells (red). As you can see, while the primals are oriented consistently, the induced orientations on the dual are opposite to each other.

First of all notice that orientation can be treated very neatly by using forms, as volume forms measure signed volume. We saw in Section 2.2.2, that a  $k$  simplex  $\sigma^k$  encodes orientation by the ordering of its vertices, and that induces an oriented basis  $v_1, \dots, v_k$  that spans its volume. In terms of forms the ordering defines a volume form

$$dv_1 \wedge \dots \wedge dv_k$$

to the  $k$ -simplex. The  $k$ -simplex lies in an  $n$ -simplex  $\sigma^n$ , oriented according to the orientation of the discrete manifold; it induces a volume form

$$dv_1 \wedge \dots \wedge dv_n$$

on its volume. We can select the vector  $v_k$  (for some fixed  $j \leq k$ ) to be a normal on the face  $\sigma^{k-1}$  pointing inside  $\sigma^k$ , and adapt  $v_1, \dots, v_{k-1}$  such that  $dv_1 \wedge \dots \wedge dv_k$  remains

the same. Then the orientation / volume form of  $\sigma^{k-1}$  induced by  $\sigma^k$  (via its border relation) is

$$dv_1 \wedge \dots \wedge dv_{k-1} (-1)^k$$

consistent with the way we defined border orientation ( preappending the 'outside normal'  $-dv_k$  leads to the form  $dv_1 \wedge \dots \wedge dv_k$ , i.e. the orientation of  $\sigma^k$ ). Furthermore we ask  $v_{k+1}, \dots, v_n$  to be orthogonal on  $v_1, \dots, v_k$ ; i.e. they should be aligned with the dual of the cell  $\sigma^k$ . Then the induced orientation of the dual simplex  $\star\sigma^k$  is given by

$$\star(dv_1 \wedge \dots \wedge dv_k) = dv_{k+1} \wedge \dots \wedge dv_n$$

The orientation of the  $j$ th border component  $\sigma_j^{k-1}$  of  $\sigma^k$  induced by  $\sigma^k$  is

$$\delta(dv_1 \wedge \dots \wedge dv_k) \Rightarrow$$

$$(-1)^k dv_1 \wedge \dots \wedge dv_{k-1}$$

its dual  $\star\sigma^{k-1}$  has the orientation

$$\star((-1)^k v_1 \wedge \dots \wedge dv_{k-1}) = (-1)^k dv_k \wedge dv_{k+1} \wedge \dots \wedge dv_n$$

Both,  $\star\sigma^k$  and  $\star\sigma^{k-1}$ , have orientations induced from the primary simplices as seen. But by its border relation  $\star\sigma^{k-1}$  also induces an orientation to  $\star\sigma^k$ . Note that  $v_k$  acts as outside pointing normal for  $\star\sigma^k$  as border of the dual  $\star\sigma_j^{k-1}$  and therefore

$$\delta(-1)^k dv_k \wedge dv_{k+1} \wedge \dots \wedge dv_n = (-1)^k dv_{k+1} \wedge \dots \wedge dv_n$$

This means that the relative orientation of the pair  $(\sigma^k, \sigma^{k-1})$  and the relative orientation of the pair  $(\star\sigma^{k-1}, \star\sigma^k)$  is related by

$$orient(\sigma^k, \sigma^{k-1}) = (-1)^k orient(\star\sigma^{k-1}, \star\sigma^k)$$

Therefore, if the border matrix

$$\delta_k$$

stores the relative orientations of  $k$  and  $k-1$  simplices  $\sigma^k$  and  $\sigma^{k-1}$ , then the relative orientation of  $n-k-1$  and  $n-k$ -dimensional dual cells  $\star\sigma^{k-1}$  and  $\star\sigma^k$ , with orientations induced by the primary simplices, is given by the dual border matrix

$$\delta_{n-k+1}^{dual} = (-1)^k (\delta_k)^T$$



# Bibliography

- [AF01] AGRICOLA, I. ; FRIEDRICH, T.: *Globale Analysis.* Vieweg, 2001 [http://books.google.ch/books?id=jNjyaS\\_2qq0C](http://books.google.ch/books?id=jNjyaS_2qq0C). – ISBN 9783528031541
- [Bac06] BACHMAN, D.: *A Geometric Approach to Differential Forms.* Birkhäuser, 2006. – ISBN 9780817645205
- [BS02] BRENNER, Susanne C. ; SCOTT, L. R.: *The Mathematical Theory of Finite Element Methods.* 2nd. Springer, 2002. – ISBN 0387954511
- [Car92] CARMO, M.P.: *Differentialgeometrie von Kurven und Flächen.* Vieweg, 1992 (Vieweg Studium). – ISBN 9783528172558
- [CM11] COLDING, T. H. ; MINICOZZI, W. P. II: Minimal surfaces and mean curvature flow. In: *ArXiv e-prints* (2011), Februar
- [DHLM05] DESBRUN, M. ; HIRANI, A. N. ; LEOK, M. ; MARSDEN, J. E.: Discrete Exterior Calculus. In: *ArXiv Mathematics e-prints* (2005), August
- [DKT08] DESBRUN, Mathieu ; KANSO, Eva ; TONG, Yiyi: Discrete Differential Forms for Computational Modeling. In: BOBENKO, Alexander I. (Hrsg.) ; SULLIVAN, John M. (Hrsg.) ; SCHRÖDER, Peter (Hrsg.) ; ZIEGLER, Günter M. (Hrsg.): *Discrete Differential Geometry* Bd. 38. Birkhäuser Basel, 2008. – ISBN 978-3-7643-8621-4, S. 287–324
- [DMA02] DESBRUN, Mathieu ; MEYER, Mark ; ALLIEZ, Pierre: Intrinsic Parameterizations of Surface Meshes. In: *Computer Graphics Forum* 21 (2002), Nr. 3, 209–218. <http://dx.doi.org/10.1111/1467-8659.00580>. – DOI 10.1111/1467-8659.00580. – ISSN 1467-8659
- [DMSB99] DESBRUN, Mathieu ; MEYER, Mark ; SCHRÖDER, Peter ; BARR, Alan H.: Implicit fairing of irregular meshes using diffusion and curvature flow. In: *Proceedings of the 26th annual conference on Computer graphics and interactive techniques.* New York, NY, USA : ACM Press/Addison-Wesley Publishing Co., 1999 (SIGGRAPH '99). – ISBN 0-201-48560-5, 317–324
- [ETK<sup>+</sup>07] ELCOTT, Sharif ; TONG, Yiyi ; KANSO, Eva ; SCHRÖDER, Peter ; DESBRUN, Mathieu: Stable, circulation-preserving, simplicial fluids. In: *ACM Trans. Graph.* 26 (2007), Januar, Nr. 1. <http://dx.doi.org/10.1145/1189762.1189766>. – DOI 10.1145/1189762.1189766. – ISSN 0730-0301

- [Flo03] FLOATER, Michael S.: Mean value coordinates. In: *Computer Aided Geometric Design* 20 (2003), Nr. 1, S. 19 – 27. [http://dx.doi.org/10.1016/S0167-8396\(03\)00002-5](http://dx.doi.org/10.1016/S0167-8396(03)00002-5). – DOI 10.1016/S0167-8396(03)00002-5. – ISSN 0167-8396
- [Fra11] FRANKEL, Theodore: *The Geometry of Physics*. Cambridge University Press, 2011 <http://dx.doi.org/10.1017/CBO9781139061377>
- [FSDH07] FISHER, Matthew ; SCHRÖDER, Peter ; DESBRUN, Mathieu ; HOPPE, Hugues: Design of tangent vector fields. In: *ACM Trans. Graph.* 26 (2007), Juli, Nr. 3. <http://dx.doi.org/10.1145/1276377.1276447>. – DOI 10.1145/1276377.1276447. – ISSN 0730-0301
- [GGT06] GORTLER, Steven J. ; GOTSMAN, Craig ; THURSTON, Dylan: Discrete one-forms on meshes and applications to 3D mesh parameterization. In: *Computer Aided Geometric Design* 23 (2006), Nr. 2, 83 - 112. <http://dx.doi.org/10.1016/j.cagd.2005.05.002>. – DOI 10.1016/j.cagd.2005.05.002. – ISSN 0167-8396
- [GP74] GUILLEMIN, V. ; POLLACK, A.: *Differential Topology*. Prentice-Hall, 1974 (Mathematics Series). – ISBN 9780132126052
- [Hir03] HIRANI, Anil N.: Discrete exterior calculus. (2003). <http://resolver.caltech.edu/CaltechETD:etd-05202003-095403>
- [MDSB02] MEYER, Mark ; DESBRUN, Mathieu ; SCHRÖDER, Peter ; BARR, Alan H.: Discrete Differential-Geometry Operators for Triangulated 2-Manifolds. In: *Proc. VisMath*, 2002, S. 35–57
- [MTAD08] MULLEN, Patrick ; TONG, Yiying ; ALLIEZ, Pierre ; DESBRUN, Mathieu: Spectral Conformal Parameterization. In: *Computer Graphics Forum* 27 (2008), Nr. 5, 1487–1494. <http://dx.doi.org/10.1111/j.1467-8659.2008.01289.x>. – DOI 10.1111/j.1467-8659.2008.01289.x. – ISSN 1467-8659
- [PS04] PERSSON, Per O. ; STRANG, Gilbert: A Simple Mesh Generator in Matlab. In: *SIAM Review* 46 (2004), Nr. 2, 329–345. <http://www.jstor.org/stable/20453511>. – ISSN 00361445
- [Rau12] RAUBER, Patrik: *Vector Field Guided Surface Crack Patterns*, Institute of Computer Science and Applied mathematics, University of Bern, Diplomarbeit, August 2012
- [SG04] SCHENK, Olaf ; GARTNER, Klaus: Solving unsymmetric sparse systems of linear equations with PARDISO. In: *Future Generation Computer Systems* 20 (2004), Nr. 3, 475 - 487. <http://dx.doi.org/10.1016/j.future.2003.07.011>. – DOI 10.1016/j.future.2003.07.011. – ISSN 0167-739X

- [WSHD07] WARREN, Joe ; SCHAEFER, Scott ; HIRANI, Anil ; DESBRUN, Mathieu: Barycentric coordinates for convex sets. In: *Advances in Computational Mathematics* 27 (2007), Oktober, Nr. 3, 319–338. <http://dx.doi.org/10.1007/s10444-005-9008-6>. – DOI 10.1007/s10444-005-9008-6